

Fred Reamer
JA64

IN-22055

REPORT RE-717

**DEVELOPMENTAL TESTING OF
A PROGRAMMABLE MULTIZONE FURNACE**

April 1986

prepared by

Edmund Y. Ting
and
David J. Larson, Jr.
Materials & Structural Mechanics Directorate
Grumman Corporate Research Center
Bethpage, New York 11714

Final Report on
Contract No. NAS-8-35607

prepared for

George C. Marshall Space Flight Center
Marshall Space Flight Center, Alabama 35812

(NASA-CR-178870) DEVELOPMENTAL TESTING OF A
PROGRAMMABLE MULTIZONE FURNACE Final Report
(Grumman Aerospace Corp.) 97 p CSCL 22A

N87-13569

Unclas
G3/29 43201

REPORT RE-717

DEVELOPMENTAL TESTING OF
A PROGRAMMABLE MULTIZONE FURNACE

April 1986

prepared by

Edmund Y. Ting
and

David J. Larson, Jr.
Materials & Structural Mechanics Directorate

Grumman Corporate Research Center
Bethpage, New York 11714

Final Report on
Contract No. NAS-8-35607

prepared for

George C. Marshall Space Flight Center
Marshall Space Flight Center, Alabama 35812

Approved by:


Richard A. Scheuing, V.P.
Corporate Research Center

ABSTRACT

A multizone furnace was evaluated for its potential utilization for process experimentation on board the Space Shuttle. A temperature gradient can be created through the use of a series of connected temperature zones and can be translated by the coordinated sequencing of zone-temperatures. The Bridgman-Stockbarger thermal configuration for directional solidification was implemented so that neither the sample nor furnace was translated. The thermal behavior of the furnace was measured and characterized. Limitations due to both thermal and electronic (computer) limits were identified. The results indicate that the multizone design is limited to low temperature gradients because of the indirect furnace-to-sample thermal coupling needed to blend the discrete thermal zones. The multizone furnace design inherently consumes more power than a similar (two temperature) conventional Bridgman type directional solidification furnace because every zone must be capable of the high cooling rates needed to produce the maximum desired temperature drop. Typical achievable static temperature gradients for the furnace tested were between 75 and 6°C/in. The maximum gradient velocity was approximately 10 in./hr. Several aspects of the tested system could be improved, but the dependence of the multizone design on high heat loss will limit Space Shuttle applications in the form tested unless additional power is available. The multizone furnace offers great flexibility but requires a high level of operator understanding for full advantage to be obtained.

CONTENTS

<u>Section</u>	<u>Page</u>
1. INTRODUCTION.....	1
2. BACKGROUND.....	3
2.1 Crystal Growth Furnace Requirements.....	3
2.2 The Multizone Directional Solidification Furnace Concept.....	5
3. EDG SYSTEM DESCRIPTION.....	7
3.1 Furnace Construction.....	7
3.2 Control System.....	7
3.2.1 Hardware.....	11
3.2.2 Temperature Control Algorithm.....	11
4. EXPERIMENTAL METHOD.....	17
4.1 Electronic Control.....	17
4.2 Thermal Control.....	17
4.3 Directional Solidification.....	19
4.4 Furnace Set-up.....	19
4.5 Data Acquisition.....	19
5. EDG PERFORMANCE EVALUATION AND DISCUSSION.....	23
5.1 Control Limits.....	23
5.1.1 Thermocouples.....	23
5.1.2 Electronic Hardware.....	25
5.1.3 Controller Software.....	25
5.2 Heat Transfer Limits.....	25
5.2.1 Radial Heat Flow.....	28
5.2.2 Axial Heat Flow.....	28
5.3 Power Consumption.....	31
5.4 Vibration.....	34
5.5 Time-Temperature Stability.....	34
5.6 Axial-Temperature Variations.....	36
5.7 Axial-Temperature Gradients.....	40
5.7.1 Control System Accuracy Limited Temperature Gradients.....	40
5.7.2 Thermal Flux Limited Temperature Gradients.....	40
5.7.3 Unachievable Furnace Temperature Gradient.....	43
5.7.4 Maximum Achievable Furnace Temperature Gradient.....	43

CONTENTS

<u>Section</u>		<u>Page</u>
5.8	Temperature Gradient Motion.....	46
5.8.1	Discontinuity of Gradient Motion.....	46
5.8.2	Errors during Gradient Motion.....	46
5.8.3	Limits of Maximum Gradient Velocity.....	51
5.8.4	Limits of Minimum Gradient Velocity.....	55
5.9	Special Considerations for the EDG Furnace.....	57
5.9.1	Furnace and Sample Temperature Gradient Differences.....	57
5.9.2	Material Thermal Conductivity Changes.....	59
6.	EVALUATION of DIRECTIONAL SOLIDIFICATION OF BiMn.....	63
6.1	Case Study A.....	63
6.2	Case Study B.....	63
6.3	Case Study C.....	68
7.	NON-BRIDGMAN TYPE FURNACE THERMAL PROFILES.....	77
8.	SPACE SHUTTLE COMPATIBILITY.....	81
8.1	Thermal and Electrical Interface.....	81
8.2	Launch Survival.....	81
9.	SUMMARY.....	83
10.	CONCLUSIONS.....	85

ILLUSTRATIONS

<u>Figure</u>		<u>Page</u>
1	Linear Temperature Gradient for Unidirectional Solidification.....	4
2	EDG Furnace System.....	8
3	Heating-element Assembly - U S Patent 4423516.....	9
4	Schematic of EDG Furnace Zone Arrangement.....	10
5	Modified Bridgman-type Directional Solidification Temperature Profile History as Programmed into the EDG System.....	12
6	Block Diagram of PID Algorithm.....	14
7a	Computer-model Furnace Response Using Proportional Control.....	15
7b	Computer-model Furnace Response Using Proportional & Integral Control.....	15
7c	Computer-model Furnace Response Using Proportional, Integral, & Derivative Control.....	15
8	Isothermal Furnace for Thermocouple Testing.....	18
9	Uncertainty of Temperature Measurement.....	26
10	Dynamic Temperature Tracking Error as Shown by Deviation from the Programmed Temperature during Ramping.....	27
11	Natural Temperature Decay (Cooling Curves) of the EDG Furnace with Various Sample Types.....	29
12	Rate of Temperature Decrease (dT/dt) vs Temperature....	30
13	Calculated Axial Heat Flux Produced in Various Materials vs Temperature Gradients.....	32
14	Maximum Furnace Temperature Gradient with Various Samples.....	33
15	Average Furnace Power at Temperature without Axial Heat Flux.....	35
16	Zone Temperature vs Time at a Fixed Furnace Power Output of 10%.....	37

ILLUSTRATIONS

<u>Figure</u>		<u>Page</u>
17	Deviation from the Programmed Temperature vs Actual Temperature Under Two Different Tuning Conditions.....	38
18	Steady-state Temperature Error at High (650°C) & Low (150°C) Temperatures.....	39
19	Measured Axial Temperature Variation during Steady-state.....	41
20	Idealized Axial Sample Heat Flow & Sample Temperature Gradient in Multizone Furnace.....	42
21	Temperature & Power vs Zone Showing Condition of Unachievable Temperature Gradient.....	44
22	Calculated & Measured Maximum Temperature Gradient vs Temperature for Stainless Steel Sample.....	45
23	Temperature Profile History of Furnace & Sample during Gradient Motion (3D View).....	47
24	Temperature vs Time for Furnace & Sample during Temperature Gradient Motion - Stainless Steel Sample.....	48
25	Temperature & Tracking Error at the End of Ramping - Stainless Steel Sample.....	49
26	Temperature & Power vs Time during Gradient Motion - Copper Sample.....	50
27	Isotherm (500°C) Position vs Time - Stainless Steel Sample.....	52
28	Isotherm (500°C) Velocity vs Time - Stainless Steel Sample.....	53
29	Deviation from Linearity During Ramp-Down.....	54
30	Temperature Oscillation at Low Temperature.....	56
31	Measured Sample Temperature Gradient.....	58
32	Axial Temperature Gradients in an Adiabatic Gradient...	60
33	Unmatched Boundary Temperature Condition Resulting in Radial Heat Flux.....	61

ILLUSTRATIONS

<u>Figure</u>		<u>Page</u>
34	BiMn Directional Solidification - Case History A.....	64
35	Detail of Temperature Tracking during BiMn Gradient Motion.....	65
36	Deviation from Linearity during Ramp-Down & Constant Temperature Hold in BiMn Run A.....	66
37	BiMn Directional Solidification - Case History B.....	67
38	Deviation from Linearity & Power during Ramp-Down & Constant Temperature Hold in BiMn Case B.....	69
39	Cooling Curve of BiMn Sample Showing Change in Slope...	70
40	Expanded Temperature vs Time for BiMn Case C.....	71
41	Isotherm Velocity vs Time for Case C.....	72
42	Power & Deviation from Linearity vs Time during Ramp-Down & Constant Temperature Hold for Case C.....	73
43	Expanded Deviation & Power vs Time for Event A.....	74
44	Sample Cooling History Showing Possible Thermal Convection within the Liquid Phase.....	76
45	Vapor-transport Crystal Growth Temperature Profile History.....	78
46	Isothermal & Gradient Furnace Temperature Profile.....	79
47	Simple Isothermal Furnace Temperature Profile.....	80

TABLES

<u>Table</u>		<u>Page</u>
1	Manufacturer's Specification for Micricon 823.....	13
2	PID Coefficients for EDG Furnace.....	20
3	Control System Accuracy.....	24

PRECEDING PAGE BLANK NOT FILMED

PAGE ~~X~~ INTENTIONALLY BLANK

ACKNOWLEDGMENT

The authors wish to acknowledge Dr. P. Adler of the Grumman Corporate Research Center for his technical assistance and Mr. W. Poit for his laboratory assistance in sample preparations.

PRECEDING PAGE BLANK NOT FILMED

1 - INTRODUCTION

The objective of this work was to evaluate the performance of a programmable multizone furnace as candidate hardware for future materials research experiments in the microgravity environment. Prior to the advent of low-cost, computer-based controllers, this type of furnace design was not practical. This developmental furnace was built by the Mellen Company (Webster, N.H.) and is commonly referred to as the Electro-Dynamic-Gradient (EDG) furnace. Although the furnace was designed for directional solidification/ crystal growth, its flexibility suggests additional applications involving heating and cooling.

Microgravity processing is ideal for solidification research because of the absence of gravity driven convection, an unavoidable phenomenon when processing on earth. Experimentation in the microgravity environment, such as that provided by NASA's Space Shuttle, can provide valuable information for improved earth-based processing. Experimental processing hardware based upon the multizone concept, might play a part in future space materials research.

The design purpose of the EDG furnace is bulk single-crystal growth. In single-crystal growth, success often depends on the proper design and operation of the furnace. This is true in the 1-g environment as well as in microgravity.

The capabilities, limitations, and problems associated with the multizone design will be addressed in this report.

2 - BACKGROUND

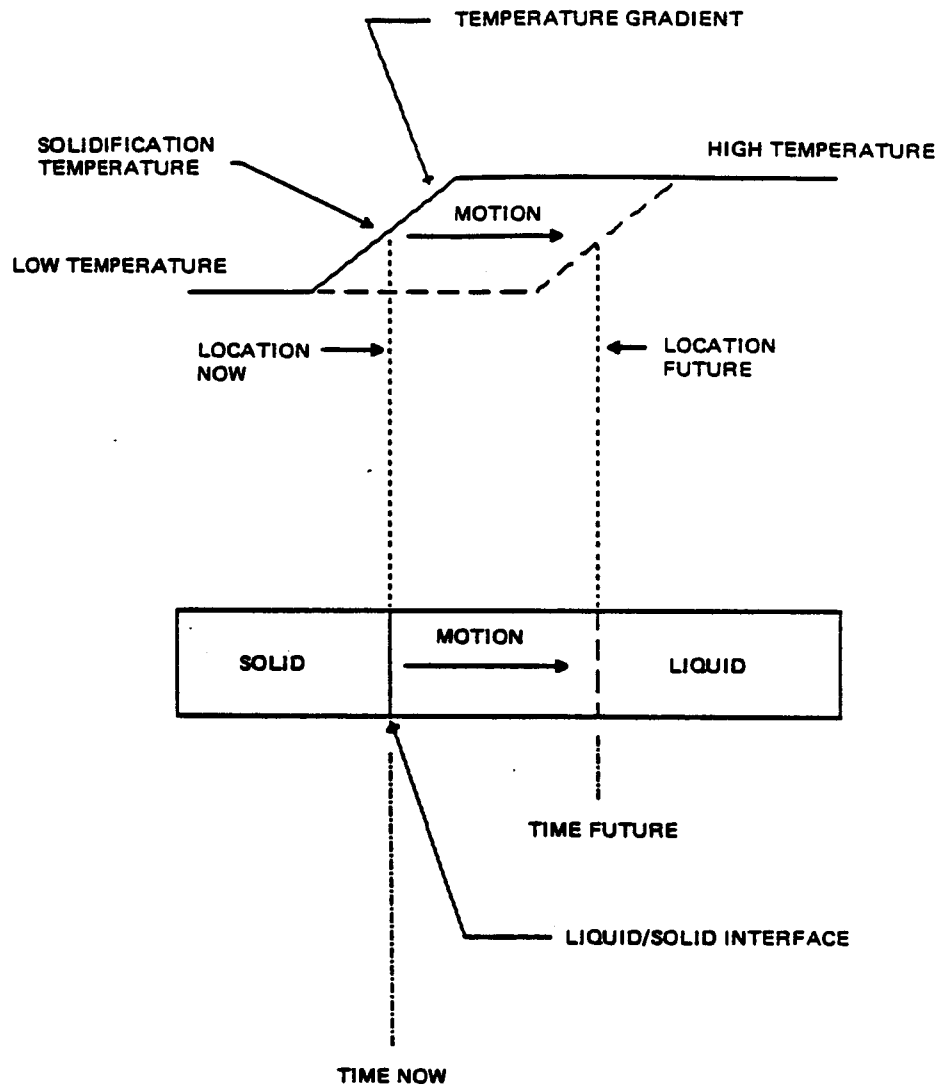
2.1 CRYSTAL GROWTH FURNACE REQUIREMENTS

Single crystal technology is an integral part of modern electronic device fabrication. The overall objective of the crystal producer is to improve device yield and performance by the production of materials with high compositional uniformity and crystallographic perfection. Both compositional variations and crystallographic imperfections can be minimized by improved crystal growth techniques.

The common objective in many bulk growth techniques is the generation of a thermal gradient across a liquid-solid interface that can be translated or changed, so as to produce a controlled liquid/solid interface motion within the subject material, to yield a single crystal (Fig. 1). Two important terms involved in plane front solidification are the temperature gradient at the interface and the interface velocity. To limit growth to only one direction, a linear temperature gradient, such as that produced in the Bridgman-type directional solidification, is used. For many materials, due to thermal stress effects, the magnitude of the temperature gradient must be limited. For these materials, a very low growth velocity must be used. During growth, the temperature gradient and interface velocity must be precisely controlled to avoid spurious nucleation ahead of the crystal growth interface. Deleterious mechanical vibrations and temperature fluctuations must be kept low. After solidification, defect generating deformation stresses in the solid must be avoided. These stresses can result from axial and radial thermal stresses generated during cooling. Thermal stresses can be reduced if the crystal is allowed to cool-down uniformly in temperature, to room temperature (isothermal lowering) while under control.

With these basic considerations, the general specification for an ideal crystal growth furnace can be established. They are:

- o A precisely controlled linear temperature gradient at the solidification interface
- o A precisely controlled gradient velocity
- o No mechanical motion that would produce vibrations



P86-0332-004(T)

Fig. 1 Linear Temperature Gradient for Unidirectional Solidification

- o Separate solidification (growth) and cooling (from post-solidification temperature to room temperature) stages to control thermal stresses.

Further requirements will be based upon considerations of:

- o Furnace internal (working) dimensions
- o Physical furnace size
- o Power requirement
- o Operational ease
- o Other operational support requirements
- o Operational flexibility.

Flexibility means that the number of gradients, as well as gradient direction, gradient magnitude, gradient velocity, gradient length, furnace heating rate, furnace cooling rate, and solidification orientation (vertical to horizontal) are all easily adjustable. With respect to the last parameter, it would be ideal if gravity could be "controlled." This would allow for the study of thermosolutal driven convection, a source of growth perturbation which even the best furnace could not eliminate.

2.2 THE MULTIZONE DIRECTIONAL SOLIDIFICATION FURNACE CONCEPT

Solidification occurs in the direction of heat flow. In order to produce a planar interface, the heat flux should be only in the axial direction at the solidification interface. This is realized by the prevention of radial heat loss in the region of solidification. Since isotherms are always perpendicular to the direction of heat flow (Fick's law), a linear temperature gradient is formed. Within the linear temperature gradient, the rate of interface motion is given by the equation:

$$R = S / G \quad (1)$$

where S is the cooling rate (deg/time), G is the temperature gradient (deg/distance), and R is the gradient velocity (distance/time).

In a conventional Bridgman-type directional solidification furnace, an adiabatic (insulation) zone is used between the hot and cold sections to ensure that within the region of solidification, no radial heat loss occurs. The temperature gradient (G) is established by the length of the adiabatic

zone and the temperature of the two adjacent heated furnace zones. The gradient velocity (R) is imposed by the mechanical motion of the furnace.

In the multizone furnace, radial heat loss in the gradient zones is prevented by the direct control of the sample temperature. If the temperature profile within the multizone gradient reproduces the same profile as if an adiabatic zone were used, then as far as the sample is concerned, there is no driving force for detrimental, radial heat transfer in the gradient zones. In the multizone furnace design, the S and G terms are controlled by programming in order to generate an effective R .

Solidification with the electronic translation of the temperature gradient eliminates mechanical binding as a problem. Thus, there should not be a lower limit for the gradient velocity in the multizone furnace (not totally true, as will be discussed). The absence of a physical adiabatic zone means that the gradient length is also variable. In addition, the absence of physical furnace or sample motion reduces the size of the furnace system by the elimination of the tracking or drive mechanisms and translational volume. The independent heating zone nature of the furnace allows many different thermal geometries to be programmed. Thermal configurations not possible with conventional directional solidification furnaces can be produced with a multizone furnace design.

3 - EDG SYSTEM DESCRIPTION

3.1 FURNACE CONSTRUCTION

The EDG system studied is shown in Fig. 2. The furnace has a 1.125 in. internal diameter. The specimen size should be limited to approximately 0.5 in. diameter. This limit is due to heat transfer reasons that will be discussed later. As received from the Mellen Company, the system consists of a furnace-heating unit (22"x22"x31"), a power controller (24"x34"x42"), and a programmer-controller electronics (18"x23"x42"). A HP9836C micro-computer was added by the Grumman Corporate Research Center.

The internal furnace construction greatly affects its performance. The following details were obtained from an external inspection of the system and a review of the EDG Furnace Patent (Ref 1). The furnace is constructed from a multitude of individual heating-element assemblies. One heating-element assembly is shown in Fig. 3. Each furnace heating-element assembly is constructed from one cast-aluminum, ring-shaped piece for structural support and cooling, one electrical heating element, and a rigid, shaped thermal insulation. Eight water cooling tubes connect all the heating-element assemblies. A flow switch prevents furnace operation at flow rates less than approximately one GPM. Two heating-element assemblies (each 0.5 in. thick) connect electrically and physically in series make up one programmable control zone. The working core of the furnace (referred to as the EDG section) contains 16 programmable control zones (also referred to as Loops), built from a total of 32 heating-element assemblies. The total length of the EDG section is 16 in., each zone or loop being one inch in length. On each end of the EDG section, there are two non-time-programmable constant temperature buffer zones. Each buffer zone is made from four heating-element assemblies, resulting in each buffer zone being 2 in. in length. Each end has a total buffer length of 4 in. The total heated length of the furnace is 24 in. The overall furnace is illustrated schematically in Fig. 4.

3.2 CONTROL SYSTEM

The EDG furnace is designed as a directional solidification furnace; its uniqueness is its ability to create a moving temperature gradient by the coordinated control of the temperature at each heating zone. Many different



R86-0332-050(T)

Fig. 2 EDG Furnace System

**ORIGINAL PAGE IS
OF POOR QUALITY**

ORIGINAL PAGE IS
OF POOR QUALITY

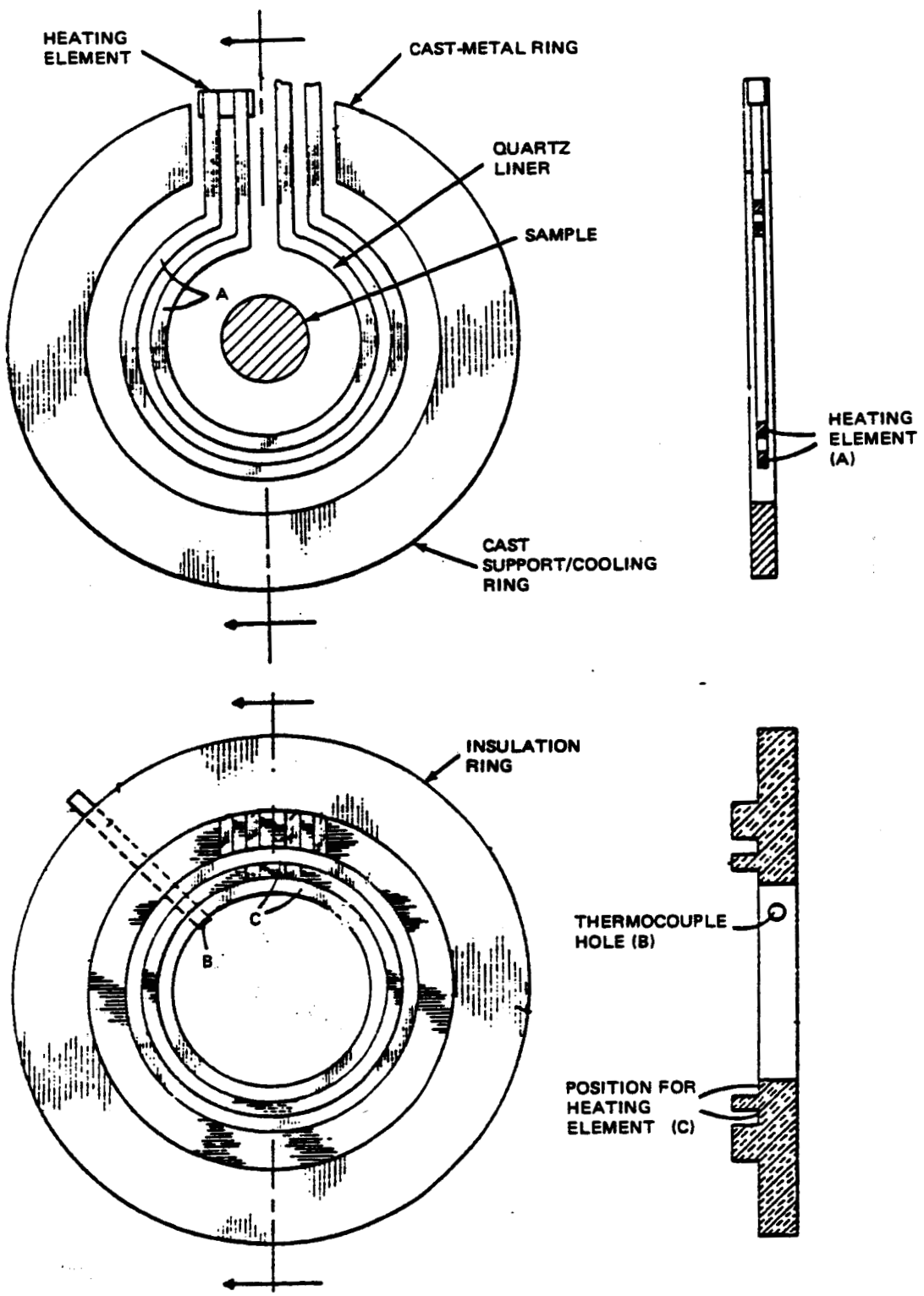
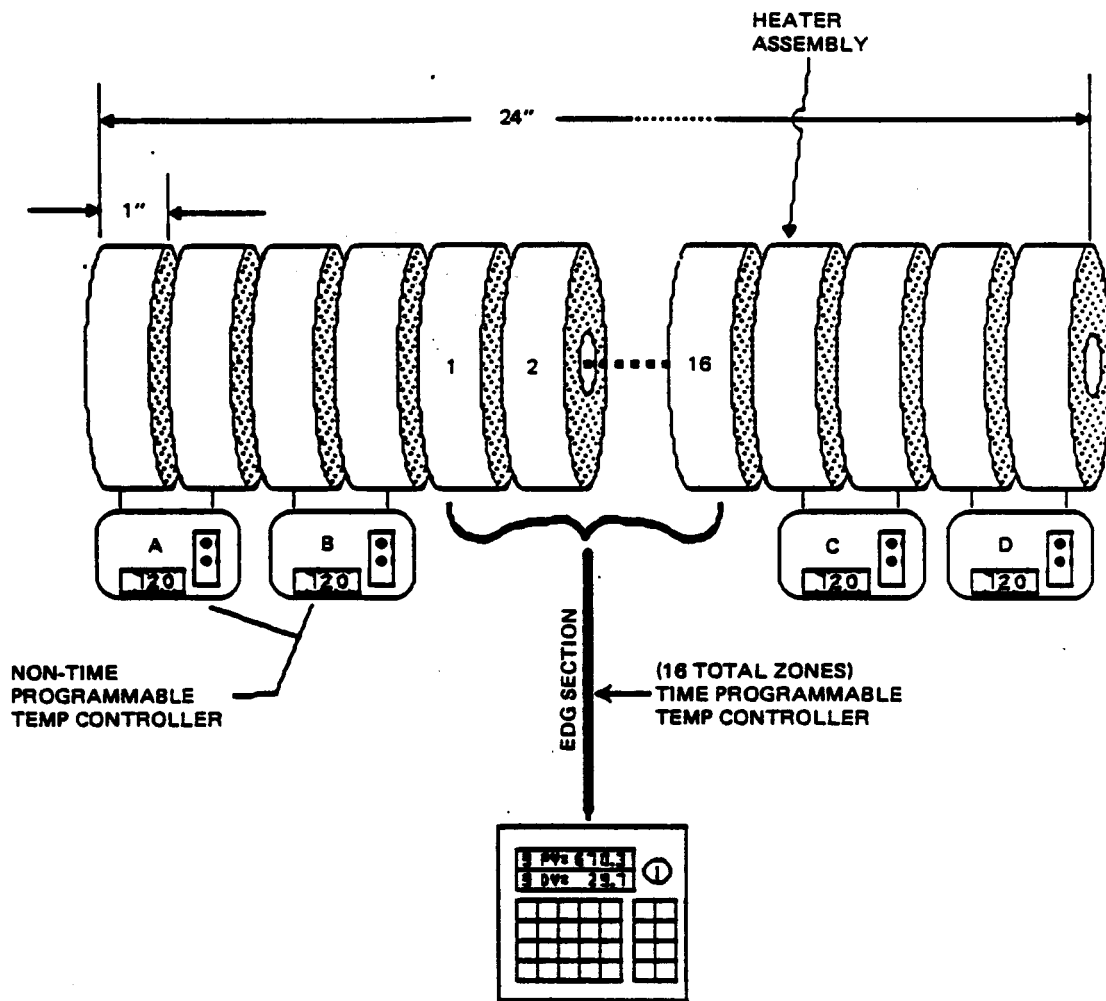


Fig. 3 Heating-element Assembly - U.S. Patent 4423516



P86-0332-006(T)

Fig. 4 Schematic of EDG Furnace Zone Arrangement

temperature-distance profiles can be created as a function of time. A modified Bridgman-type thermal profile history is shown in Fig. 5. The figure shows rapid heat-up, a melt-back sequence (for seeding), and then temperature gradient motion for directional solidification.

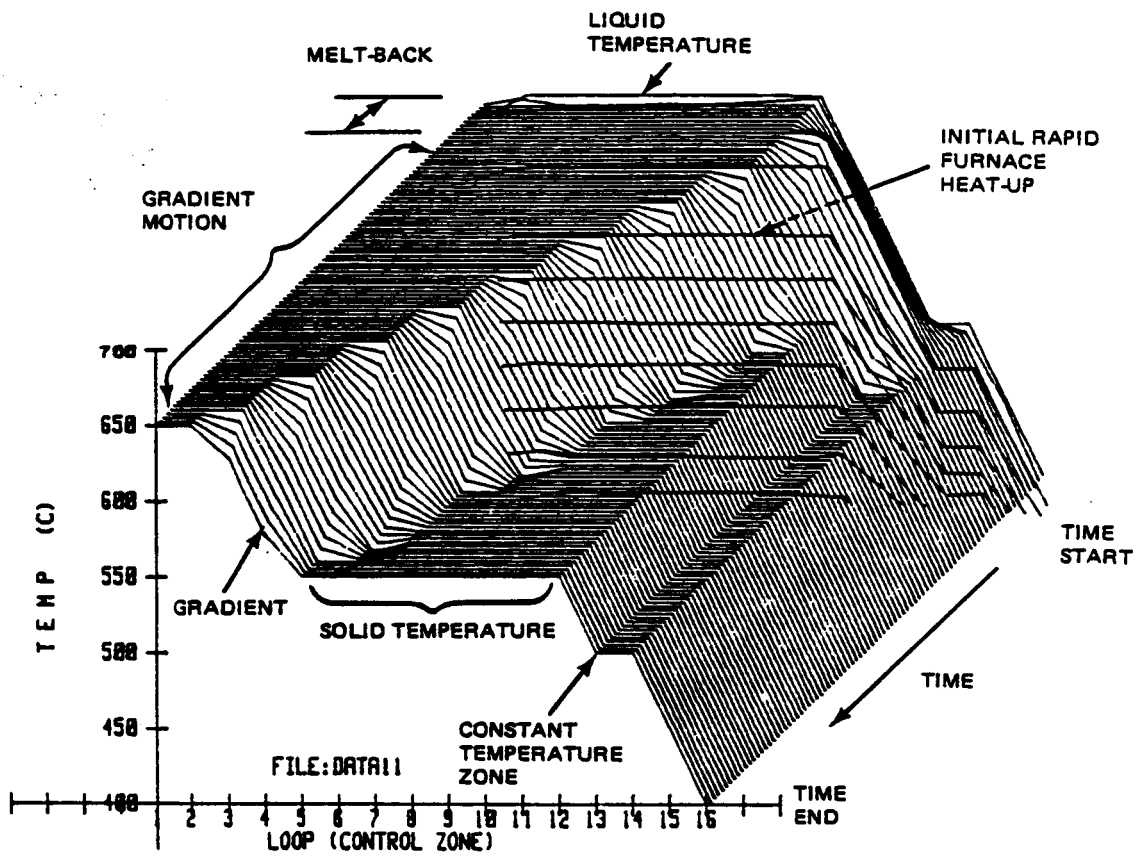
3.2.1 Hardware

The control system used for the EDG is a Micricon 823 digital process controller manufactured by Research Incorporated. The Micricon 823 uses a 2650A CPU (1.25 MHz) and operates using a conventional PID algorithm. The Micricon is configured to its maximum capacity of 16 control channels. The I/O process is divided between 8 I/O cards, with 2 control zones per card. The data update rate for each channel is approximately 4 seconds. Each channel is dedicated to the temperature control of one heating (control) zone. The furnace feed-back temperature is measured by thermocouples placed in contact with the sample (ampoule wall). Each control zone can be programmed to ramp linearly to or from a set-point temperature in a specified time, or to hold a constant temperature. Temperature control for the end (buffer) zones is provided by conventional Eurotherm 919 controllers. The manufacturer's specifications for the Micricon 823 are given in Table 1.

3.2.2 Temperature Control Algorithm

The PID control algorithm is represented in Fig. 6. The power directed to a control zone is determined by the proportional (P), integral (I), and derivative (D) control terms. The Micricon has the ability to adjust (linearize) the values of the P and I coefficients as a function of temperature based upon optimized coefficients at five points (0, 187, 375, 562, 750°C) within its span (0-750°C).

The proportional power contribution equals the temperature error (difference between the actual and the programmed temperature) multiplied by a proportional gain (K_p). Proportional power (pPower) alone cannot achieve the programmed temperature in a critically damped manner since pPower reduces to zero as the temperature error approaches zero. If a furnace is operated on proportional power alone, and because no furnace is adiabatic (there is always heat loss), the final temperature of the furnace will be somewhat less than the programmed temperature (Fig. 7a).

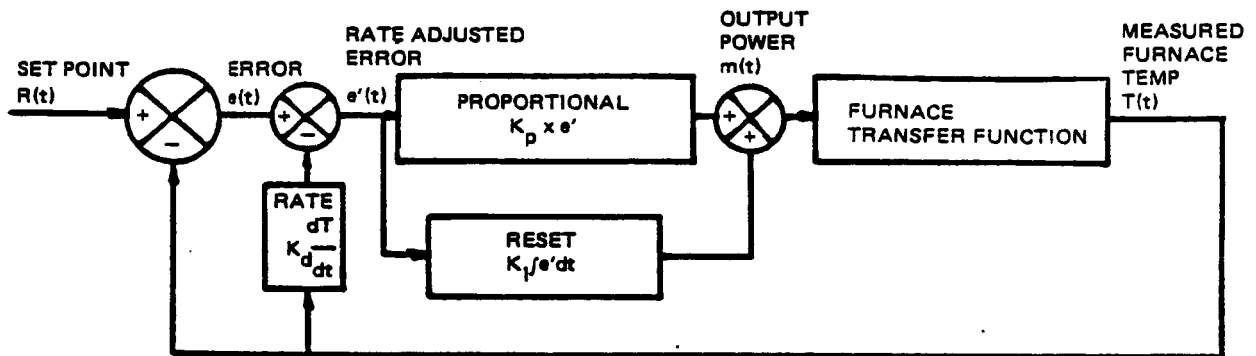


P86-0332-007(T)

Fig. 5 Modified Bridgman-type Directional Solidification Temperature Profile History as Programmed into the EDG System

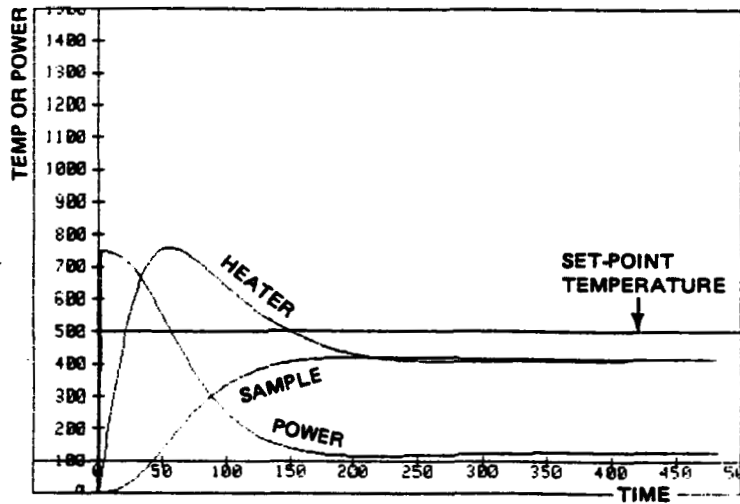
Table 1 Manufacturer's Specifications for Micricon 823

CONTROLLER SPECIFICATIONS											
INPUT:	OUTPUT:										
<p><u>LOOP PERFORMANCE</u></p> <p>MINIMUM INPUT SPAN: 10 mV</p> <p>MINIMUM INPUT IMPEDANCE: 1 MEG OHM – THERMOCOUPLE & mV</p> <p>10 OHMS: MA</p> <p>TEMPERATURE INFLUENCE: .01% OF SPAN/°C</p> <p>CONFORMITY: .1%</p> <p>COMMON MODE REJECTION: DC</p> <p>INPUT-TO-INPUT: 80 dB @ ± 10V, MAX</p> <p>INPUT-TO-OUTPUT: 120 dB @ ± 200V, MAX</p> <p>NORMAL MODE REJECTION: AC 50/60 Hz, 60 dB</p> <p>RESOLUTION: 12 BITS BINARY (.025%)</p> <p>ACCURACY: .15 ± .01% TYPICAL</p> <p>LINEARITY: .1%</p> <p>INPUT UPDATE TIME:</p> <table style="margin-left: auto; margin-right: auto;"> <thead> <tr> <th style="text-align: center;"><u># OF CONTROL LOOPS</u></th> <th style="text-align: center;"><u>UPDATE TIME</u></th> </tr> </thead> <tbody> <tr> <td style="text-align: center;">2</td> <td style="text-align: center;">1/2 SEC</td> </tr> <tr> <td style="text-align: center;">4</td> <td style="text-align: center;">1 SEC</td> </tr> <tr> <td style="text-align: center;">8</td> <td style="text-align: center;">2 SEC</td> </tr> <tr> <td style="text-align: center;">16</td> <td style="text-align: center;">4 SEC</td> </tr> </tbody> </table>	<u># OF CONTROL LOOPS</u>	<u>UPDATE TIME</u>	2	1/2 SEC	4	1 SEC	8	2 SEC	16	4 SEC	<p><u>OUTPUT SPECIFICATIONS</u></p> <p>CURRENT: 4 – 20 mA INTO 750 OHM MAX 1 – 5 mA INTO 3000 OHM MAX</p> <p>VOLTAGE: 0 – 5 VDC INTO 500 OHM MIN 0 – 10 VDC INTO 500 OHM MIN</p> <p>TIME PROPORTIONAL: SOLID STATE RELAY RATED 3A @ 120 VAC RESISTIVE</p> <p>ALARM: SSR RATED, 3A @ 120 VAC RESISTIVE</p> <p><u>OUTPUT PERFORMANCE SPECIFICATIONS</u></p> <p>OPTICAL ISOLATION FROM LOGIC & INPUTS</p> <p>RESOLUTION: 10 BIT BINARY (.1%)</p> <p>SPAN ACCURACY: .5%</p> <p>TEMPERATURE INFLUENCE: –.05%/°C</p> <p><u>CONTROL PARAMETERS</u></p> <p>GAIN: 0 – 64.12</p> <p>RESET: 0 – 60.23 PER MIN</p> <p>RATE: 0 – 8.5 MIN</p> <p>OUTPUT LIMITING: –100 TO +100% (INDEPENDENT MIN/MAX ADJUST)</p>
<u># OF CONTROL LOOPS</u>	<u>UPDATE TIME</u>										
2	1/2 SEC										
4	1 SEC										
8	2 SEC										
16	4 SEC										
R86-0332-002(T)											

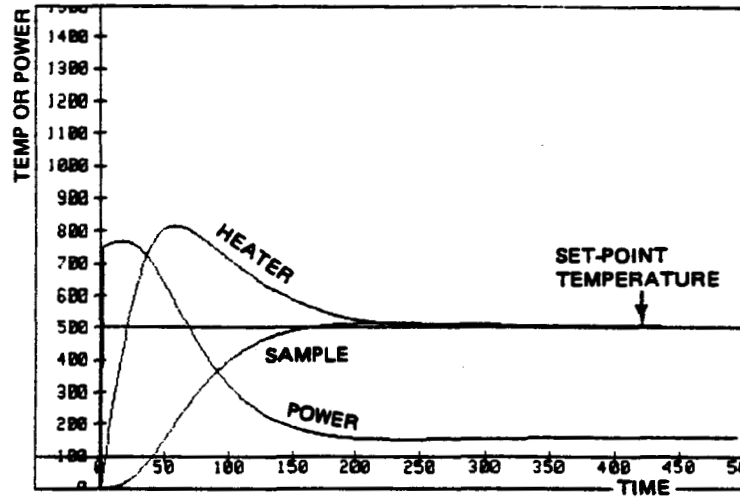


P66-0332-008(T)

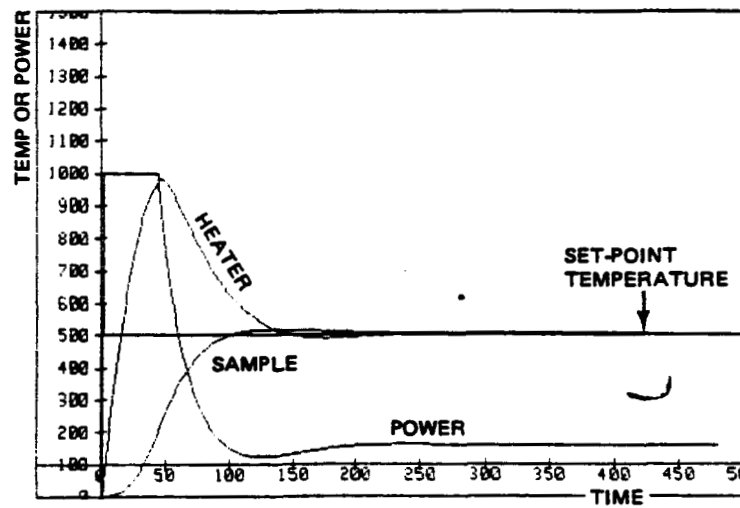
Fig. 6 Block Diagram of PID Algorithm



(a) PROPORTIONAL CONTROL



(b) PROPORTIONAL & INTEGRAL CONTROL



(c) PROPORTIONAL, INTEGRAL & DERIVATIVE CONTROL

P86-0332-009(T)

Fig. 7 Computer-Model Furnace Response Using Proportional, Integral, & Derivative Control

In order to correct for the temperature deviation associated with pPower, the integral (I) coefficient is used. The integral power (iPower) is equal to the cumulative error since the start of the process multiplied by the integral gain (K_i). Although the iPower term can be used alone to reach the programmed temperature, the combination of the two terms (iPower + pPower) results in a more rapid establishment of the programmed temperature. In a constant-programmed-temperature furnace with a nonvarying environment, the iPower term will be equal to the amount of steady state furnace heat (energy) lost to the environment (Fig. 7b).

In order to achieve the programmed temperature as rapidly as possible using the P and I terms, the P and I coefficients are often set such that the furnace temperature overshoots the programmed temperature. The derivative (D) term attempts to anticipate the overshoot by adjusting the error signal according to its rate of change (Fig. 7c). The derivative (or rate) adjusted error value is equal to the nonderivative-adjusted error minus the quantity of the derivative gain (K_d) times the rate of temperature change. In practice, the derivative term is limited to gross error anticipation. The derivative's sensitivity to noise makes it unusable for precise temperature control. As a result, the K_d coefficient is often set to a very low value.

The gain values for P, I and D for the test furnace are experimentally determined in the tuning process. For more information on PID see Ref 2.

4 - EXPERIMENTAL METHOD

The evaluation of the EDG furnace is divided into three parts.

- o Electronic control - computer hardware and software
- o Thermal control - static and dynamic heat flux and power
- o Crystal growth - directional solidification.

4.1 ELECTRONIC CONTROL

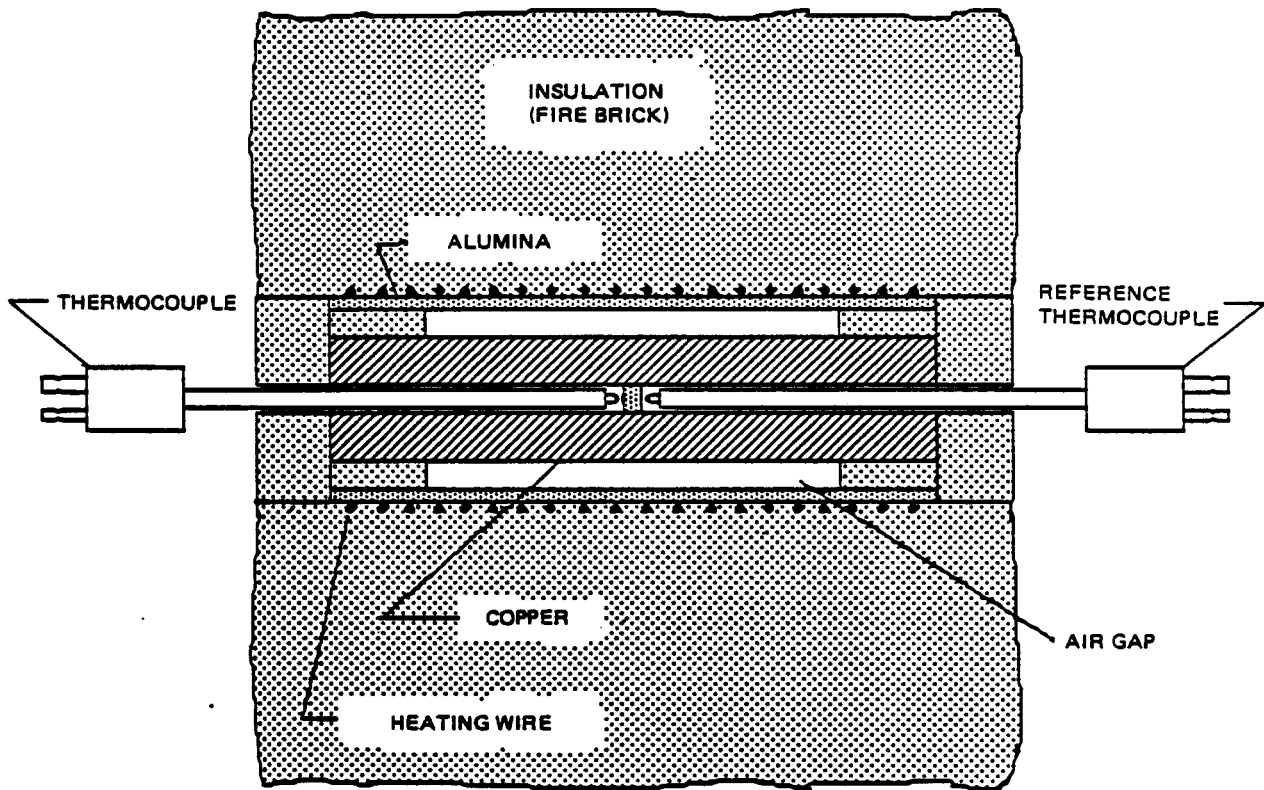
The electronic accuracy of the system was measured. Thermocouple accuracy was measured by the comparison of each thermocouple with a reference thermocouple in a specially constructed isothermal furnace (Fig. 8). The analog to digital converter (A/D) accuracy was measured by replacing the thermocouples with a Leeds and Northrup precision potentiometer. For the evaluation of electrical noise, a constant temperature source at room temperature was simulated by allowing a 0.5 in. diameter stainless steel rod within the unpowered EDG furnace to come to equilibrium for at least 20 hours.

4.2 THERMAL CONTROL

Thermal profile experiments were designed to study the thermal characteristics of the furnace. The experiments can be classified as:

- o Ramp rate effects - the dynamic dependence of accuracy on the rate of temperature change
- o Steady state stability - static time and location dependent accuracy
- o Thermal balance - axial and radial heat transfer within the furnace
- o Bridgman-type temperature gradient motion - effect of discrete furnace zone design and gradient motion stability
- o Nonbridgman-type temperature profiles - demonstrate temperature profiles of interest to NASA.

The influence of sample conductivity was studied by the use of dummy samples. Samples used were: a copper rod (inside a quartz tube), a stainless steel rod (without a quartz tube), and an empty quartz tube. The stainless steel rod was instrumented with three thermocouples spaced 1.0 in. apart, placed in holes drilled into the center line of the rod. This enabled the measurement of the sample center line temperature.



P86-0332-012(T)

Fig. 8 Isothermal Furnace for Thermocouple Testing

4.3 DIRECTIONAL SOLIDIFICATION

Directional solidification experiments were performed on BiMn eutectic samples with a diameter of 0.380 in. and a length of between 3 and 4 in.

Quartz ampoules (0.482 in. OD) of the design previously referred to (Ref 3) were used. Thermocouples and/or Peltier lead wires are incorporated into the ampoules for temperature and interface monitoring. The closed ampoules were inserted into a quartz guide-tube with a measured inside diameter of 0.520 in. and a wall thickness of 0.036 in.

4.4 FURNACE SET-UP

In the as-received condition, the zone-control thermocouples were found to be incorrectly connected. After proper thermocouple connection, the PID coefficients were obtained by tuning for best furnace response. These values and the general effect on furnace performance by each term are listed in Table 2.

The Mellen Company recommended sample diameters no larger than approximately 0.5 in. A sample size smaller than the bore of the furnace is needed to provide a physical gap between the sample and the furnace wall. The gap of 0.25 in. was recommended to smooth out the transition effect between zone due to the discrete heating zone construction of the furnace. A water pressure regulator was added to steady flow rate at approximately 1.5GPM.

4.5 DATA ACQUISITION

The data acquisition system used in the analysis of the furnace was a HP9836C microcomputer. The software was developed internally. Data was transmitted to the HP9836C from the Micricon through an RS232 connection. The data was then displayed in real-time and stored for analysis. Once stored, the data could be processed for further studies. Analyzed data was displayed under various screen formats. These formats incorporated parameters of: time (t), zone number (X), temperature (T), rate of temperature change (dT/dt), local temperature gradient (dT/dX), deviation from set-point, power, average power, and d^2T/dt^2 . The use of colors for zone identification in the computer monitor enabled the display of all zones on any one screen. When furnace parameters were displayed as a function of time, the display could be

Table 2 PID Coefficients for EDG Furnace

PROPORTIONAL	TEMPERATURE (C)				EFFECT ON SYSTEM
	187	375	562	750	
P	5	24	50	64 (MAX)	LARGE P MAKES SYSTEM MORE RESPONSIVE BUT CAN CAUSE OSCILLATIONS. SYSTEM SHOULD BE SET TO AS HIGH A P AS POSSIBLE. P ALONE CANNOT ACHIEVE SET-POINT TEMPERATURE DUE TO HEAT LOSS.
CONSTANT VALUES AT TEMPERATURES					
INTEGRAL	TEMPERATURE (C)				EFFECT ON SYSTEM
	187	375	562	750	
I	0.5	2	4	12	LARGE I MAKES SYSTEM MORE STABLE, BUT REDUCES SYSTEM RESPONSE TIME. AVOID LARGE I WHERE TEMP RAMPING IS NEEDED, SUCH AS DURING GRADIENT MOTION. I IS NEEDED TO REACH SET-POINT TEMPERATURE. POWER DUE TO THE I TERM EQUALS THE STEADY-STATE HEAT LOSS.
CONSTANT VALUES AT TEMPERATURES					
DERIVATIVE	TEMPERATURE (C)				EFFECT ON SYSTEM
	187	375	562	750	
D	0.05	0.05	0.05	0.05	D IS USED ONLY TO PREVENT GROSS OVERSHOOT CONDITIONS. D IS TOO SENSITIVE TO NOISE, THUS NOT USEFUL FOR DIRECT CONTROL.
CONSTANT VALUES AT TEMPERATURES					

THESE ARE TYPICAL VALUES FOR STAINLESS STEEL SAMPLE. THE SPECIFIC VALUES DEPENDED ON GRADIENT MAGNITUDE. PROPORTIONAL CONSTANTS ARE INCREASED FOR HIGH CONDUCTIVITY SAMPLE, AND LARGE TEMPERATURE GRADIENT CONDITIONS. INTEGRAL CONSTANTS CAN BE INCREASED FOR MORE STABILITY UNDER SLOW GRADIENT MOTION CONDITIONS.

R86-0332-003(T)

rapidly or slowly sequenced (forward or backward) through time for review. The figures shown in this report are derived from the data analysis program, the colors, however, are missing.

5 - EDG PERFORMANCE EVALUATION

The multizone furnace design can be thought of as a series of thermally interconnected furnaces controlled by a microcomputer. The performance limits of the EDG furnace system were defined by two independent factors:

- o Control system limits
- o Heat transfer limits.

The control system determined the overall temperature resolution and accuracy. This accuracy depends on sensors, electronic hardware and software factors. Heat flow, as determined by the rate of heat gain and the rate of heat loss, defined the limits of both static and dynamic thermal behavior. Heat flow was in the axial and/or the radial direction, and was influenced by the furnace's physical design and the sample within the furnace.

5.1 CONTROL LIMITS

Results of the control system accuracy evaluation are summarized in Table 3.

5.1.1 Thermocouples

Temperature accuracy was critical to the EDG for the generation of the temperature gradient and its motion. When new, thermocouples can be quite accurate. Testing of 20 new type K thermocouples showed a total deviation less than $\pm 0.1^\circ\text{C}$ at 200°C . After over 100+h of use at various temperatures between 200 to 750°C , they showed a deviation range of $+1.3$ to -0.6°C at 200°C and $+1.3$ to -0.8 at 700°C . The inability to determine the exact temperature at a location (zone) prevented the establishment of an exact gradient. The temperature gradient established was as good as the measured temperature used to produce that gradient. The absolute accuracy limit of thermocouples is typically $\pm 1.1^\circ\text{C}$ or 0.4 % whichever is greater for type K thermocouples (Ref 4). To a certain extent when establishing a temperature gradient in the EDG furnace, absolute accuracy is not needed. What is required is that all thermocouples be true, relative to each other. But, because of unpredictable thermocouple drift on aging, there does not appear to be any simple method to ensure relative accuracy. Thermocouple temperature accuracy can be improved only with constant calibration.

Table 3 Control System Accuracy

THERMOCOUPLE ERROR			
ABSOLUTE	$\pm 1.1^{\circ}\text{C}$ OR 0.4%	WHICHEVER IS GREATER	REF 3
RELATIVE	$\pm 0.1^{\circ}\text{C}$ (NEW)	$\pm 1.0^{\circ}\text{C}$ (100h+)	MEASURED
COMPUTER A/D ERROR			
PER A/D CARD	$\pm 0.15^{\circ}\text{C}$	BETWEEN THE TWO CHANNELS ON CARD	MEASURED
BETWEEN A/D CARD	$\pm 1.0^{\circ}\text{C}$	ROOM TEMPERATURE COMPENSATION ERROR BETWEEN CARDS	MEASURED
COMBINED SYSTEM ERROR			
ABSOLUTE	± 2.25 (BEST)	$\pm 4.15^{\circ}\text{C}$ (WORST)	CALCULATED FROM ABOVE
RELATIVE	$\pm 1.25^{\circ}\text{C}$ (BEST)	$\pm 2.15^{\circ}\text{C}$ (WORST)	CALCULATED FROM ABOVE

R86-0332-001(T)

5.1.2 Electronic Hardware

The Micricon 823 had a temperature display resolution of $\pm 0.1^\circ\text{C}$. In reality, each I/O card could not distinguish a temperature change with a certainty of greater than $\pm 0.25^\circ\text{C}$. This limit was set by the resolution of the signal processing (wiring and amplifier noise) and A/D converter resolution, as shown in Fig. 9. In order to resolve $\pm 0.1^\circ\text{C}$ in a range of 0 to 750°C , an A/D converter of at least 13-bit (1/8192 resolution) was needed. The Micricon's 12-bit A/D at best yielded only 1/4096 or 0.25% ($\pm 0.18^\circ\text{C}$ in 750°C) resolution.

Another source of temperature error was in the cold junction compensation. Between the 8 I/O cards, the maximum deviation was found to be $\pm 1.0^\circ\text{C}$. These errors resulted from the inconsistent room temperature compensation between I/O cards and were measured directly after calibration.

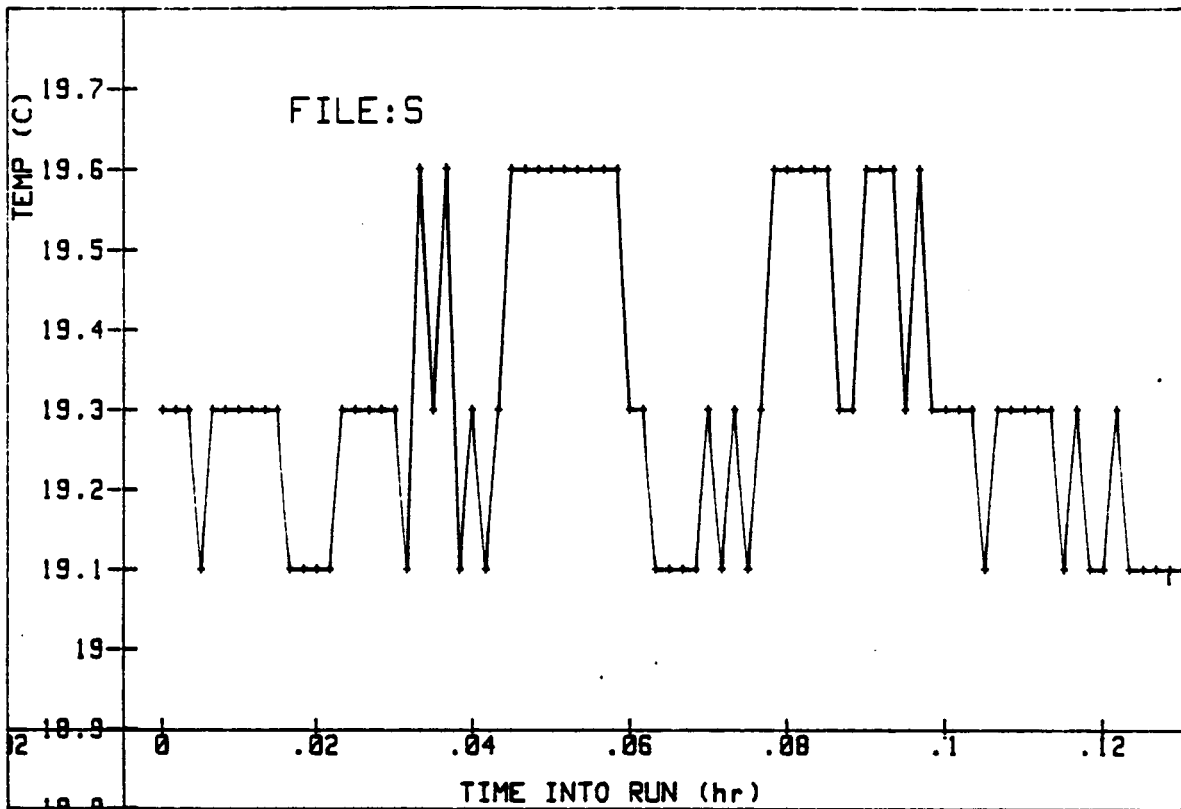
5.1.3 Controller Software

The PID algorithm was designed for static, noninteracting, furnace temperature control. The use of the PID algorithm for control during temperature ramping, although possible, failed to take into account the time (rate) dependent nature of dynamic temperature changes. The integral (I) term within the PID algorithm did not take into consideration the difference between a steady state or a dynamic $[d(\text{programmed temperature})/d(\text{time}) \neq 0]$ condition. As a result, deviation from the programmed temperature was lowest at steady state, and worsened as the rate increased. This is illustrated in Fig. 10 for different programmed heating and cooling rate changes.

The algorithm also did not consider the thermal interaction between neighboring control zones. When a zone was near a temperature gradient, the extra heat flux received is not anticipated, resulting in poor control. The poorest control, therefore, occurred during the most critical portion of the process, that involving the gradient and its motion. Most of these hardware and software shortcomings can be corrected with a new control system.

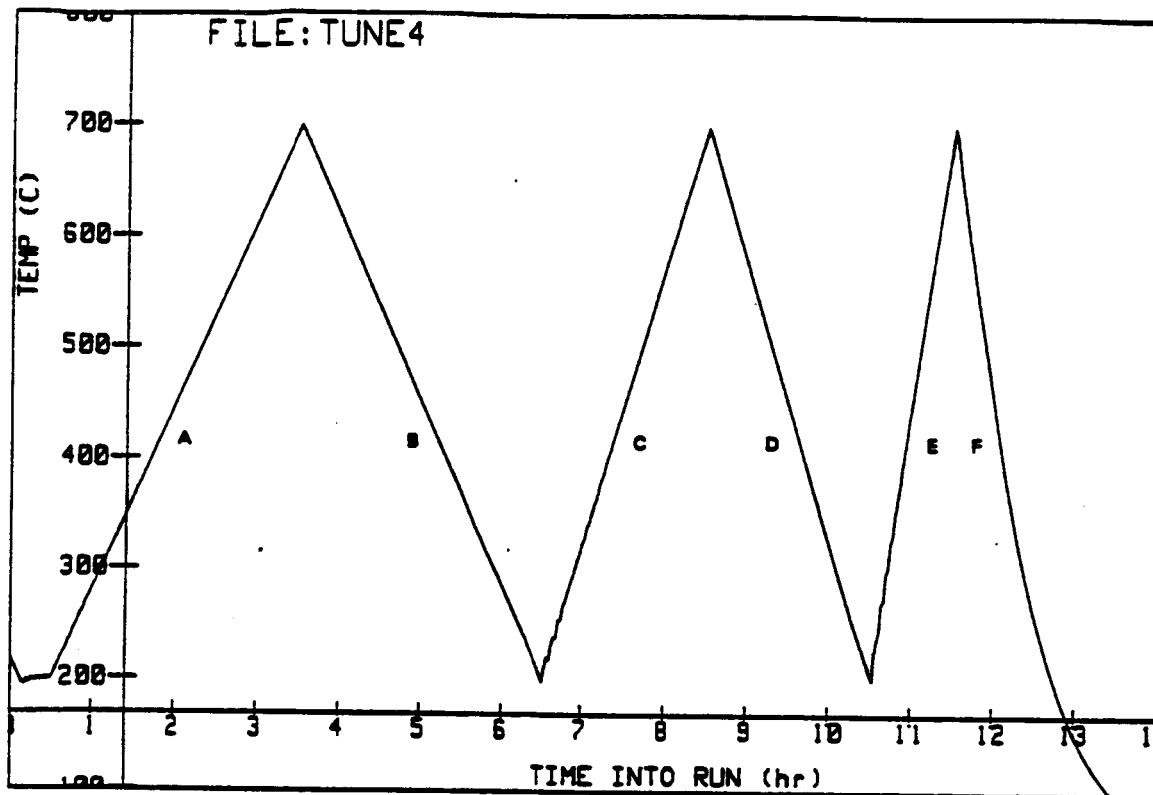
5.2 HEAT TRANSFER LIMITS

The heat transfer in the EDG furnace can be characterized by describing the radial and axial components of heat transfer.

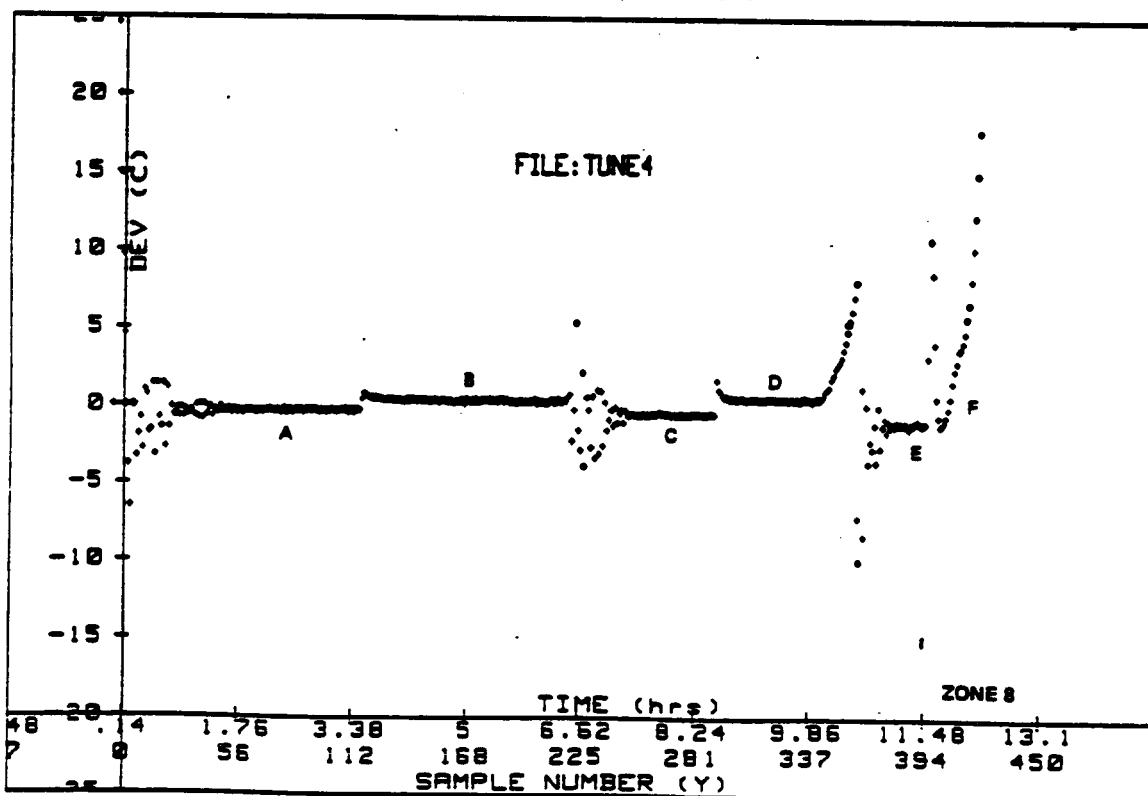


P86-0332-013(T)

Fig. 9 Variation of Temperature Measurement System



TIME-TEMPERATURE TESTING HISTORY



P86-0332-014(T)

Fig. 10 Dynamic Temperature Tracking Error as Shown by Deviation from the Programmed Temperature during Ramping

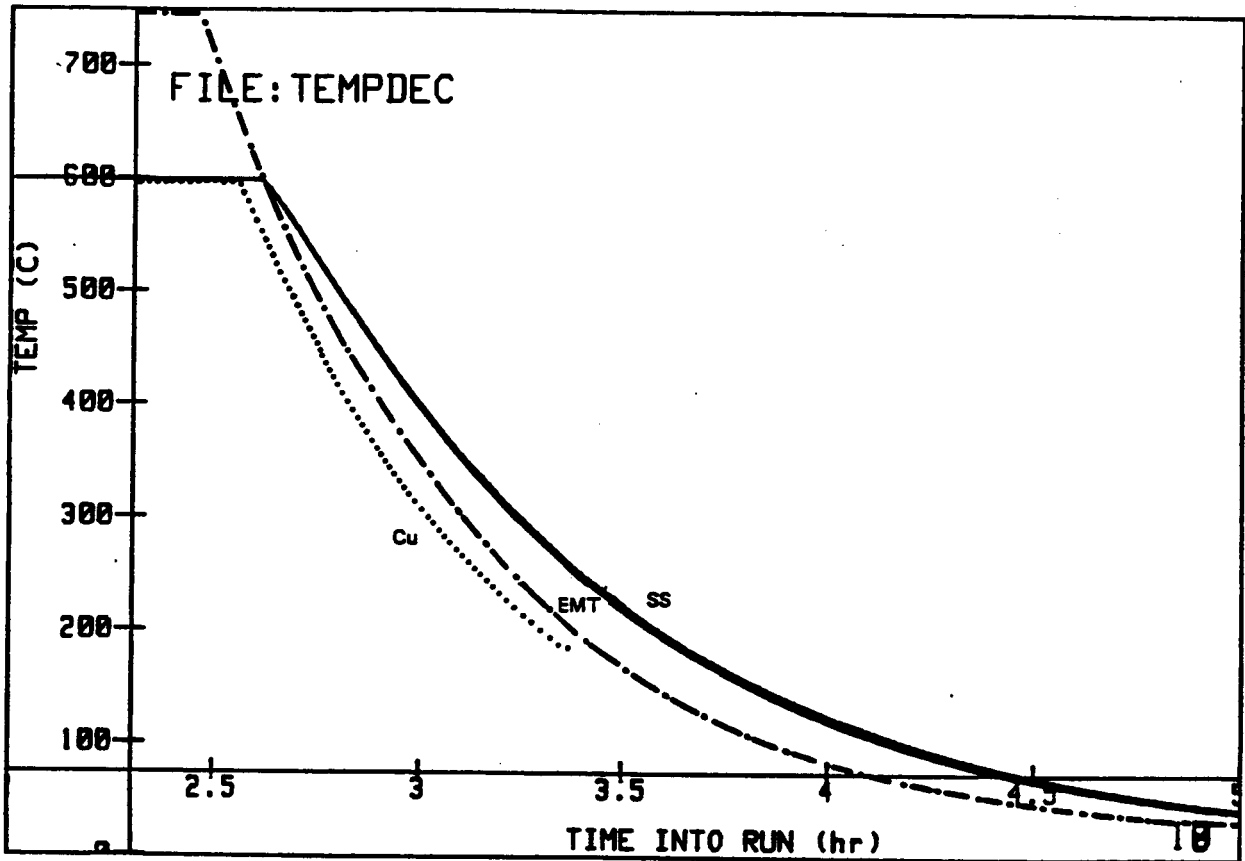
5.2.1 Radial Heat Flow

Heat flow from the EDG furnace to the environment is needed to reduce temperature. In the absence of axial heat flow, radial heat loss is necessary. Water cooling, combined with the design of the heating-element assembly provides the high radial heat-loss characteristic in the EDG furnace. The radial heat loss of the furnace was found to be insensitive to the sample type. Figure 11 shows the temperature/time decay of the furnace with different sample materials. The measured time constant (the time needed to drop to 36.8% of the initial value) of the furnace was approximately between 0.3 and 0.4 hours. The insensitivity of the decay time to the sample type is a result of the significantly greater thermal mass of the hot components of the furnace as compared to the thermal mass of sample. For example, the thermal mass contribution by a 0.5 in. diameter sample per zone (one inch in length), is only approximately 1/6 of the thermal mass contribution of the furnace heating elements used in that zone (see Fig. 3). Thus, the rate of temperature decrease (dT/dt) as a result of radial heat flux was insensitive to the sample type within the furnace and was proportional to temperature up to approximately 500°C (Fig. 12). Above 500°C, the slope increased due to increased radiative effects. The radial heat loss at constant temperature (steady state) is equal to the steady-state power consumption given in Section 5.3.

This condition of radial heat loss being almost independent of the sample will not be expected for larger EDG furnace designs. At some larger furnace bore size, the mass contribution of the sample will equal that of the heating elements. Based on the same heating element diameter, a 0.25 in. sample-to-furnace liner gap, and a one inch zone length, the cross-over point would be expected to occur at a furnace diameter of approximately 1.5 in. Furnaces greater than this diameter should have sample sensitive radial thermal behavior.

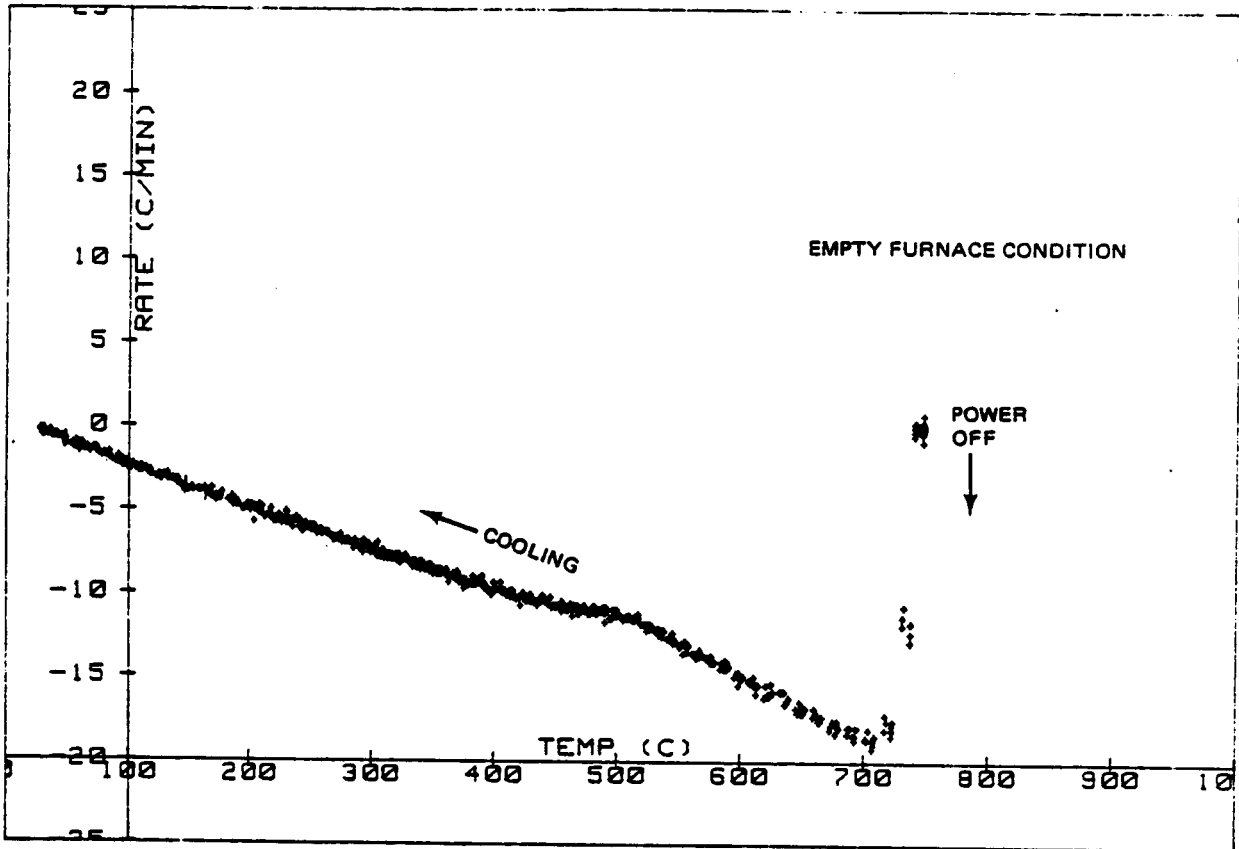
5.2.2 Axial Heat Flow

Axial heat flow will only occur within an axial temperature gradient. When an axial gradient exists in the EDG furnace, the axial heat flow occurs in the sample and furnace. The magnitude of axial-sample heat flux was governed by the size and thermal conductivity of the solid sample material and the magnitude of the temperature gradient. Axial heat flow is dependent only



P86-0332-010(T)

Fig. 11 Natural Temperature Decay (Cooling Curves) of the EDG Furnace with Various Sample Types



R86-0332-011(T)

Fig. 12 Rate of Temperature Decrease (dT/dt) vs Temperature

on gradient magnitude and is independent of the length of the temperature gradient. Based upon the 0.5 in. diameter sample size, the calculated axial heat flux is plotted in Fig. 13 as a function of temperature gradient and material type. The background values were experimentally determined.

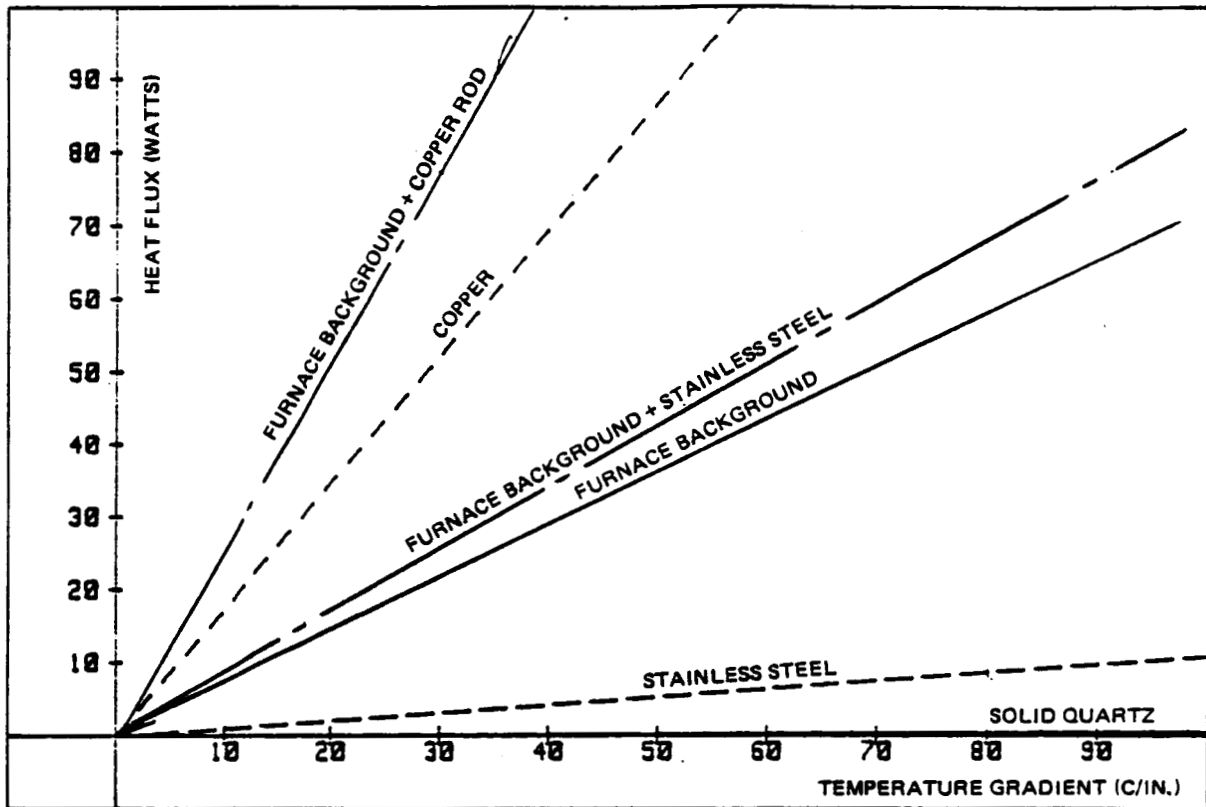
To illustrate the effect of sample thermal conductivity on axial heat transfer, half the length of the furnace was set to a constant high temperature while the other half was turned off. When empty, the furnace showed a background amount of axial heat transfer (Fig. 14). This background amount was due to thermal convection and conduction inside the furnace. When loaded, the axial heat flux was influenced by the thermal conductivity of the sample material. The copper sample produced a greater axial heat flux than the stainless steel sample, as indicated by the lower temperature gradient established by the copper. The inability to carry away the increased axially transferred heat (of the higher conductivity sample) by the unpowered zones (because radial heat loss is limited) resulted in a lower temperature gradient. A nonlinear temperature decay profile is generated as each successive unpowered zone removed less heat in the radial direction.

5.3 POWER CONSUMPTION

Time-proportioned (duty cycle) power control was used in the EDG furnace. The power was pulsed (on-off) to the heating elements at a rapid rate such that an average power level was achieved over time.

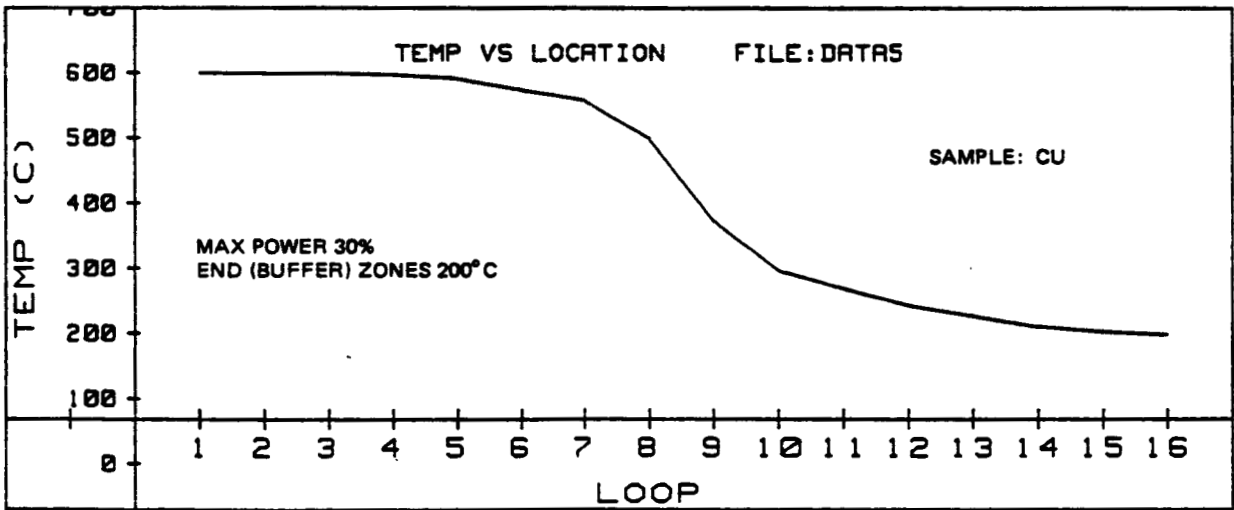
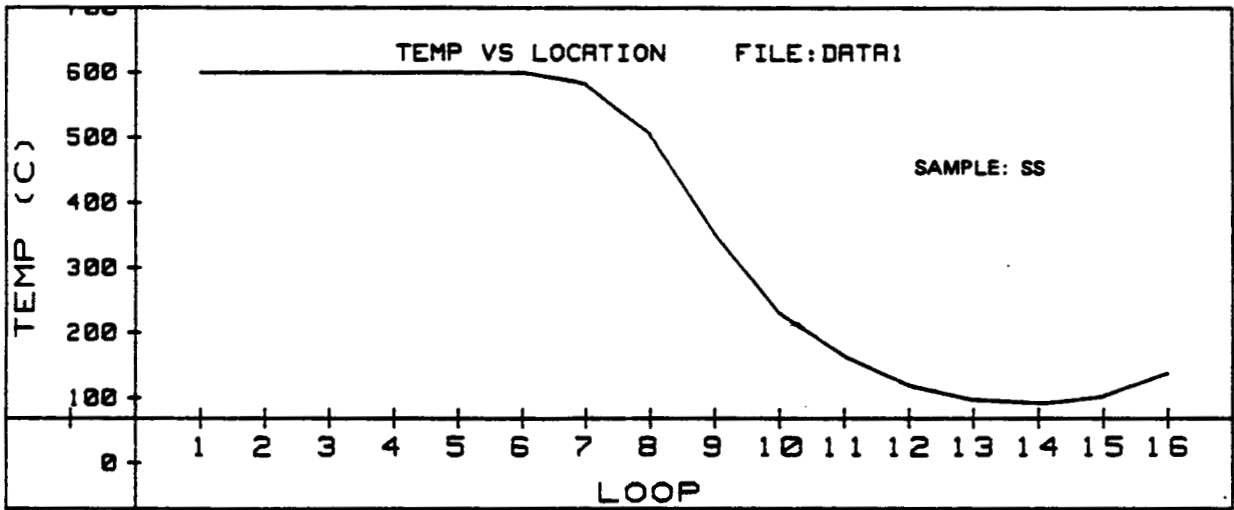
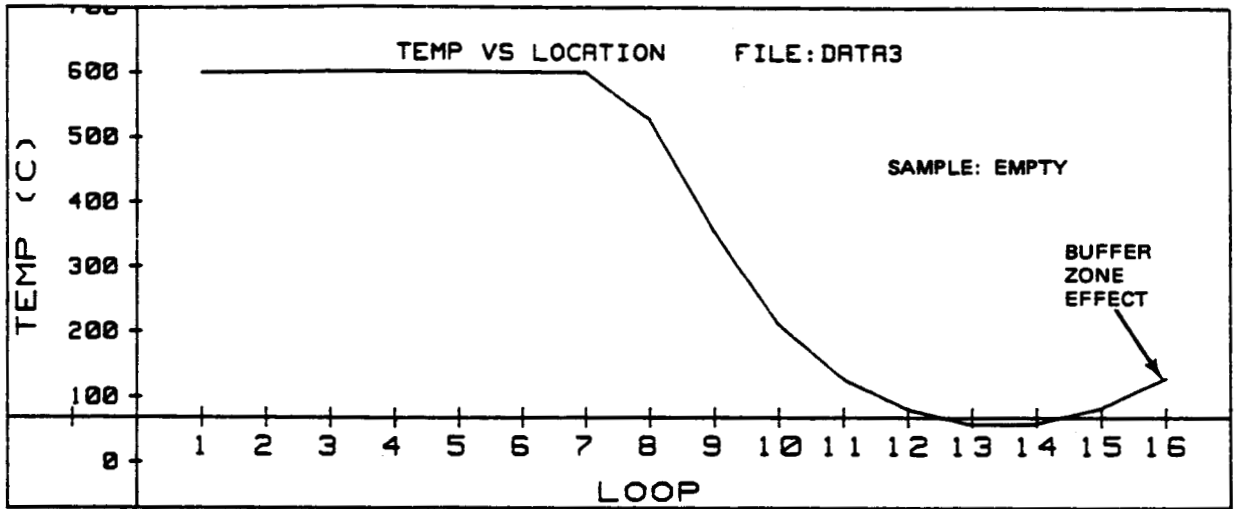
At full power, each heating element required 132 watts. With 2 heating elements per zone, each zone required 264 watts. Overall, the furnace with a total of 48 elements required 6.3 kw. This was based on a measured voltage at the heating element of 2.2 Vac and a measured element current of 60 amps during full (100%) furnace power. Since power was time proportioned, the power demand per zone when energized was always 264 watts. There is no reason (other than cost) why other power control methods, such as voltage proportionation, cannot be used to reduce peak-power demand.

The difference between the energy input (heat gain) and energy output (heat loss) is equal to the change in the internal energy. Internal energy change is reflected by either a state change (ie. solidification or melting),



R86-0332-015(T)

Fig. 13 Calculated Axial Heat Flux for a 0.5 in. Diameter Rod vs Temperature Gradients



R86-0332-016(T)

Fig. 14 Maximum Achievable Furnace Temperature Gradient with Indicated Samples

or a temperature change. As stated earlier, without axial thermal gradients the performance of the furnace was not very sample-type dependent. The power needed to achieve furnace temperatures are plotted in Fig. 15. The values plotted are equal to the steady-state, radial heat loss at temperature. Water cooling flow rate changes did not measurably change the power. In Fig. 15 the power levels for zones 1 and 16 are higher because of the axial heat loss at these zones due to their proximity to the lower temperature end buffer zones (set at 200°C). Zones 2 and 15 are affected by zones 1 and 16. Typical power at 700°C was approximately 70 watts per in. (radial heat loss only).

5.4 VIBRATIONS

At high power output, a small but noticeable humming occurred in the base unit of the EDG that houses the power transformers. Since the base was mechanically connected to the furnace section, the humming was also felt at the furnace. Under the same high power output condition, a noticeable vibration was also generated at the heating elements. Since high power was only needed for a very rapid positive temperature change, these vibrations were not felt under normal operating power levels. The extent of this vibration that was transmitted to the sample was not investigated.

5.5 TIME-TEMPERATURE STABILITY

In a real furnace, even in a programmed constant temperature condition, due to fluctuations in environment and the finite resolution of any control system, small temperature fluctuation within the furnace can occur. These environmental changes include changes in power-line voltage, room temperature and coolant (water) temperature or flow rate.

For example, if the amount of energy delivered to the heating element when set to 10% power changed due to power line voltage variations, then the achieved temperature within the furnace will also change (until the control system makes a correction). Variations in incoming line voltage will cause variations in real power output because no further voltage regulation is performed by the system. In the laboratory, the line voltage is regulated to 8% (by Grumman). The power variation will be a square function of the line voltage variation since:

$$\text{Power} = \text{Voltage}^2 / \text{Resistance} \quad (2)$$

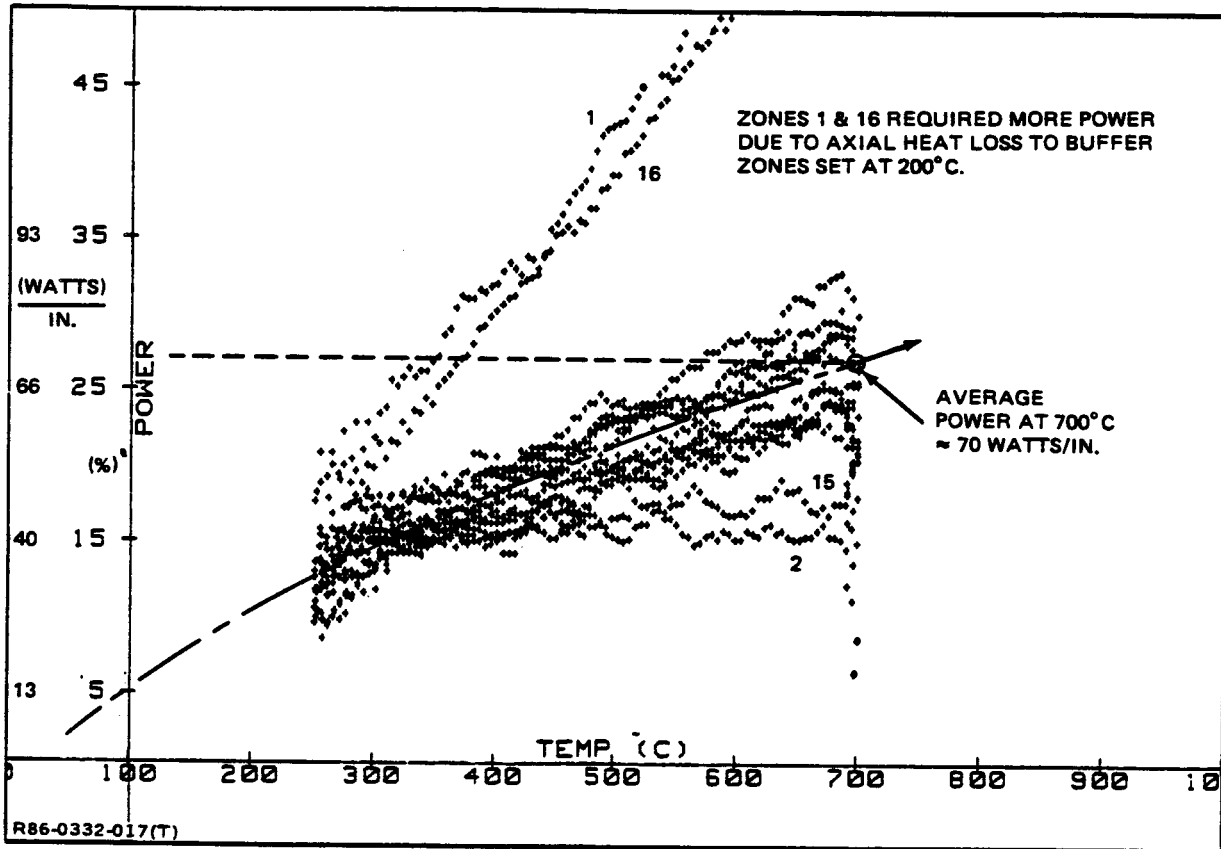


Fig. 15 Average Furnace Power at Temperature Without Axial Heat Flux

Runs at constant power (with no temperature control) had shown variations in achieved temperatures (Fig. 16). The exact reason for the furnace temperature change at constant power is not clear. It most likely is a combination of room temperature change and line voltage change. A line voltage regulator, along with better room temperature control, can lessen these variations. Coolant flow regulation was improved with a flow pressure regulator. The extent of environmental influence depended on the furnace operation temperature.

At high temperatures, greater natural heat loss improved the overall controllability of the furnace. Conversely, the accuracy of the furnace was poorer at lower temperatures. Figure 17 shows the deviation from the programmed temperature as a function of furnace temperature for two different tuning conditions. Furnace controllability noticeably improved at temperatures above 400°C. If properly tuned for low temperature operation, the errors at low temperatures can be reduced, but not as low as at high temperature levels. Under steady state at high temperatures, the controller can control the temperature as read by its control thermocouple to within $\pm 0.2^\circ\text{C}$ (true resolution limit of the control system), as shown in Fig. 18a for high temperatures above approximately 400°C. Fig. 18b shows the steady state error at low temperature. Note that in this condition the power output resolution becomes a problem at low temperatures.

5.6 AXIAL-TEMPERATURE VARIATIONS

When empty at 700°C, observation of the EDG quartz furnace liner showed a zebra stripe appearance, evidence of the discrete-zone nature of the EDG furnace. These bright-to-dark bands, indicative of temperature variations, did not correspond to the interheating-element assembly spacing (0.5 in.). The number of stripes were less than the number of heater assemblies. The exact relationship between the observed spacing and furnace design is not known, but one possible cause could be nonuniform furnace construction. Axial temperature variations at the furnace liner were measured with a surface thermocouple over a random 2 in. furnace length near the middle of the furnace. The results indicated no temperature fluctuation as a function of heating element spacing, but rather variations of a larger and uneven

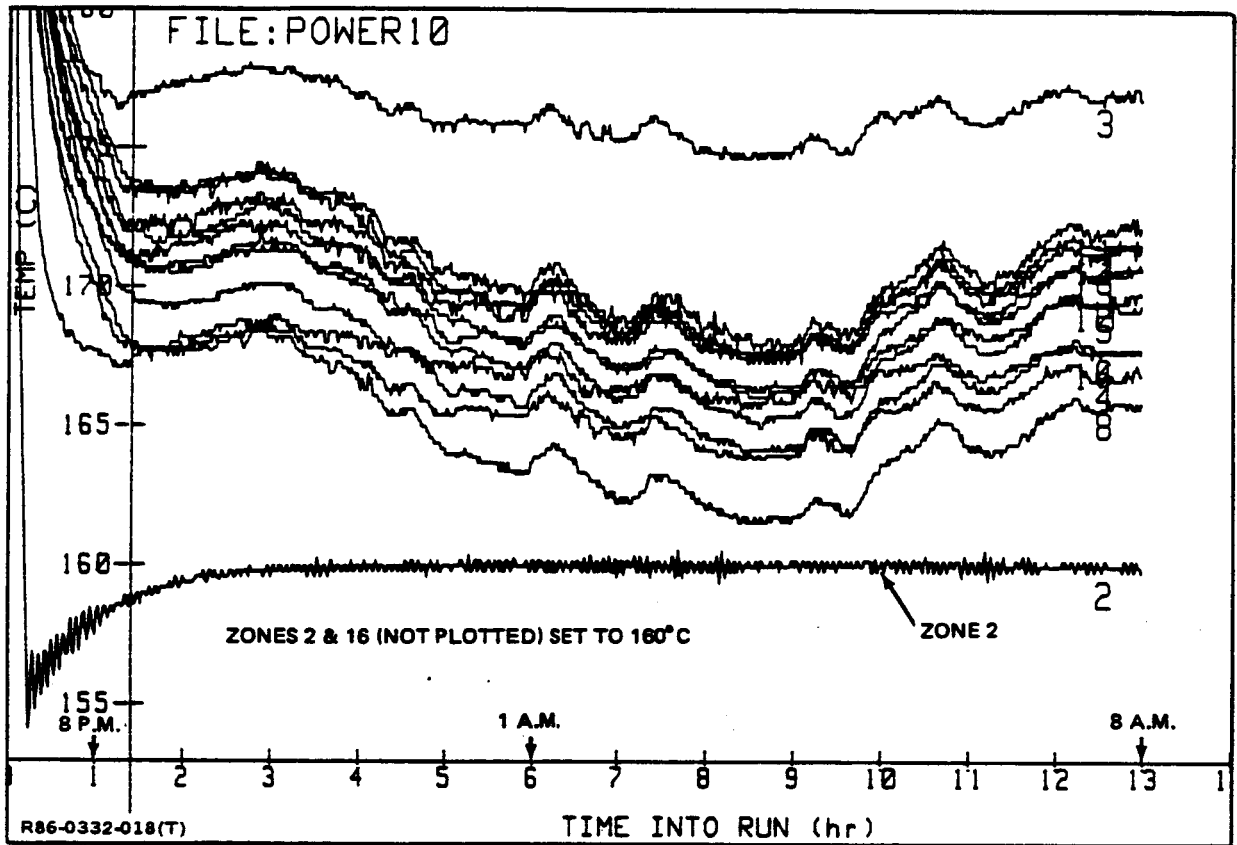
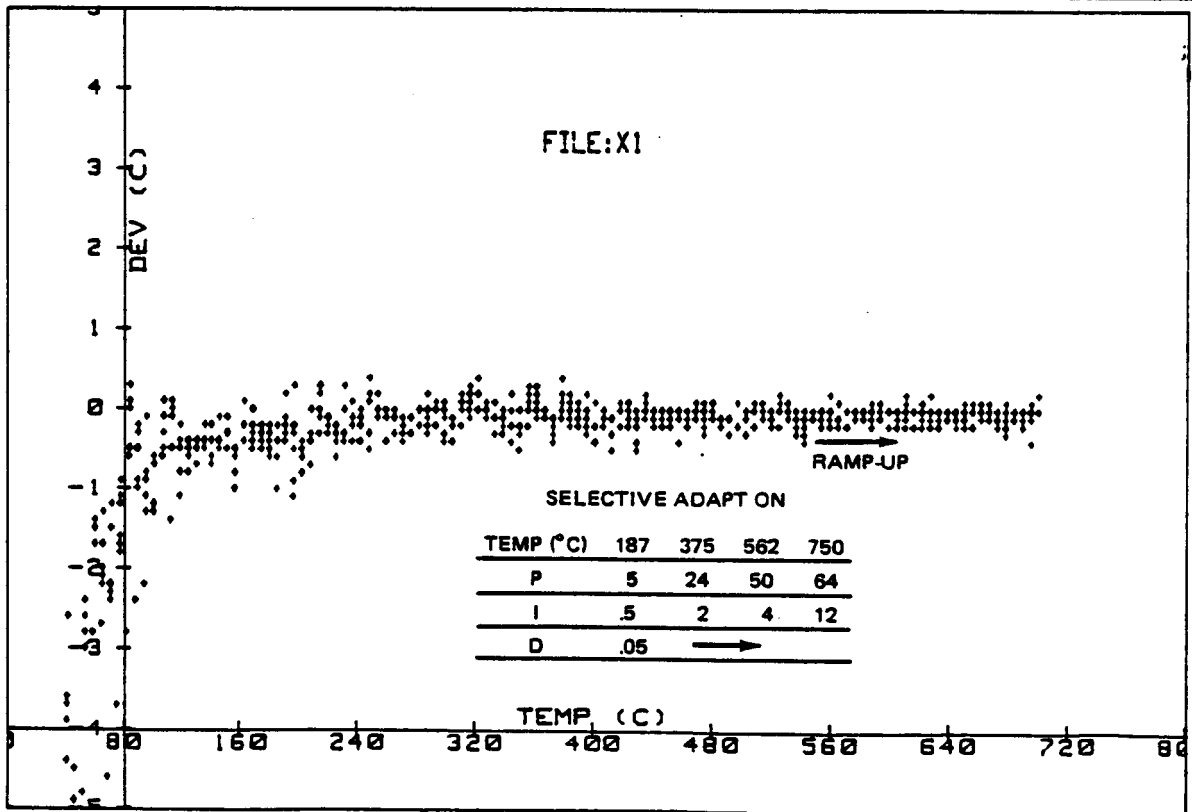
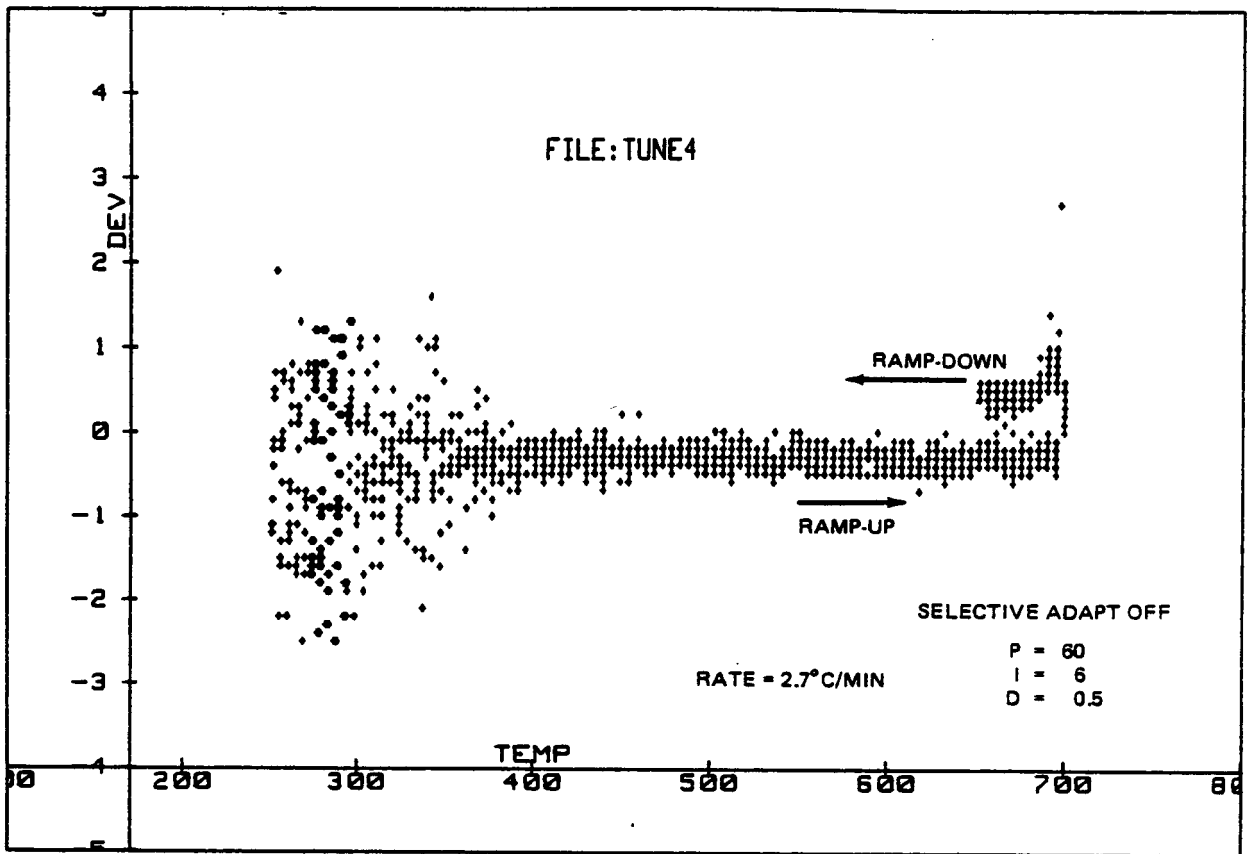
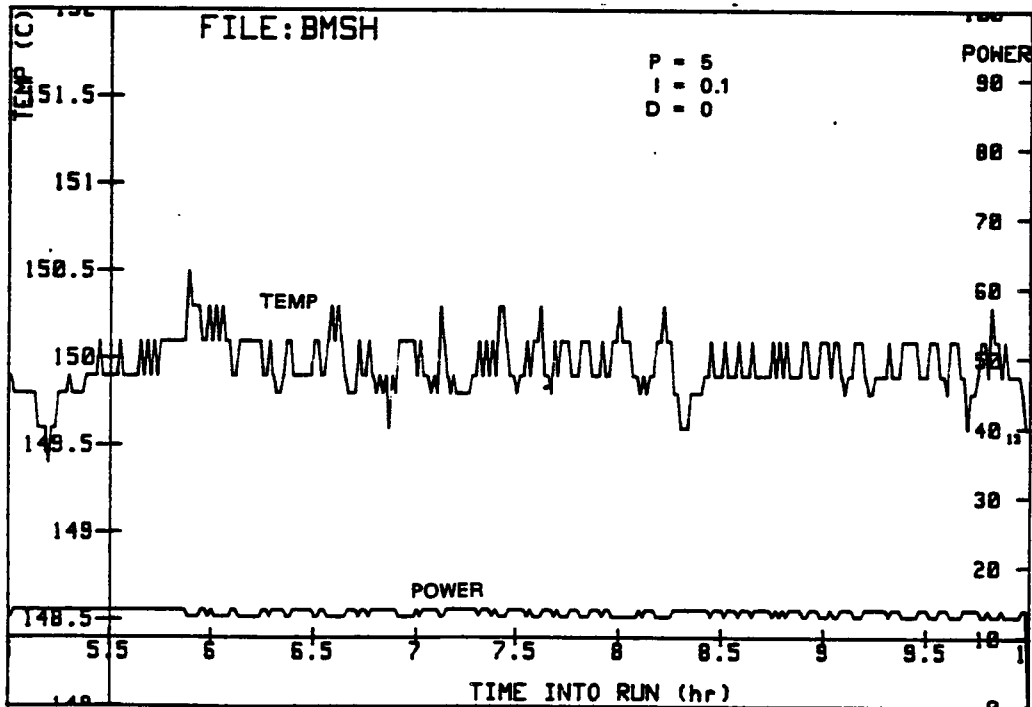
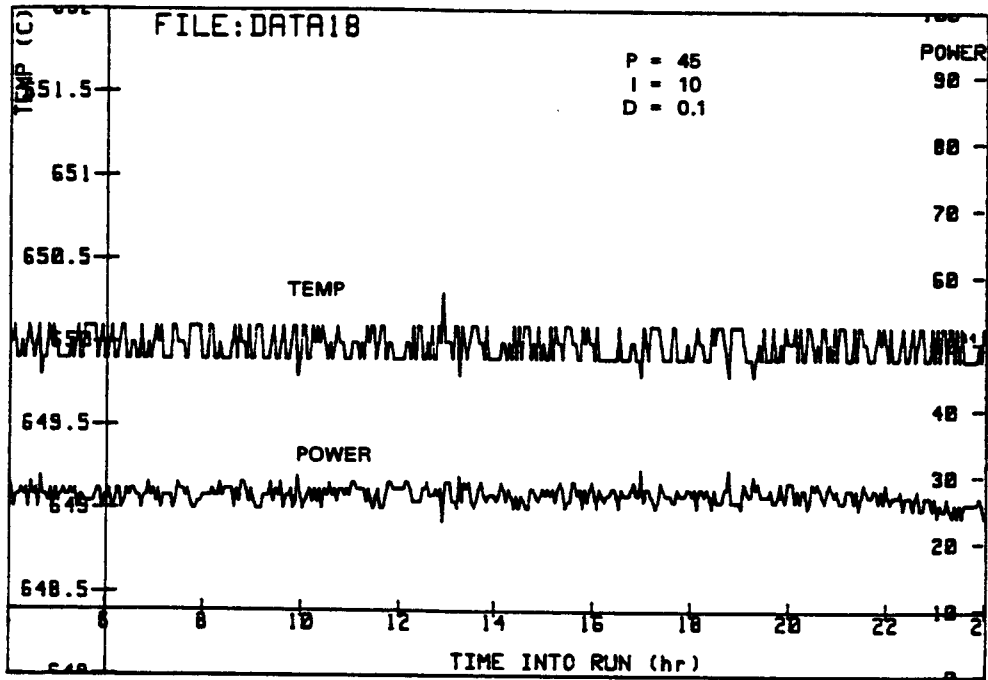


Fig. 16 Zone Temperature vs Time at a Fixed Furnace Power Output of 10%



R86-0332-019(T)

Fig. 17 Deviation from the Programmed Temperature vs Actual Temperature under Two Different Tuning Conditions



R86-0332-020(T)

Fig. 18 Steady-state Temperature Error at High (650°C) & Low (150°C) Temperatures

wavelength were found. An axial temperature variation of $\pm 2.5^{\circ}\text{C}$ was observed as shown in Fig. 19.

5.7 AXIAL TEMPERATURE GRADIENTS

Although any temperature gradient can be programmed into the EDG control system, the achievable sample temperature gradients are determined by the heat transfer and the control accuracy limits of the system. The former sets the maximum gradient, while the latter sets the minimum gradient achievable.

The sample temperature gradient limits were set by:

- o Control system accuracy for low temperature gradients
- o Radial thermal loss for high temperature gradients.

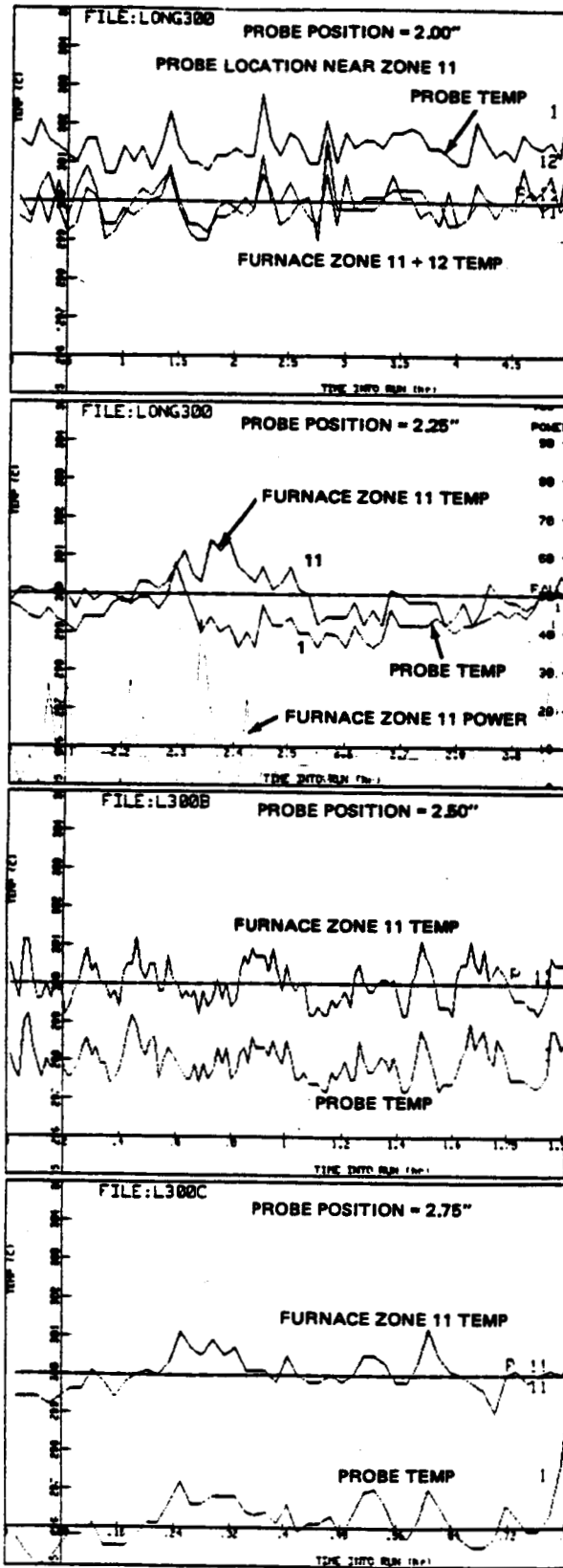
5.7.1 Control System Accuracy Limited Temperature Gradients

The lowest gradient that can be achieved is determined by the relative accuracy of the control system. The accuracy of the gradient is no better than the control system used to create it. For example, in the EDG furnace, at a temperature gradient of $6^{\circ}\text{C}/\text{in.}$, an error of 100% is possible. This is based on a thermocouple accuracy of 0.4% ($\pm 3\text{C}$) at 750°C (refer to Section 5.1.1).

5.7.2 Thermal Flux Limited Temperature Gradients

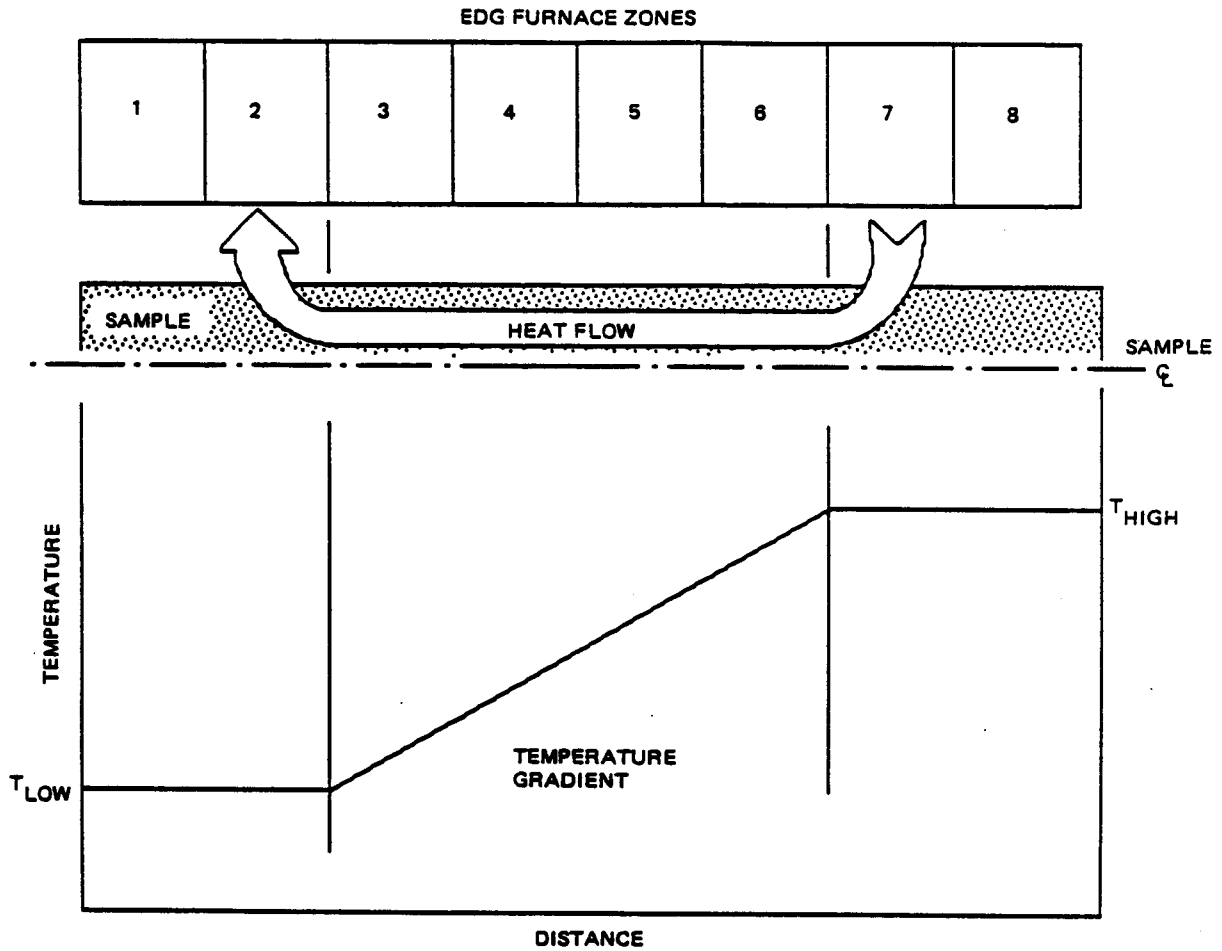
As stated in Section 5.2, the axial heat flow within the furnace was governed by the nature of the sample material and the magnitude of the temperature gradient. The axial heat transferred as a result of the sample axial temperature gradient must be radially lost at the first zone at the base of the gradient in order for the linear gradient to be achievable (Fig. 20).

Conversely, the same axial heat flux must be gained by the high temperature zone just prior to the start of the gradient. At this zone, the power needed to maintain a steady temperature is equal to the radial heatloss at their respective temperatures. If more or less heat is gained, then the gradient will not be linear.



R86-0332-021(T)

Fig. 19 Measured Axial Temperature Variation during Steady-state



P86-0332-022(T)

Fig. 20 Idealized Axial Sample Heat Flow & Sample Temperature Gradient in Multizone Furnace

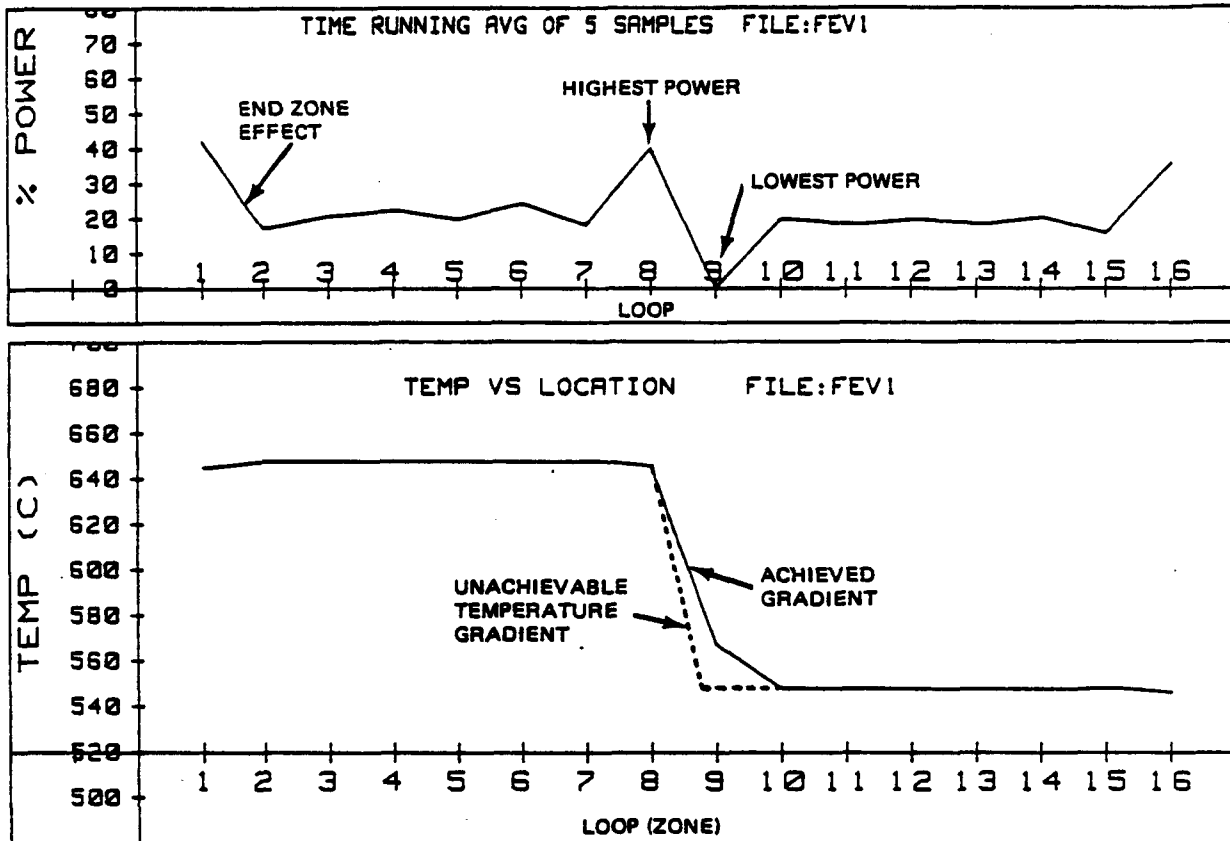
5.7.3 Unachievable Furnace Temperature Gradient

An example of an unachievable axial temperature gradient is shown in Fig. 21. Note that as expected, the zone at the bottom of the gradient has the lowest power consumption, while the zone at the top of the gradient has the highest. However, due to the inability of the bottom zone to radially lose the axially transported heat (power level was already equal to 0), the programmed axial temperature gradient cannot be created.

5.7.4 Maximum Achievable Furnace Temperature Gradient

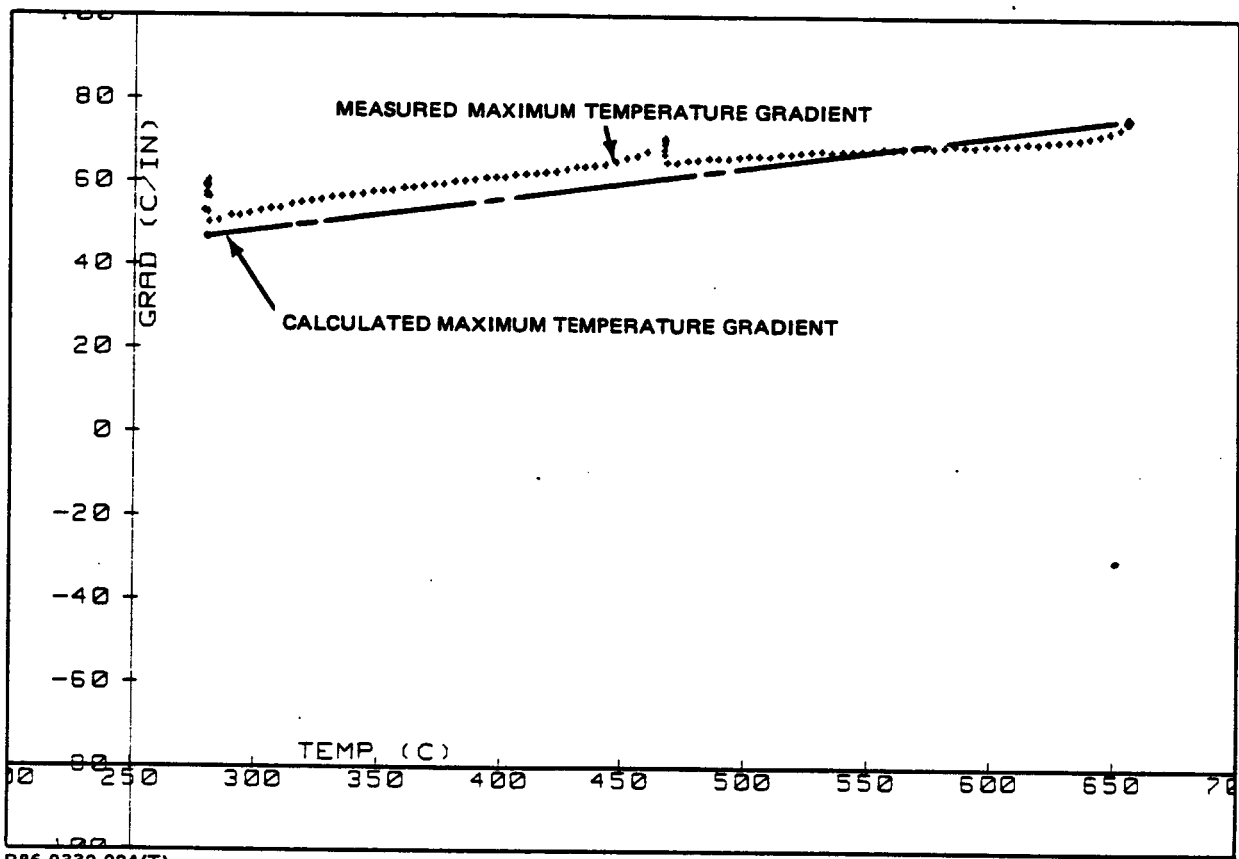
Unlike the lower limit, the limit of the maximum temperature gradient in the EDG furnace was more complex, since what can be achieved within the furnace might not be the same as what was achieved within the sample. A maximum temperature gradient is produced when the axial heat flux generated by the gradient (in the sample and in the furnace) is equal to the maximum radial heat loss in the first zone at the base of the gradient. Based upon the power dissipation of Fig. 15, and the calculated axial heat transfer of Fig. 13, the maximum sample gradient can be calculated; this is plotted in Fig. 22. As the amount of radial heat loss is a function of temperature (Fig. 15), the maximum temperature gradient possible will be expected to increase as furnace temperature increases. This trend is shown in Fig. 22 in which the measured maximum gradient established with the stainless steel sample is also plotted. This data was obtained by ramping a thermal geometry with an unattainable gradient through various temperatures. The achieved gradient values were then plotted as a function of temperature. The calculated and measured values are approximately the same.

It must be emphasized that since the temperature gradient is created from discrete thermocouples located outside the bulk of the sample, the measured furnace temperature gradient might not be the sample temperature gradient. This is more important when dealing with larger gradients and samples of higher conductivity. A distinction between the achievable furnace temperature gradient and the achievable sample temperature gradient should be made. More information on furnace vs sample temperature gradients will be presented in Section 5.9.



R86-0332-023(T)

Fig. 21 Temperature & Power vs Zone Showing Condition of Unachievable Temperature Gradient



R86-0332-024(T)

Fig. 22 Calculated & Measured Maximum Temperature Gradient vs Temperature for Stainless Steel Sample

5.8 TEMPERATURE GRADIENT MOTION

The ultimate criterion for any directional solidification gradient furnace is its ability to move a liquid/solid interface while controlling the temperature gradient and velocity. Important issues for gradient motion in the EDG furnace are:

- o Smoothness of zone transition
- o Smoothness of gradient motion
- o Maximum gradient velocity
- o Minimum gradient velocity.

5.8.1 Discontinuity of Gradient Motion

The discrete-zone nature of the EDG furnace design cannot create a smooth continuous change in the programmed temperature gradient at all furnace locations as a function of time if only two control zones are used. This, however, is not a problem if more than two zones are used to produce the gradient. Fig. 23 shows a temperature-distance history from a run with a gradient using five control zones. The discontinuity (the bend) appeared at the start and end of each gradient. Note that this produced a greater length of constant gradient than that shown in Fig. 5, which used fewer control zones.

5.8.2 Errors During Gradient Motion

The temperature-distance history of Fig. 23 is replotted in Fig. 24. The cause for the inability of certain zones to track the last portion of the ramp-down (enlarged section shown in Fig. 25) is unclear. This might be due to uneven furnace construction, which produced zones with slightly higher cooling than others. Note that the control is lost after the power dropped to zero. The reason for the control inaction after the 400°C programmed temperature was passed was due to the large integral coefficient used in the PID (An example of the effect of large integral coefficients). A run with a copper sample is shown in Fig. 26. Note that the tracking error can be reduced, but a small error still occurred because of the axially transferred heat. (This is a complex run which can be misinterpreted; it will be discussed in detail in Section 5.9.).

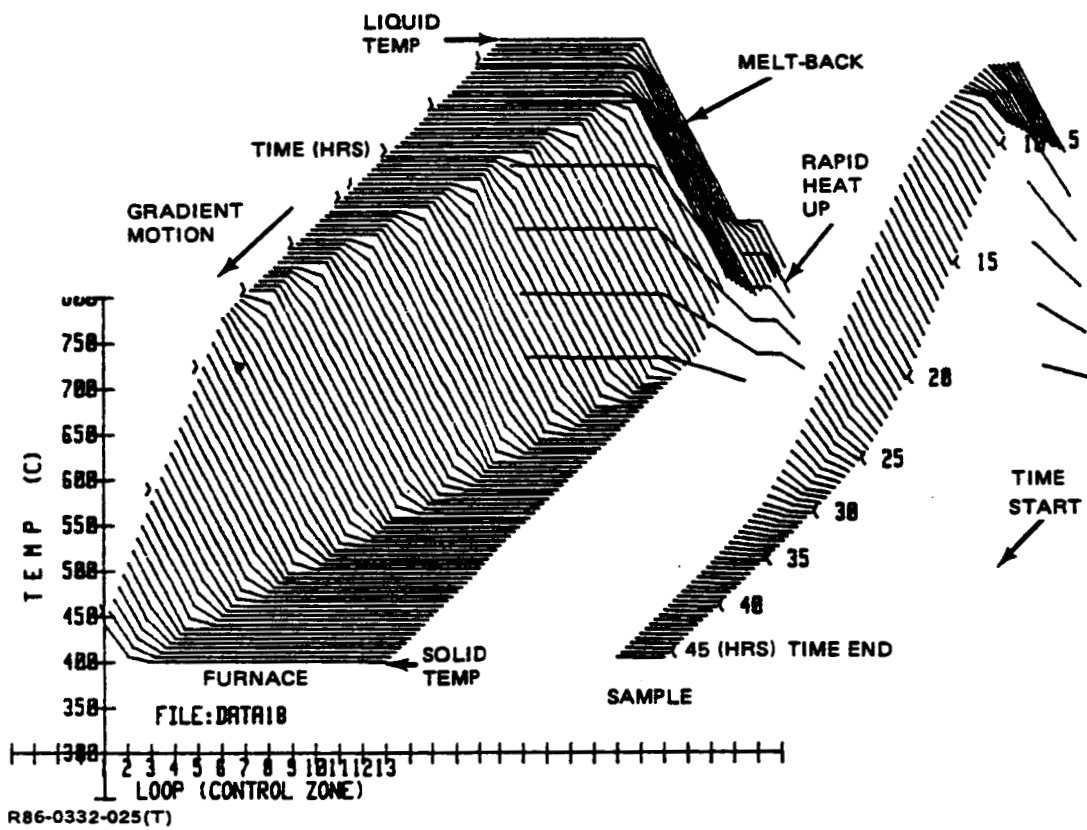
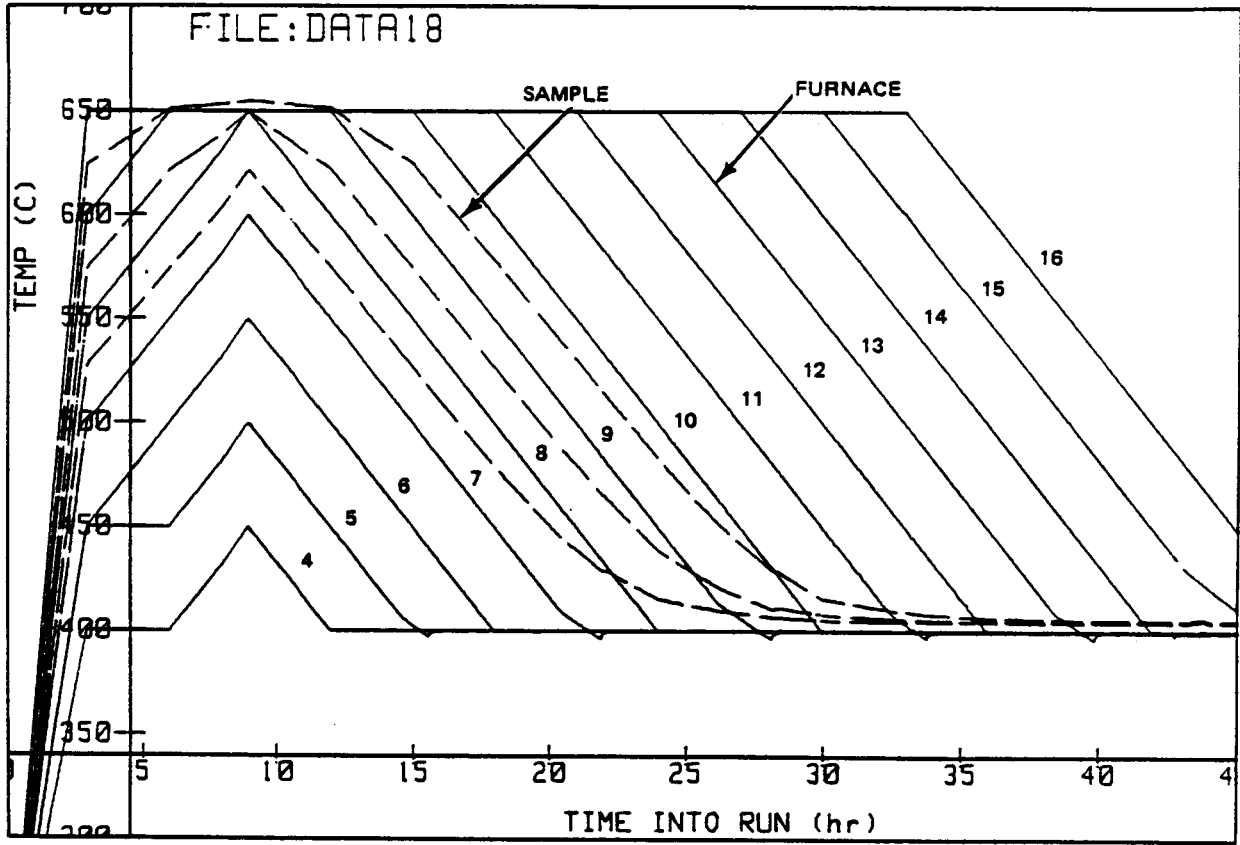
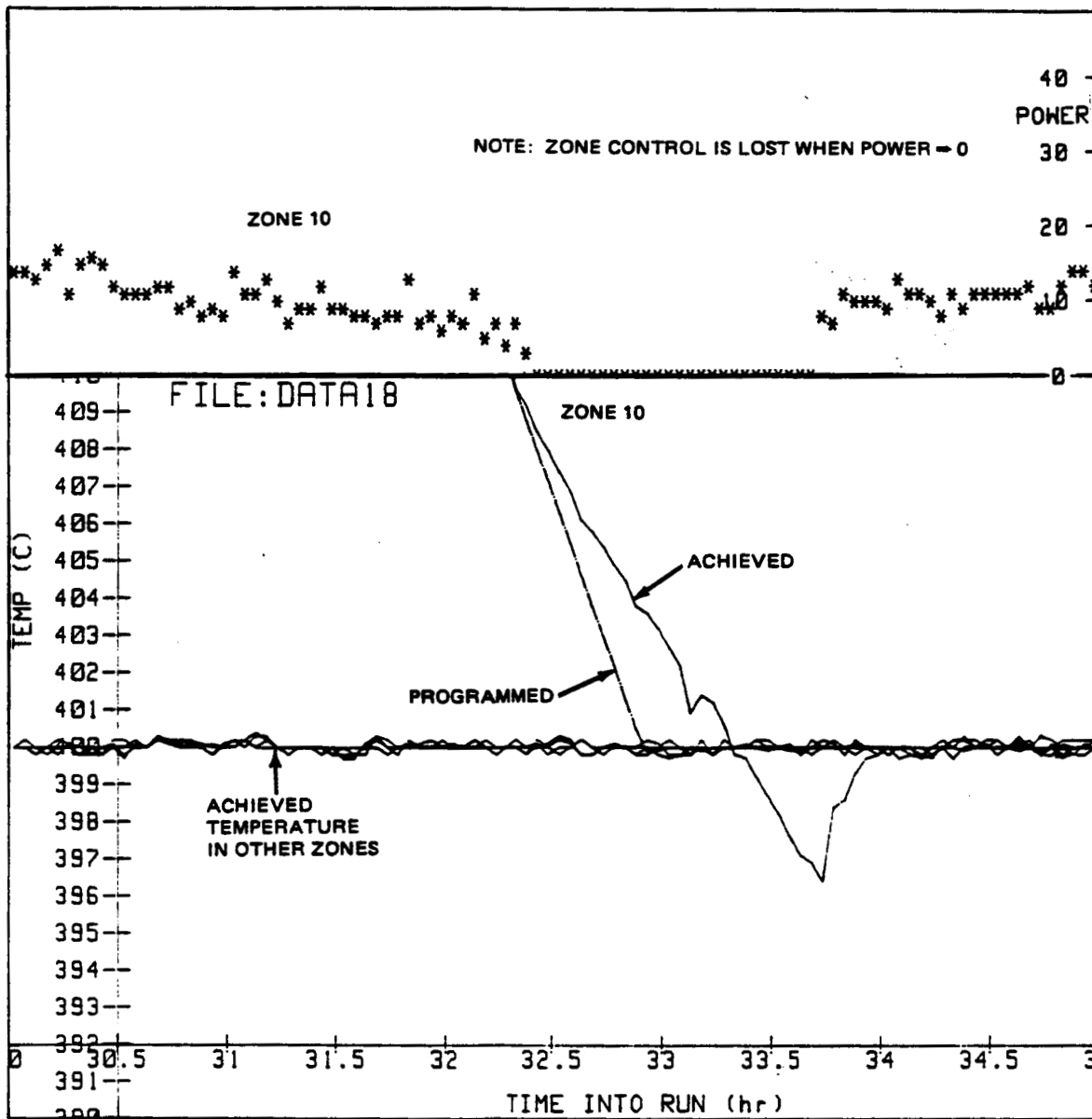


Fig. 23 Temperature Profile History of Furnace & Sample during Gradient Motion (3D View)



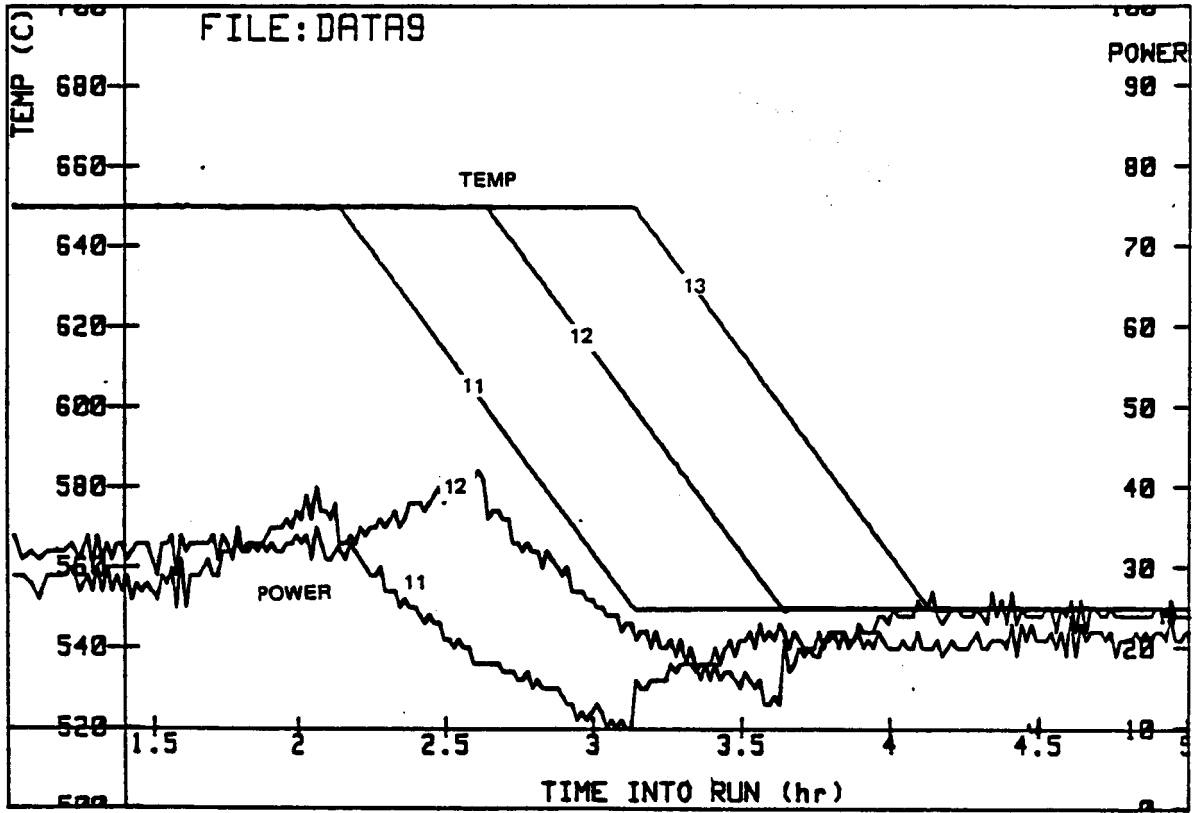
P86-0332-026(T)

Fig. 24 Temperature vs Time for Furnace & Sample during Temperature Gradient Motion with Stainless Steel Sample



P86-0332-027(T)

Fig. 25 Temperature & Tracking Error at the End of Ramping – Stainless Steel Sample



R86-0332-028(T)

Fig. 26 Temperature & Power vs Time during Gradient Motion — Copper Sample

Based on the data shown in Fig. 24, one isotherm temperature (500°C) location vs time is plotted in Fig. 27. The isotherm temperature velocity, when plotted, appeared more noisy (Fig. 28). This noise is due to the slight fluctuations in temperature within the gradient zones and/or electronic errors in temperature measurement magnified by the derivative (dx/dt) calculation. The deviations from the programmed temperatures during ramping are shown in Fig. 29.

5.8.3 Limits of Maximum Gradient Velocity

The maximum gradient velocity in the EDG furnace was set by the maximum cooling rate of the furnace and the amount of axial heat flux (ie. the value of the temperature gradient, thermal conductivity, size, and heat of fusion of the sample). It can be calculated based upon Fig. 12, 13, and 15. The maximum gradient velocity is equal to:

$$V_{max} * G_s = S_{max} * (1 - ((Q_a + Q_b) / Q_r)) \quad (3)$$

where:

V_{max} (in./min) = maximum gradient velocity

G_s (°C/in.) = sample temperature gradient

S_{max} (°C/min) = zone maximum cooling rate; obtained from Fig. 12

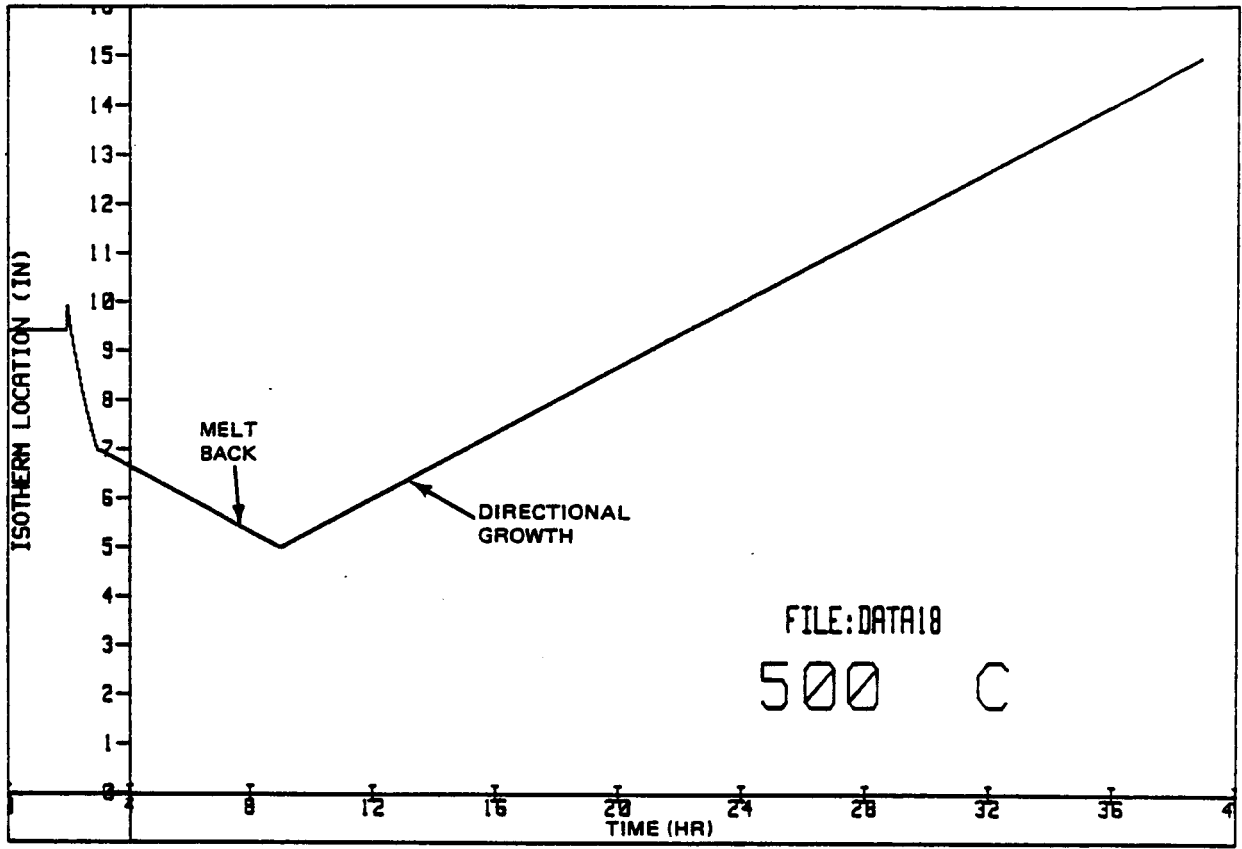
Q_a (watts) = sample axial heat flux due to temperature gradient; obtained from Fig. 13

Q_b (watts) = background axial heat flux in furnace due to temperature gradient; obtained from Fig. 13

Q_r (watts) = steady state heat loss; obtained from Fig. 15.

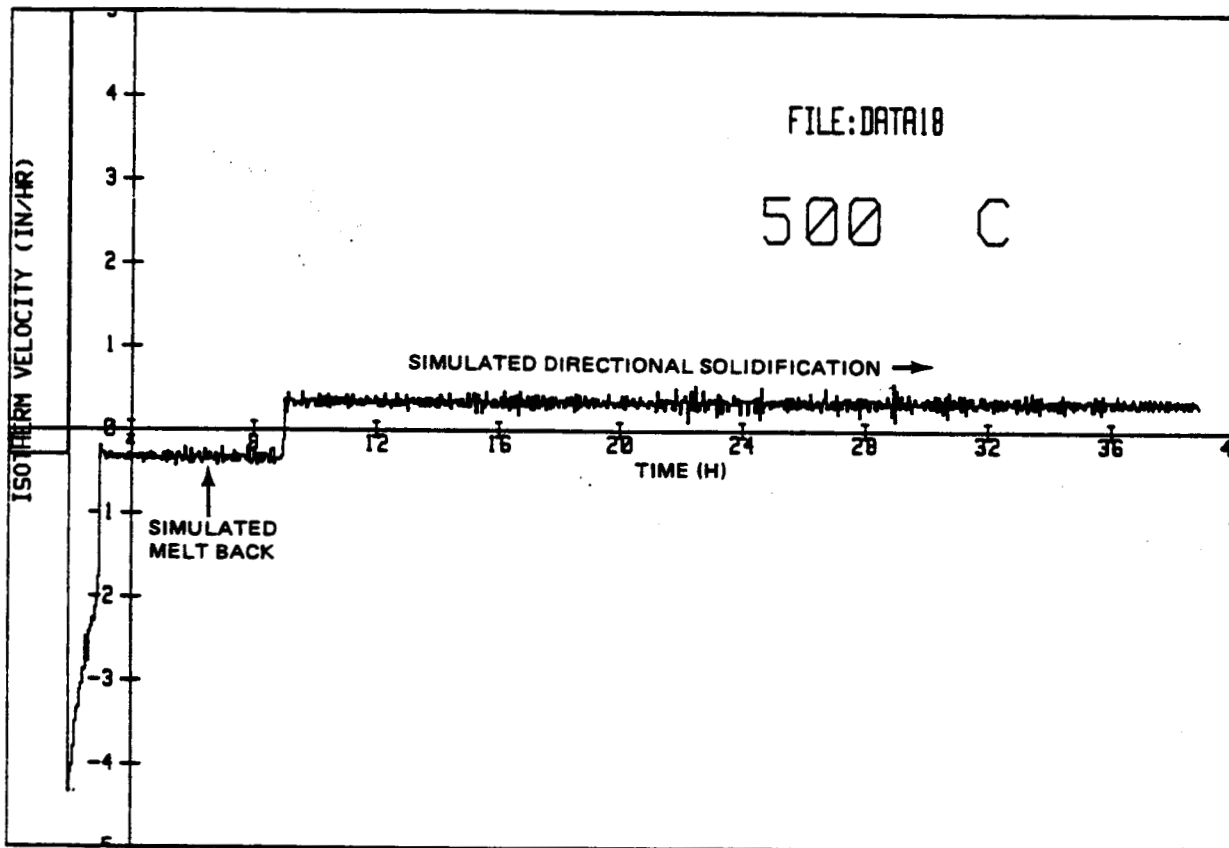
If $(Q_a + Q_b) > Q_r$ then an unachievable temperature gradient condition exists. This calculation is an approximation since radiation heat transfer from the sample is not considered.

A typical maximum limit will be approximately 10 in./hr, based upon a stainless-steel like conductivity and the following conditions: $T(\text{high}) = 700^\circ\text{C}$, $T(\text{low}) = 650^\circ\text{C}$, $G_s = 50^\circ\text{C}/\text{in.}$, $S_{max} = 17^\circ\text{C}/\text{min}$, $Q_a = 8\text{w}$, $Q_b = 25\text{w}$, and $Q_r = 66\text{w}$. At this fast rate, the current control system might not be able to track correctly.



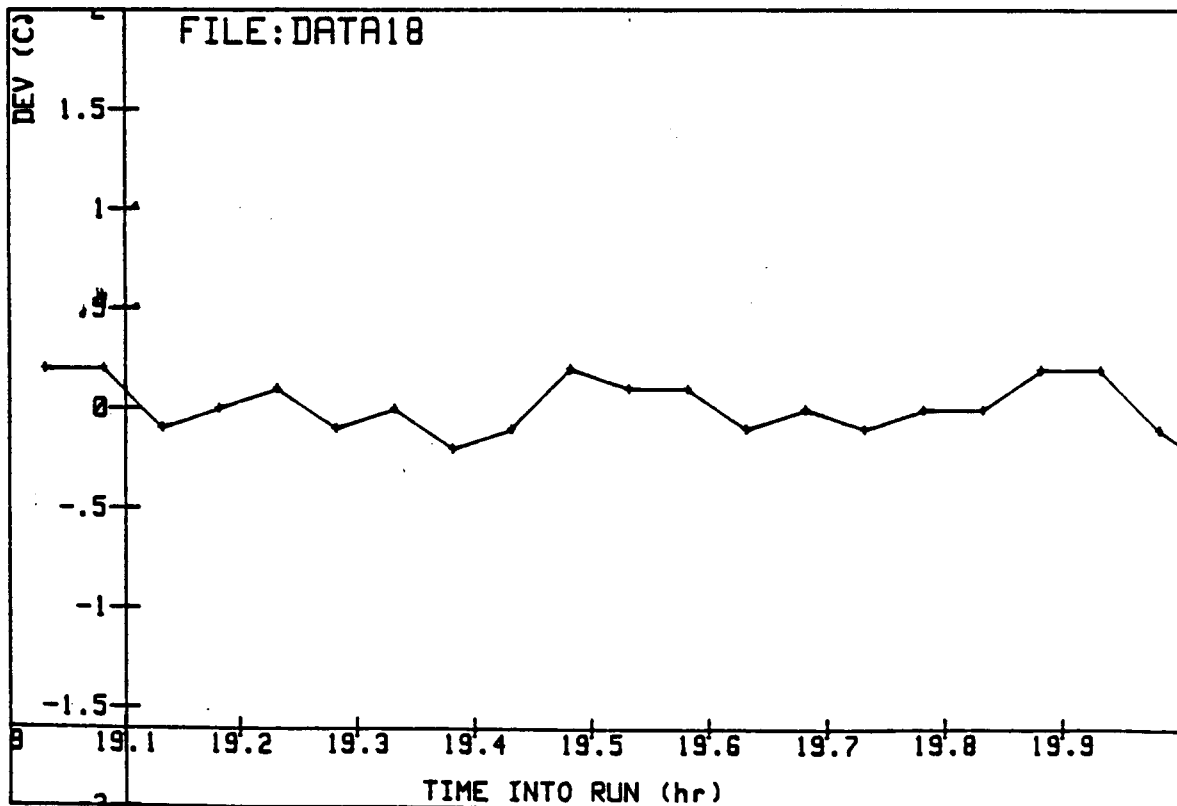
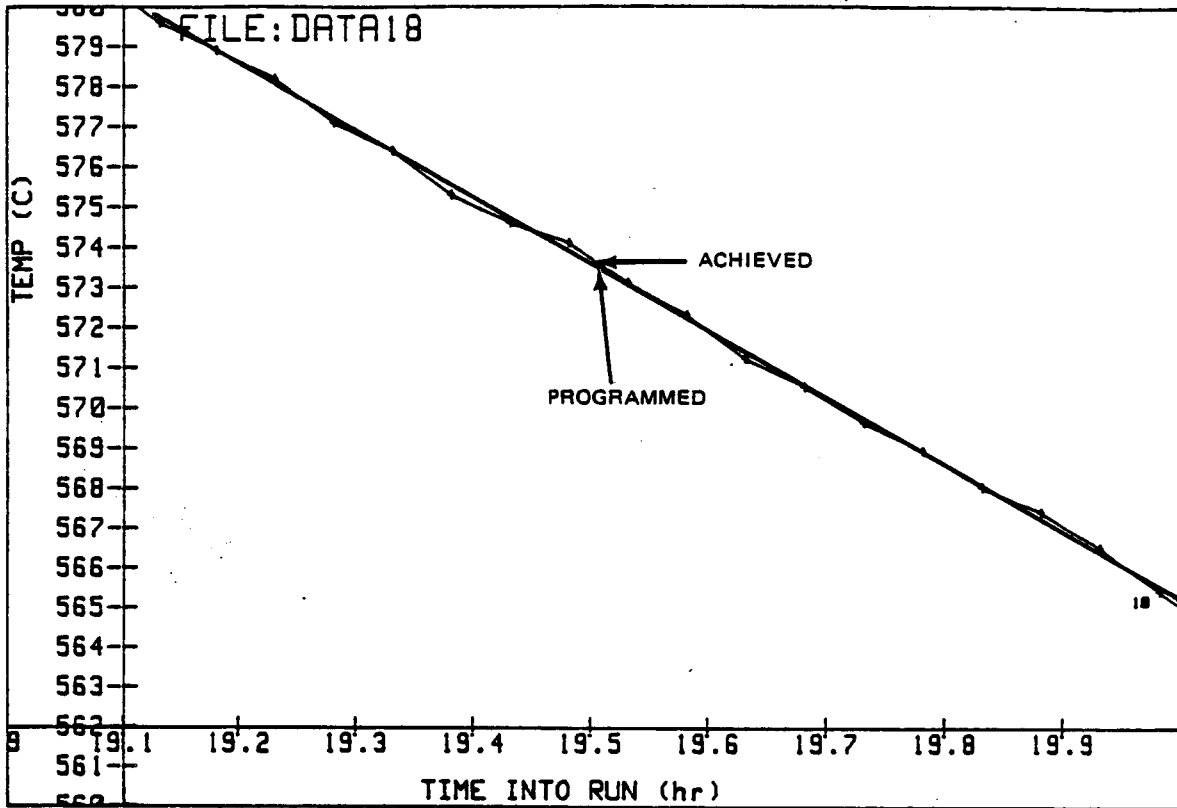
R86-0332-029(T)

Fig. 27 Isotherm (500°C) Position vs Time with Stainless Steel Sample



R86-0332-030(T)

Fig. 28 Isotherm (500°C) Velocity vs Time with Stainless Steel Sample



P86-0332-031(T)

Fig. 29 Deviation from Linearity during Ramp-Down

5.8.4 Limits of Minimum Gradient Velocity

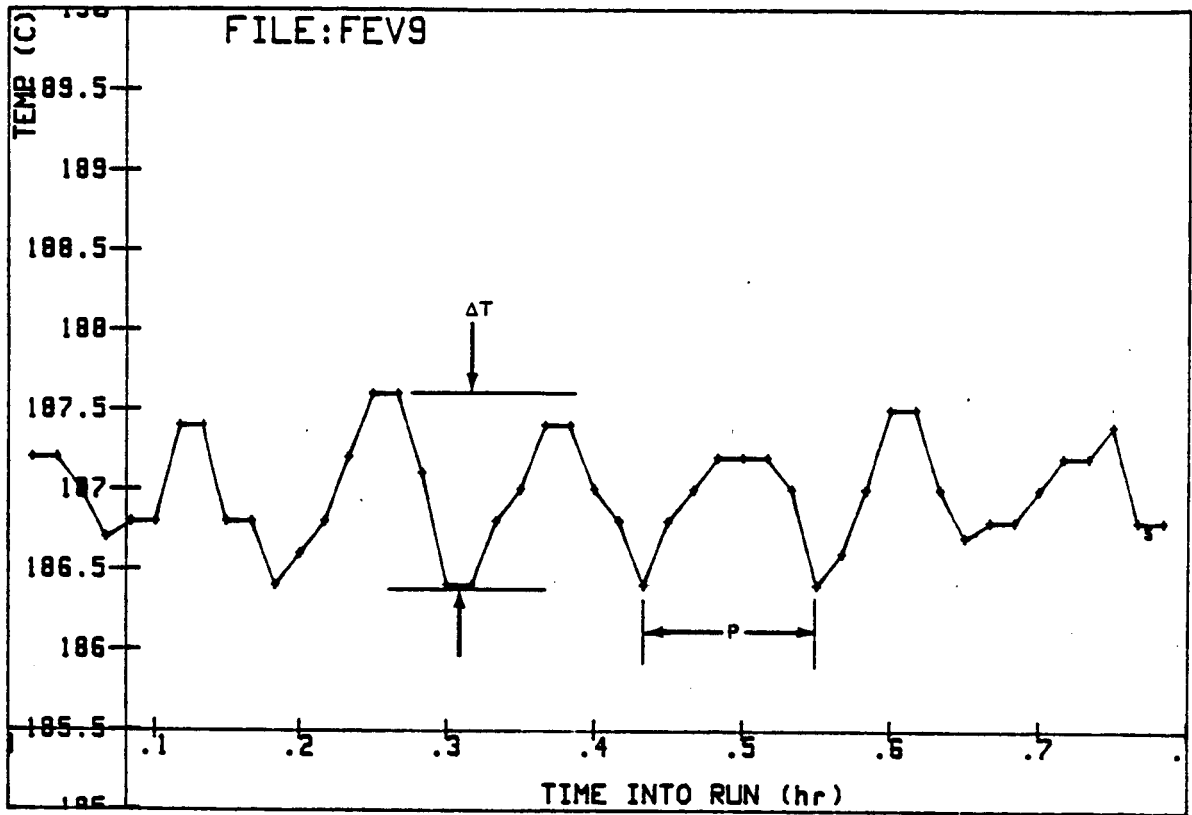
The minimum temperature gradient velocity in the EDG furnace was set by the stability of the temperature control system. Oscillation of the interface (ratcheting) will occur if the programmed cooling rate becomes less than the drift and/or furnace control induced temperature oscillation rates. For example, under certain conditions, such as at low programmed temperatures, and poor PID tuning, control is difficult and the furnace temperature often undergoes small oscillations even at a steady state (Fig. 30). Under this condition, the gradient velocity lower limit is set by the temperature oscillation and the period of the oscillation.

Effective interface rate (R) as a result of temperature oscillation:

$$R = (2 \cdot \Delta T / P) / G \quad (4)$$

A ΔT value of 1°C and a period (P) of 0.1 hours (typical oscillation period) at a gradient of $20^\circ\text{C}/\text{in.}$ would set a lower limit of one in./hr. Under these conditions, the furnace temperature oscillations dominate the interface motion, and no useful control growth can be expected. In reality, temperature stability becomes a significant factor at low temperatures (see Section 7).

Another factor which can influence furnace temperature stability is the stability of the furnace environment. For example, if the furnace is operating at around 750°C and the room temperature changes 5°C in 5 hr, this will result in a measured temperature error of 0.75°C (based on a 0.1% controller temperature influence - see Table 1). Over 5 hr, this is equal to a 0.15 C/hr rate of change. If the gradient was $20^\circ\text{C}/\text{in.}$, then the effective interface velocity as a result of this room temperature change is $(0.15 \text{ C/hr} + 20^\circ\text{C}/\text{in.})$ 0.0075 in./hr. If the programmed rate of interface velocity is equal to or less than this, then ratcheting of the interface can occur. At high temperatures (above 400°C), where tuning oscillations are not likely, then a practical lower gradient velocity limit based upon the above room temperature stability and gradient velocity at a precision of 10% is thus approximately 0.075 in. per hour. The precision can be improved with better room temperature control, better electronic stability, and/or higher gradient magnitudes.



R86-0332-032(T)

Fig. 30 Temperature Oscillation at Low Temperature

5.9 SPECIAL CONSIDERATIONS FOR THE EDG FURNACE

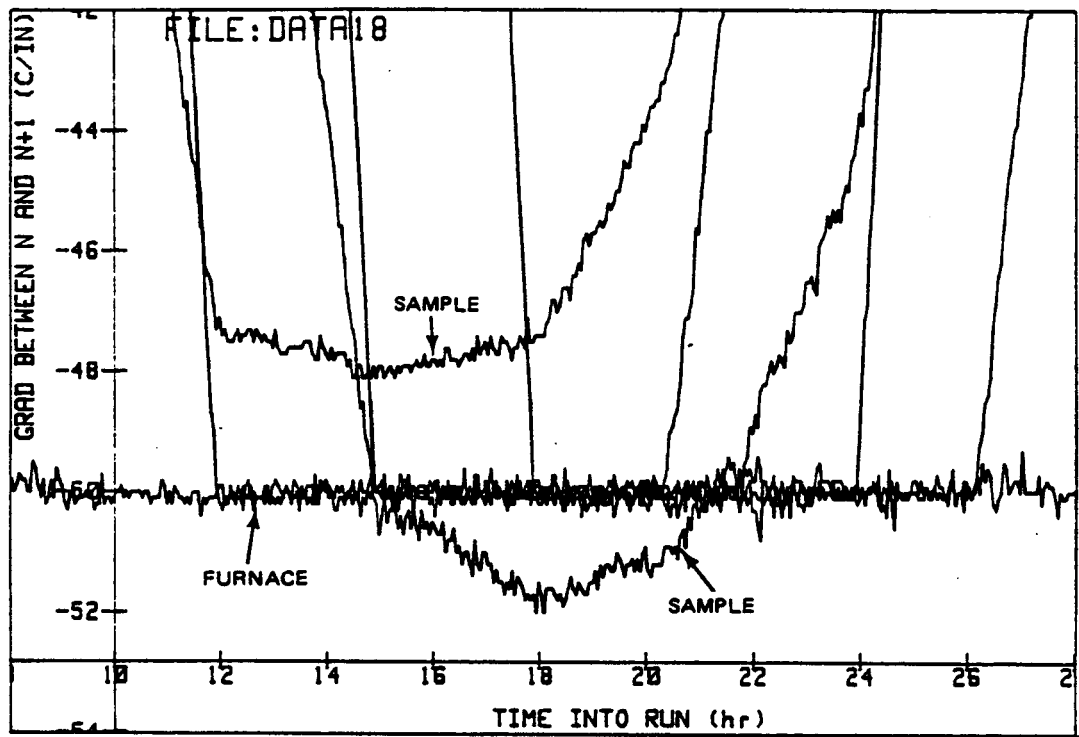
Special consideration must be given to the EDG furnace with regard to:

- o Furnace and sample temperature gradient differences
- o Gradients in materials involving thermal conductivity changes.

5.9.1 Furnace and Sample Temperature Gradient Differences

As stated in Section 2.2, in the multizone furnace design, the S term in equation (1) is controlled in order to generate an effective R, while holding G constant. But in fact, the G term is only constant when the temperature measured by the control system is the actual sample temperature. Because control thermocouples are only in surface contact with the sample ampoule, the measured and actual sample temperature might differ. If the two temperatures are equal, then the slope of the sample cooling curve (if measured) should correspond to the slope of the furnace zone cooling curve. This is observed in Fig. 24, where the instrumented stainless-steel sample shows the same cooling curve slope as the furnace zones. When plotted as gradient vs time in Fig. 31, the two samples gradients (calculated from three thermocouples inside the sample) are relatively close to the programmed furnace gradient of 50°C/in. The amount of difference shown might be due to small radial temperature gradients an/or the discrete zones of the furnace.

Based upon the prior sections, it was clear that the maximum gradient possible is set by the maximum rate of radial heat loss. Gradients and samples that result in larger axial heat flow cannot be controlled. Runs with the copper sample, however, showed gradients of larger magnitudes being achieved (Fig. 26); the explanation for this apparent contradiction stems from the fact that the copper runs were made with a quartz ampoule (the stainless steel sample was without an ampoule). So it seems that for the copper sample, the programmed gradient was achieved only at the surface of the ampoule. The actual copper sample temperature gradient must be of a lower value. A radial gradient must have existed between the center of the sample and the quartz ampoule surface, resulting in a significantly nonlinear heat flux path within the sample. The situation in which the sample gradient differs from the furnace gradient is illustrated in the BiMn runs (see Section 6). In the BiMn runs, the gradient within the sample was measured with one thermocouple by the motion of a known furnace temperature gradient through the sample. In these



R86-0332-033(T)

Fig. 31 Measured Sample Temperature Gradient

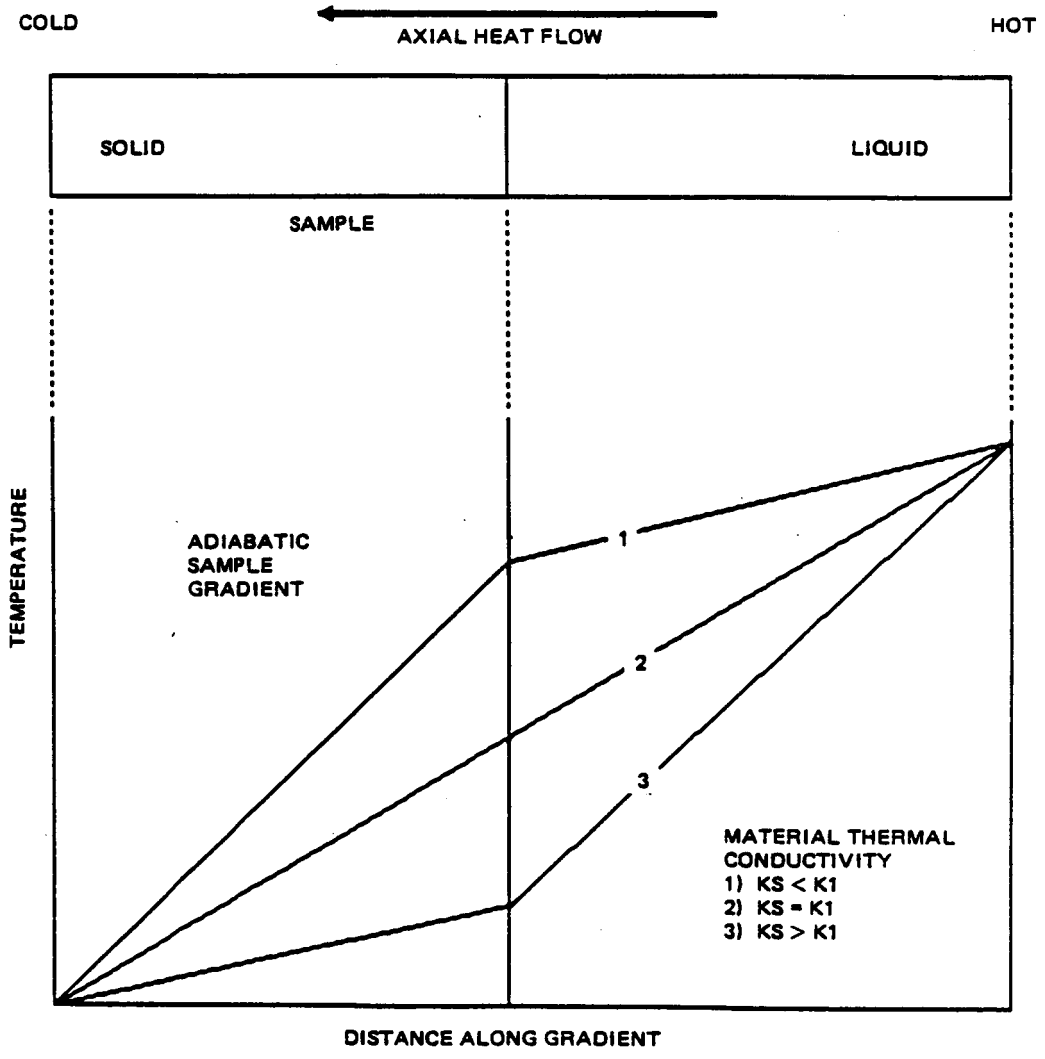
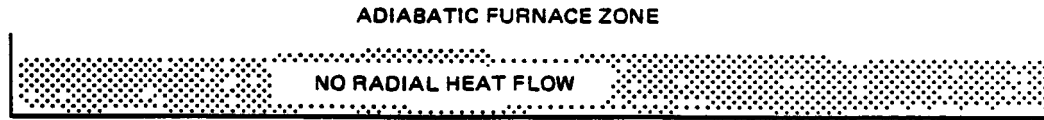
cases, it was found that the sample cooling curves were different from the furnace zone cooling curves (different slopes) indicating a sample temperature gradient lower than that programmed.

Because radial heat transfer is limited, the higher the sample axial heat flux, the lower the gradient that can be established without significant deviations from the programmed value.

5.9.2 Material Thermal Conductivity Changes

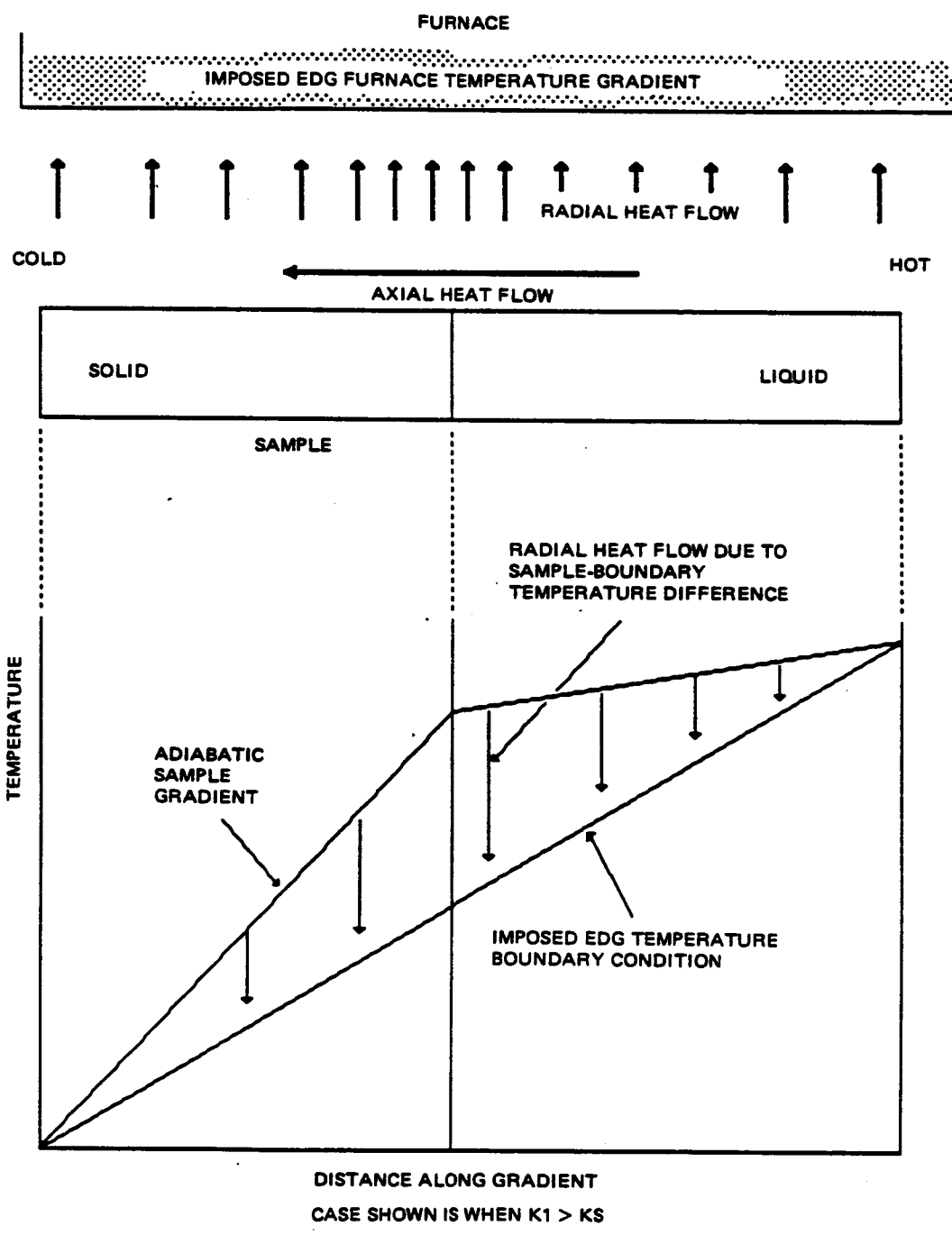
During solidification, the thermal conductivity changes significantly. In an adiabatic type furnace, this results in a nonlinear temperature profile within a liquid/solid sample (Fig. 32). The occurrence of this nonlinear temperature profile is a direct effect of the thermal conductivity change between the liquid phase and the solid phase.

In the EDG furnace, since no adiabatic zone exist, radial heat flow is minimized by the generation of an ampoule (temperature) boundary condition which mimics the temperature profile that would have been produced by an adiabatic gradient zone. With a liquid/solid sample, the use of a linear temperature gradient will result in radial heat loss within the gradient as shown in Fig. 33. Since the temperature at the ampoule is an artificial boundary condition unless it is matched exactly to the temperature boundary condition of the adiabatic gradient case, it will result in radial heat loss (or gain) within the gradient section. Radial heat transfer within the gradient zone(s) will result in an non-planar interface and additional thermal convection. The critical influence of radial temperature gradients is well known and efforts to minimize radial heat transport by the programming of nonlinear temperature gradient profiles although not studied, might be important in the future.



P86-0332-034(T)

Fig. 32 Sample Axial Temperature in an Adiabatic Gradient



P86-0332-035(T)

Fig. 33 Unmatched Boundary Temperature Condition Resulting in Radial Heat Flow

6 - DIRECTIONAL SOLIDIFICATION OF BiMn

The directional solidification of eutectic BiMn ($T_m.p.=265^{\circ}C$) involved Bridgman-type solidification temperature profiles. Application of the furnace for directional solidification at this low solidification temperature was difficult due to poor furnace temperature control. Three case studies of the BiMn directional solidification runs are presented. The run samples showed indications of nonplanar interface growth and convection. Admittedly, only a limited number of attempts were made at BiMn growth. It was felt, however, that the temperature needed for BiMn was under the effective control range of the EDG furnace tested.

6.1 CASE A

- o Thermal history (Fig. 34) - a temperature gradient of $50^{\circ}C/in.$ was passed over the initial solid eutectic BiMn sample at a rate of one in./hr. until approximately $2/3$ of the sample was melted. At this point, the gradient was held for one hour. Then the gradient direction was reversed and the sample was resolidified at one inch per hour at $50^{\circ}C/in.$ A thermocouple was placed within the sample approximately between zones 5 and 6, near where the interface direction was reversed
- o Results - the following observations can be made. First, note that the sample temperature response was shifted with respect to the furnace response. This was typical of the lag between furnace action and sample reaction. Second, upon expansion of the details of zones 9 and 10, deviation from linearity appeared small (Fig. 35). But, an enlarged plot of the deviation vs time (Fig. 36) clearly showed temperature tracking errors. It was clear that very precise control is required for smooth isotherm motion.

6.2 CASE B

- o Thermal history (Fig. 37) - this case was different from case A due to the total melting of the BiMn sample. After the furnace was heated to an isothermal temperature of $650^{\circ}C$ in one hour, it was held at the constant temperature of $650^{\circ}C$ for one hour. Then, during a period of one hour, a $50^{\circ}C/in.$ temperature gradient was formed. The gradient was held static for one hour prior to the start of gradient motion at

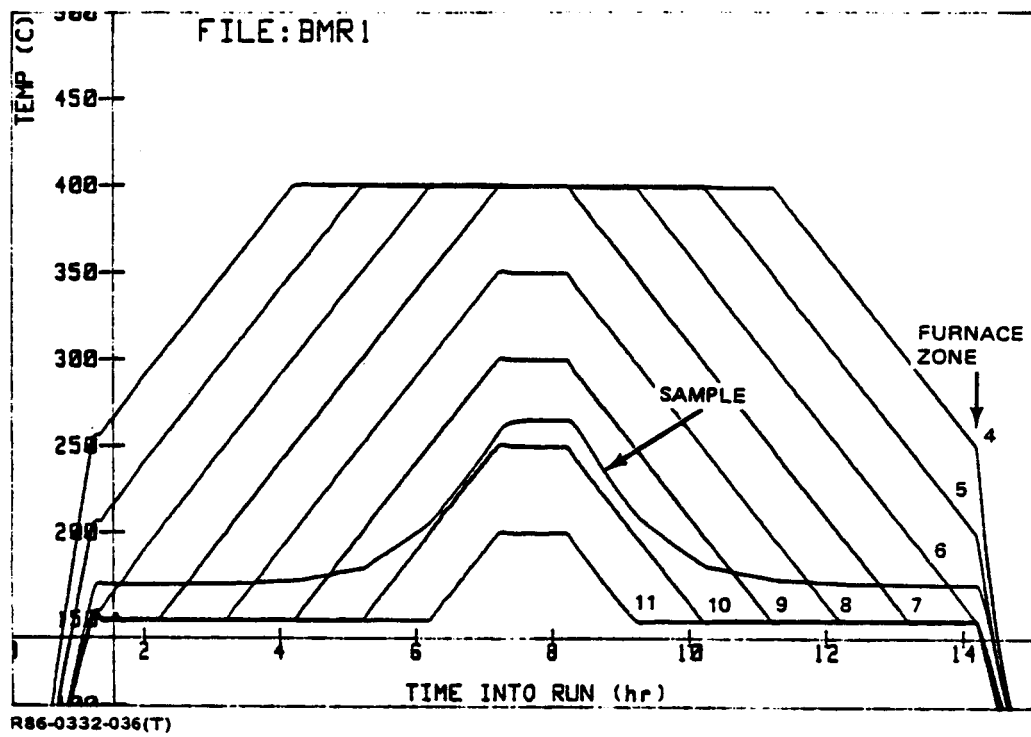
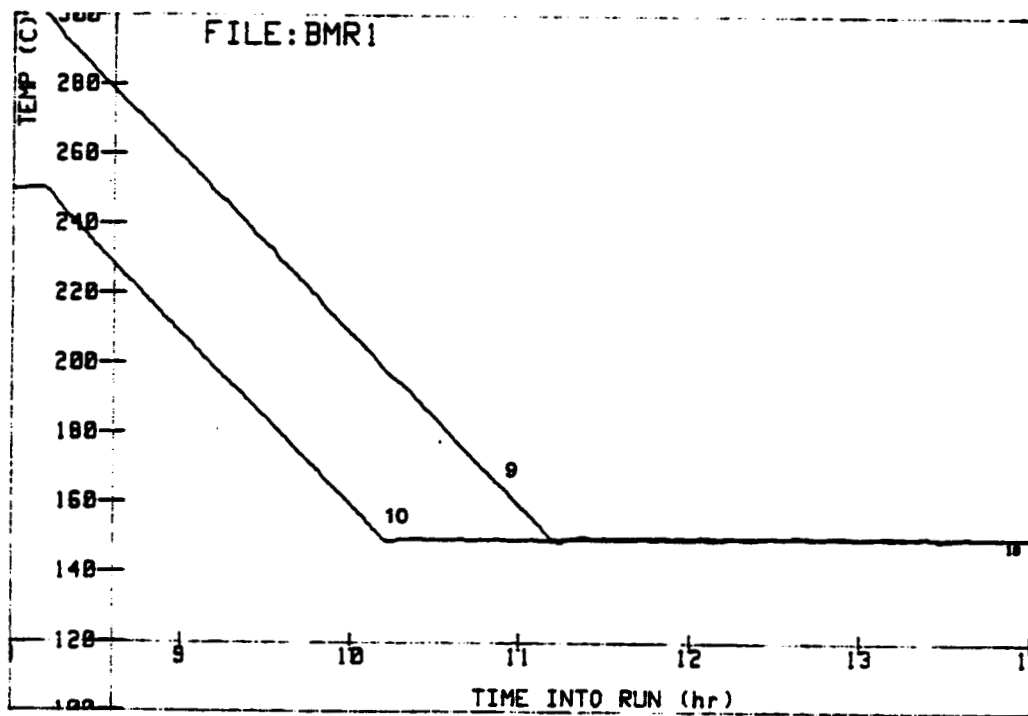
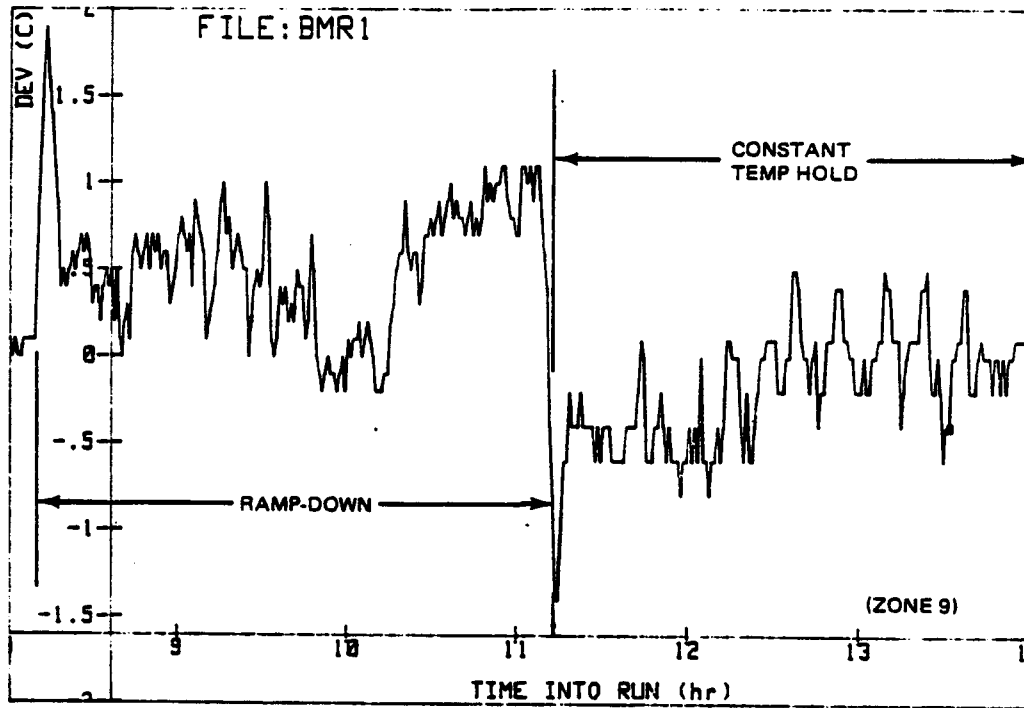


Fig. 34 BiMn Directional Solidification - Case History A



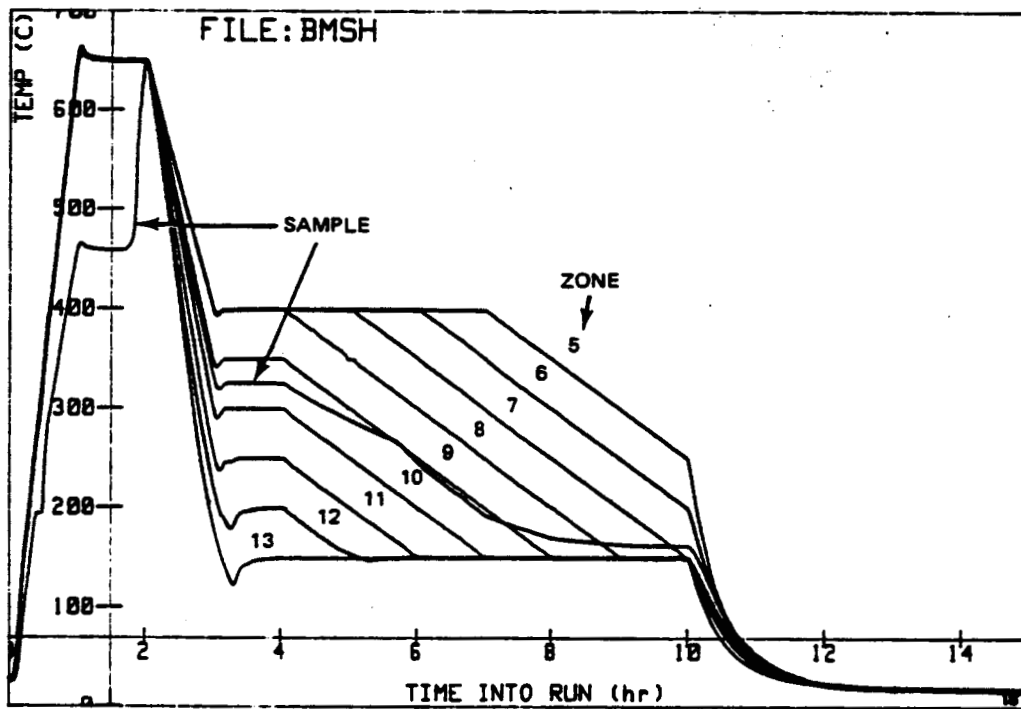
R86-0332-037(T)

Fig. 35 Detail of Temperature Tracking during BiMn Gradient Motion



R86-0332-038(T)

Fig. 36 Deviation from Linearity during Ramp-Down & Constant Temperature Hold in BiMn Run A



R86-0332-039(T)

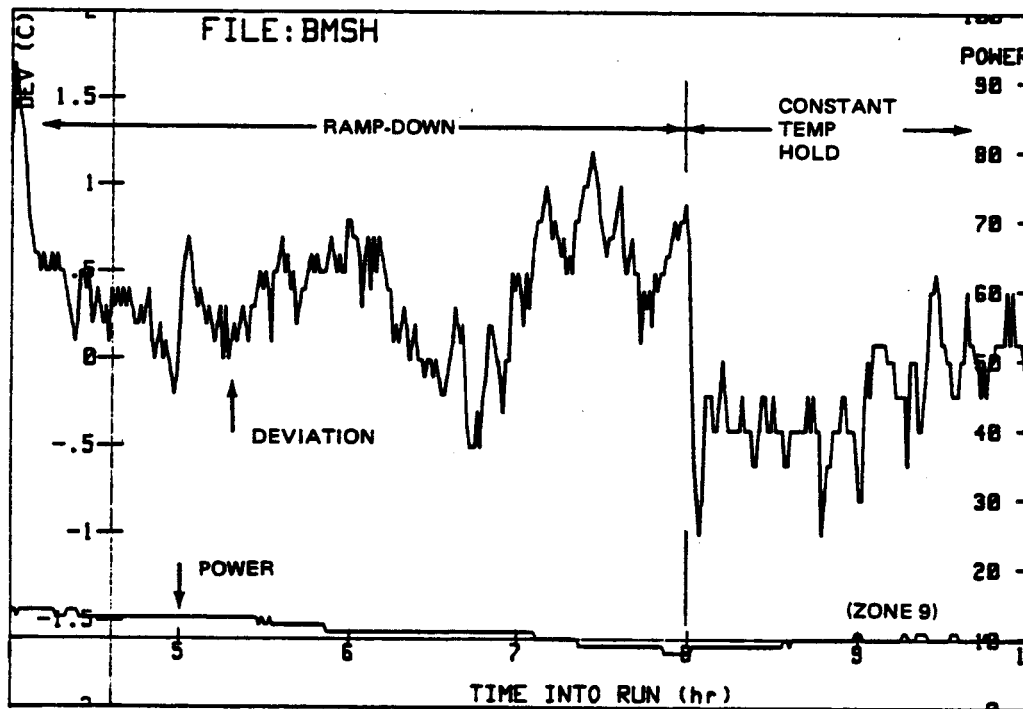
Fig. 37 BiMn Directional Solidification - Case History B

one in./hr. The furnace power was turned off at the 10th hour. The sample temperature showed a plateau at 460°C due to the melting of the alloy. The plateau was not at 265°C because the sample thermocouple was placed between the sample and the ampoule, and only came into intimate contact with the sample after it melted. (On runs where the thermocouple was placed inside the sample, the true melting temperature was indicated.)

- o Results - this run showed behavior (Fig. 38) similar to Case A (Fig. 35). In this figure, the power is also plotted. It is observed that the power level is low (approximately 10%) and that the power level (step) changes are near the resolution limit of the control system. The change in slope of the sample temperature (Fig. 39) was due to the fact that the temperature gradient in the sample was lower than the temperature gradient of the furnace. It can be calculated from the lower slope that the sample temperature gradient was approximately 33°C/in. in the liquid phase, and changed to approximately equal to, or slightly greater than, the programmed temperature gradient (50°C/in.) after solidification. This was due to the change in thermal conductivity of the sample upon solidification. It was clear that what was programmed into the furnace was not what was achieved during the run in the sample.

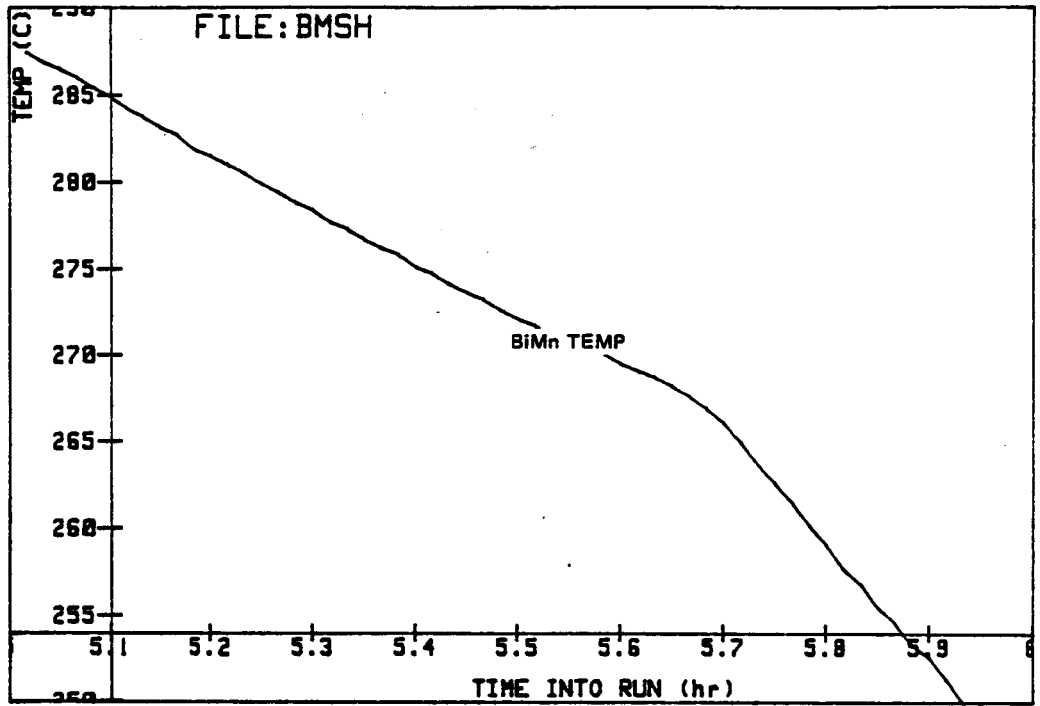
6.3 CASE C

- o Thermal history (Fig. 40) - this is an example of poor thermal control. Figure 40 is an expanded portion of a thermal history similar to Case B, except that the PID coefficients were different, and not capable of stable control
- o Results - the noisy cooling curves of the furnace and sample indicated poor control. An isotherm velocity plot at 350°C vs time (Fig. 41) showed large deviations from the programmed one in./hr velocity. A study of the deviation history of the control zone showed repeated oscillations in temperature (Fig. 42). Note that the power oscillation was in response to the initial temperature oscillation, due to overcompensation the temperature went through a period of decaying temperature oscillation (ringing). This was clearly shown in Fig. 43.



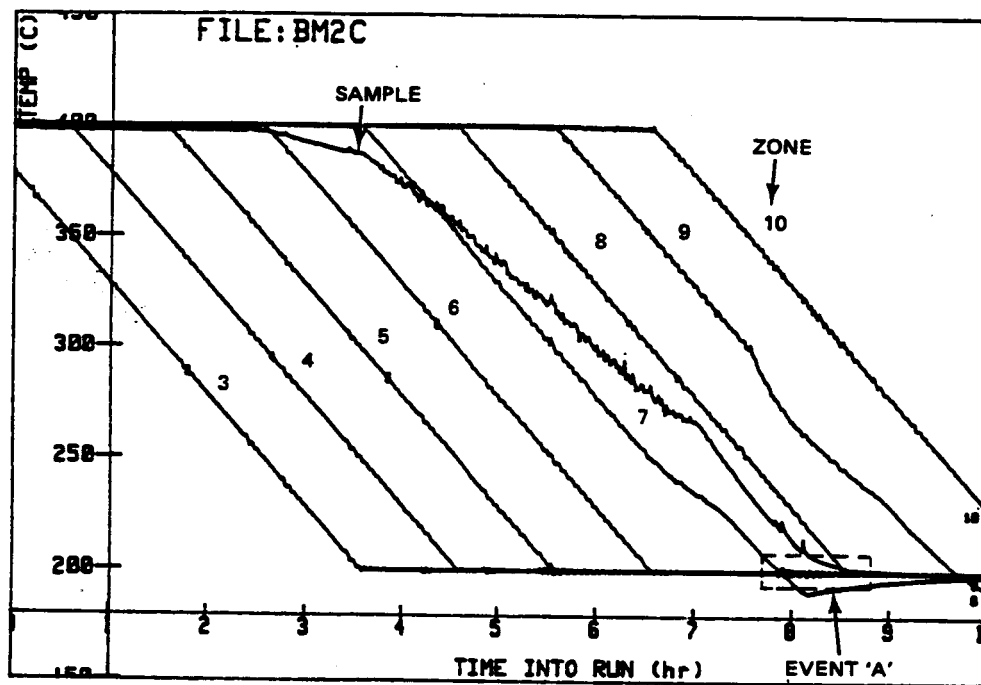
R86-0332-040(T)

Fig. 38 Deviation from Linearity & Power during Ramp-Down & Constant Temperature Hold in BiMn Case B



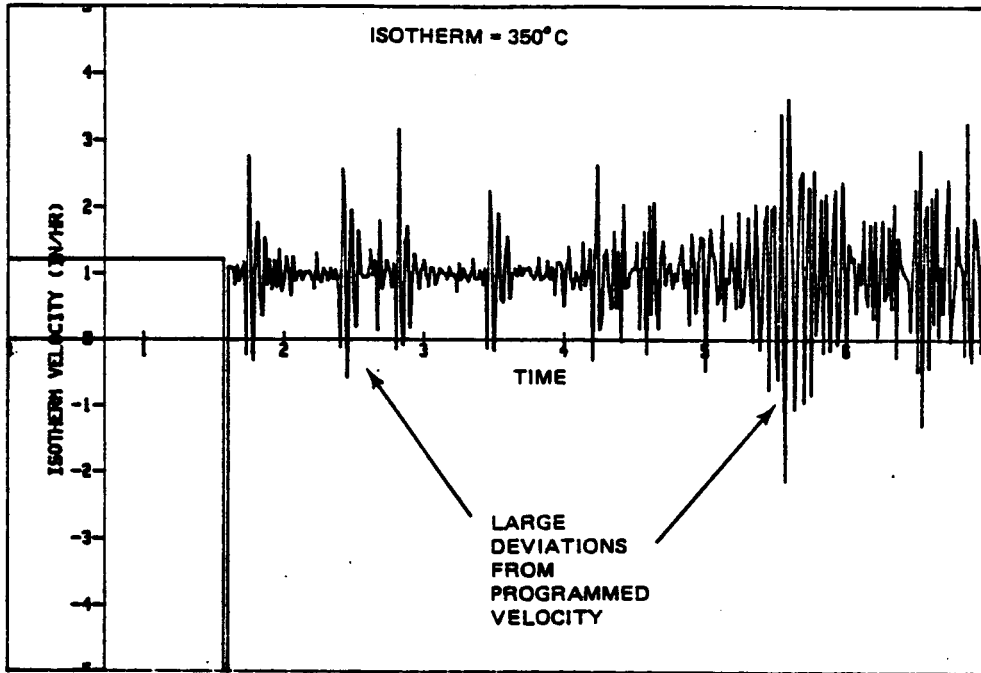
R86-0332-041(T)

Fig. 39 Cooling Curve of BiMn Sample Showing Change in Slope



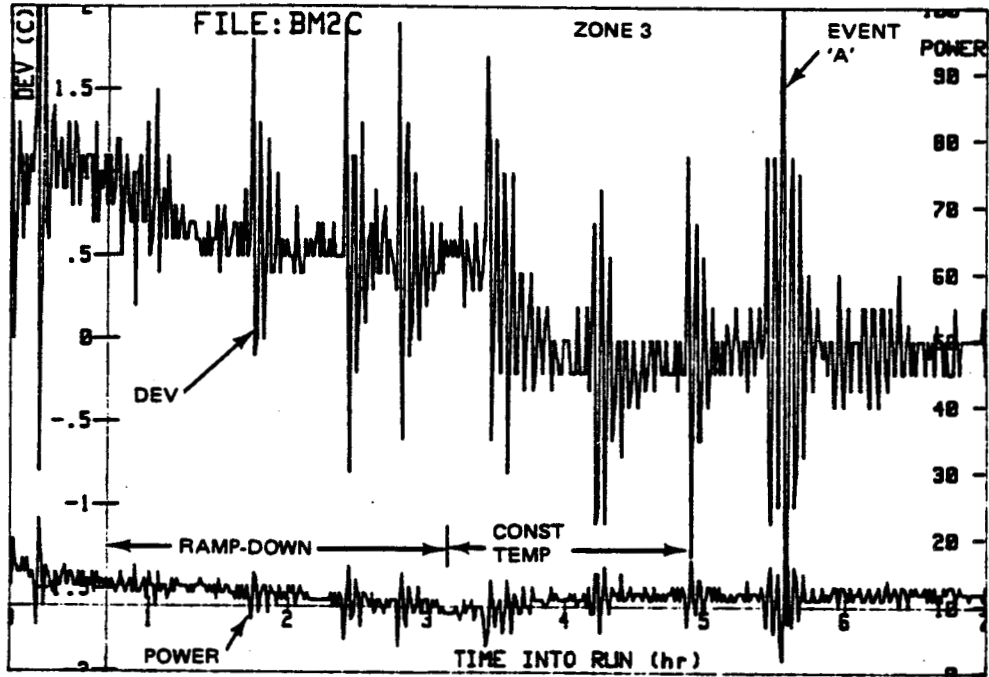
R86-0332-042(T)

Fig. 40 Expanded Temperature vs Time for BiMn Case C



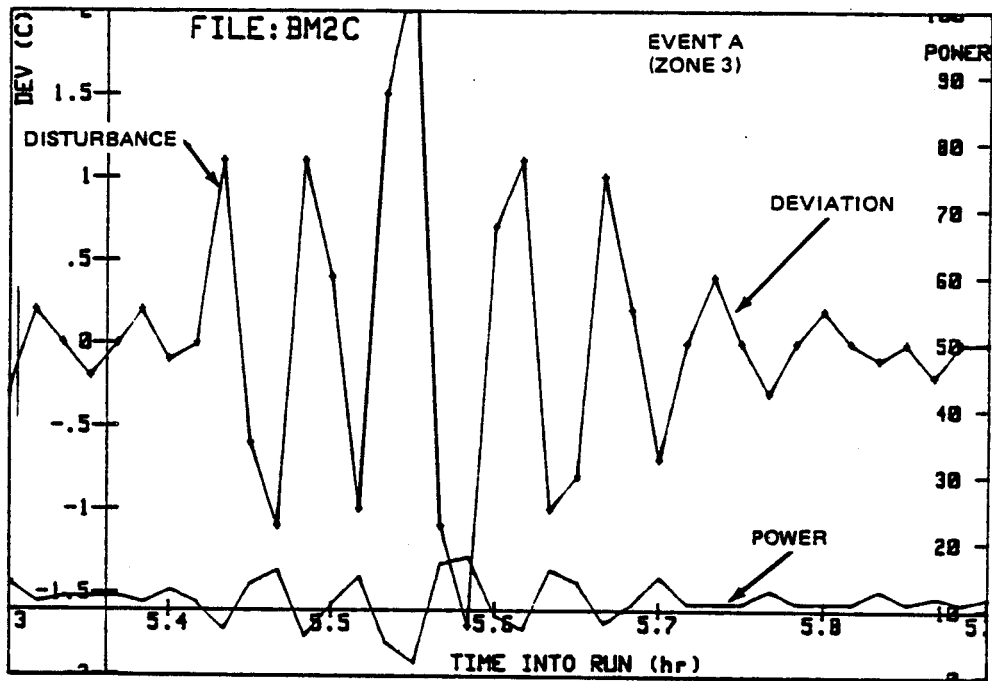
R86-0332-043(T)

Fig. 41 Isotherm Velocity vs Time for Case C



R86-0332-044(T)

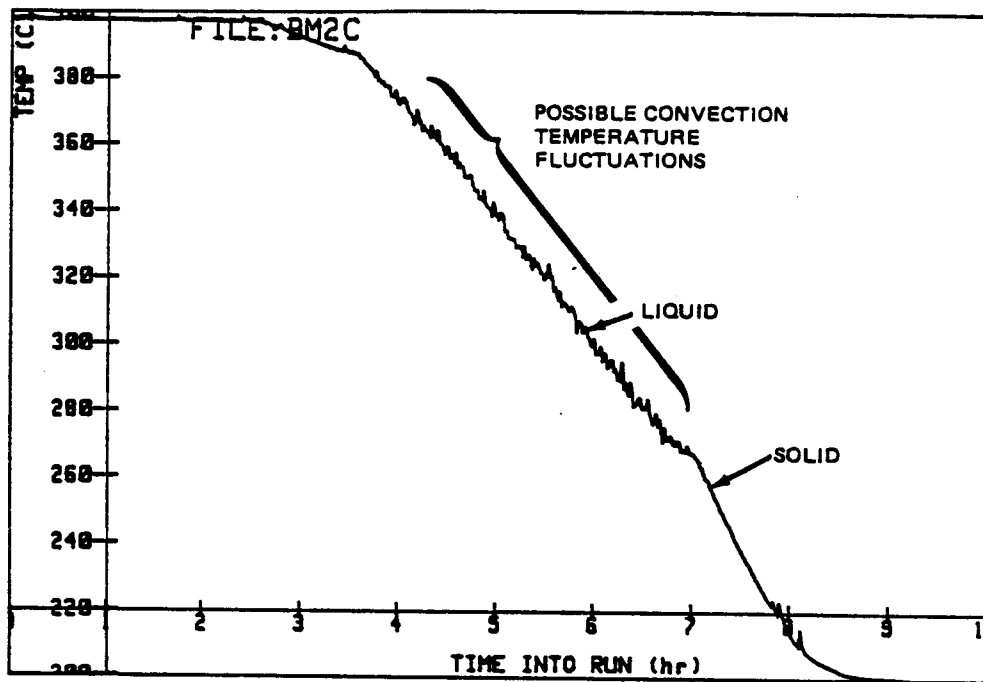
Fig. 42 Power & Deviation from Linearity vs Time during Ramp-Down & Constant Temperature Hold for Case C



R86-0332-045(T)

Fig. 43 Expanded Deviation & Power vs Time for Event A

The source of the initial temperature disturbance was not known, but could very well be electrical in nature as it appeared to affect all zones at the same time. The observed noise in the sample cooling curve (Fig. 44) might be direct indication of thermal convection cells as most of it disappeared after the solidification point. The strange behavior of zone 9 was due to a program error. Zone 7 deviated due to the influence of the sample.



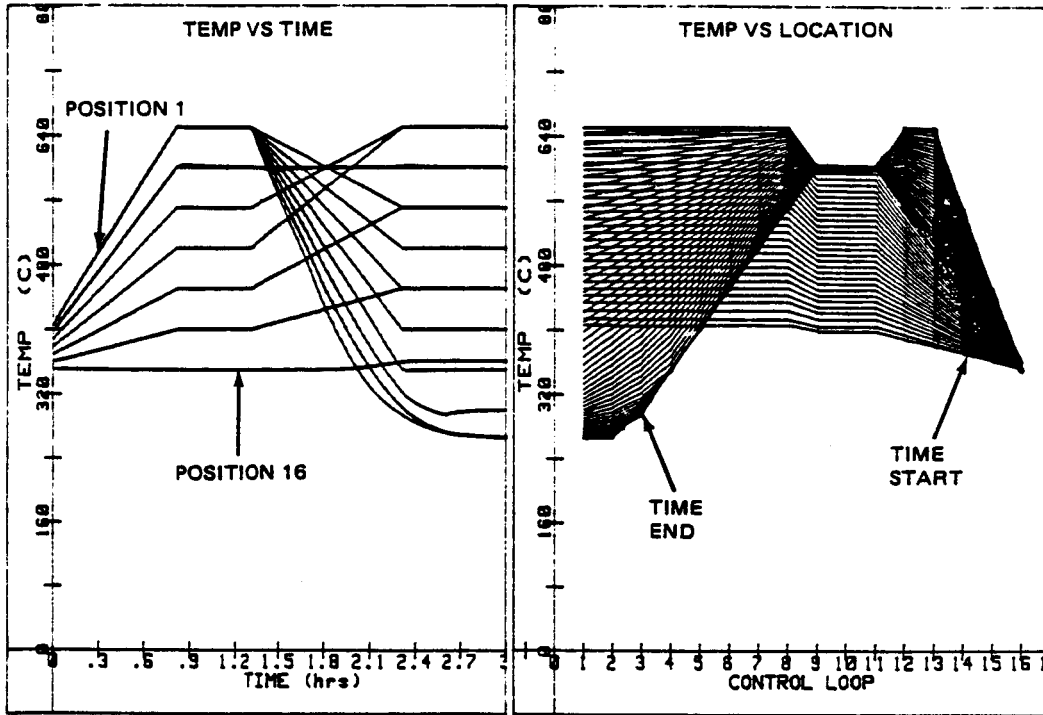
R86-0332-046(T)

Fig. 44 Sample Cooling History Showing Possible Thermal Convection in the Liquid Phase during Cooling

7 - NONBRIDGMAN-TYPE FURNACE THERMAL PROFILES

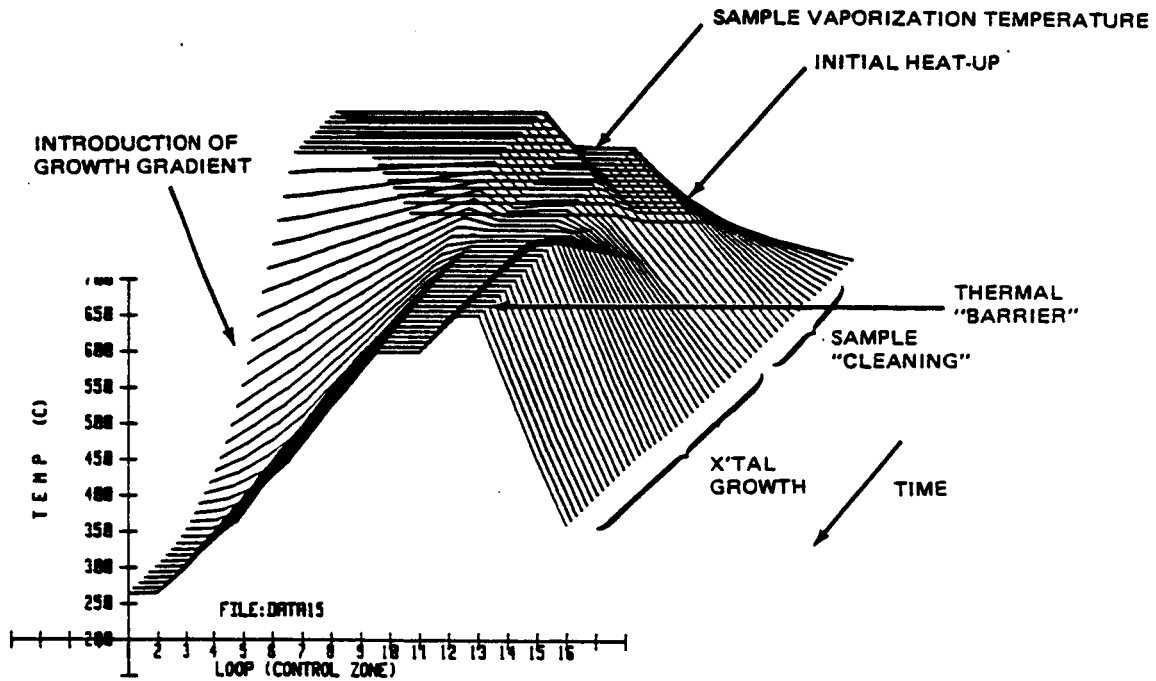
The versatility of the multizone design enabled the generation of other interesting thermal geometries. Besides the Bridgman-type thermal geometry described earlier, thermal history suitable for crystal growth by the vapor transport technique is possible. Figure 45 shows a 3D time-temperature-location view of a thermal history associated with the EDG furnace configured for vapor transport. The profile involves heating a material in a temperature gradient to vaporize the initial surface layers which contain contaminants. These contaminants will then be collected on a cold surface to the right side. After a certain period, a temperature gradient for vapor transport negative relative to the first gradient will be introduced for vapor transport to the left (crystal seed) side. A thermal barrier to now minimize transport to the right side is also created.

Other useful complex or simple profiles can be generated. Two typically programmed temperature profiles are shown in Fig. 46 and 47.



2D VIEW OF:

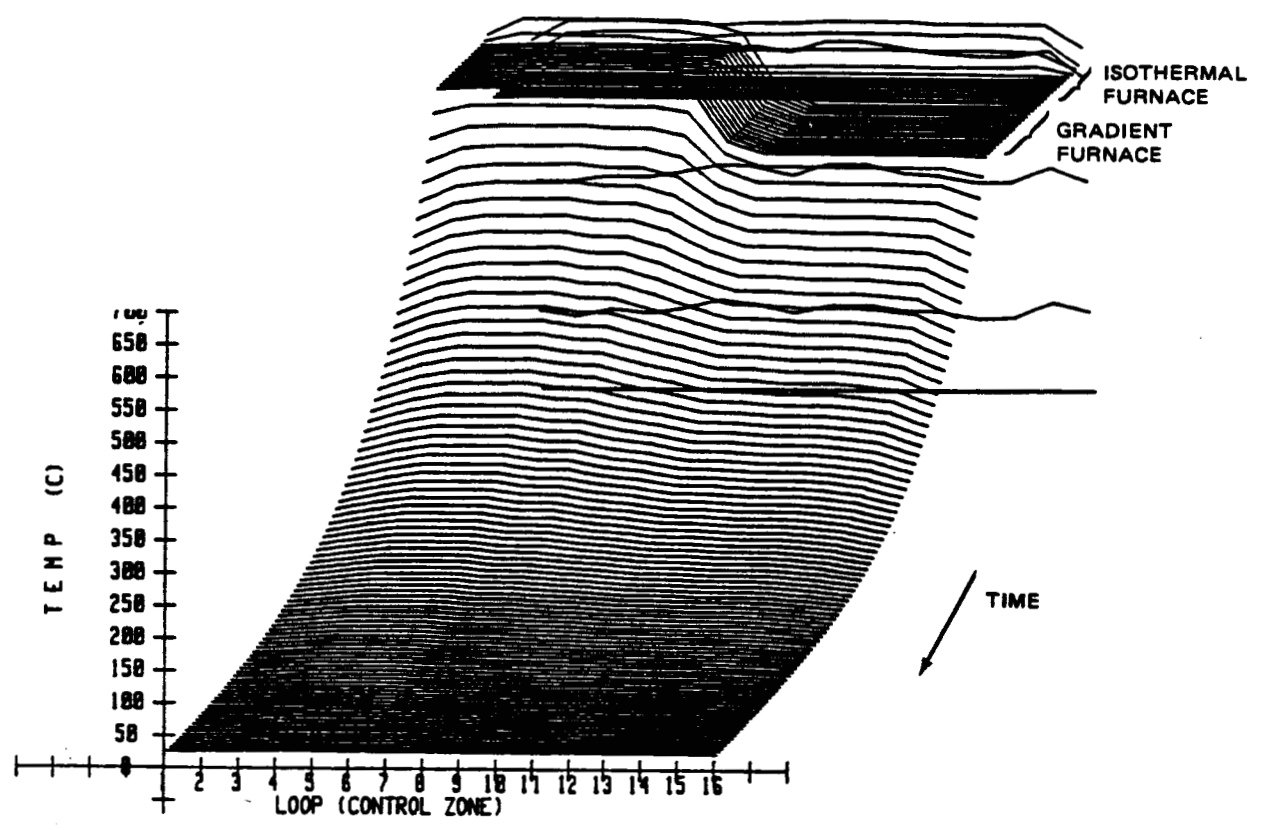
TEMP VS TIME
&
TEMP VS LOCATION



R86-0332-047(T)

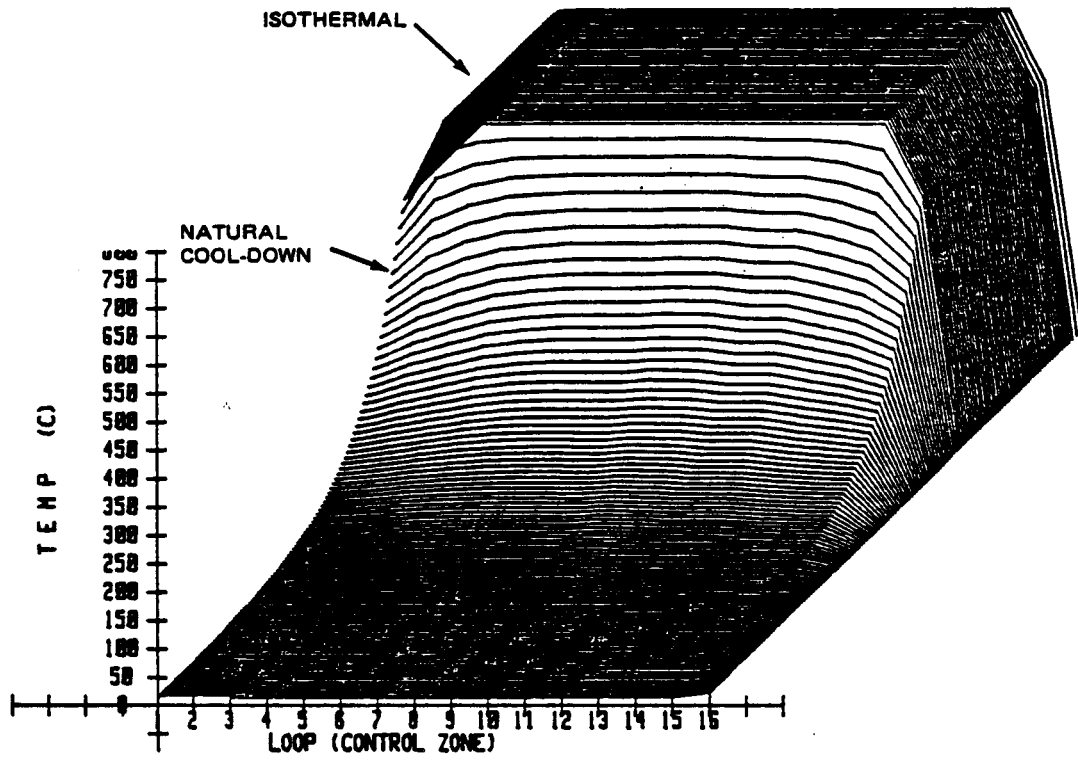
Fig. 45 Vapor-transport Crystal Growth Temperature Profile History

ORIGINAL PAGE
OF POOR QUALITY



R86-0332-048(T)

Fig. 46 Isothermal & Gradient Furnace Temperature Profile



R86-0332-049(T)

Fig. 47 Simple Isothermal Furnace Temperature Profile

8 - SPACE SHUTTLE COMPATIBILITY

The two factors which determine whether the EDG can be used on the Space Shuttle are :

- o Power compatibility
- o Physical survivability during launch.

8.1 THERMAL AND ELECTRICAL INTERFACE

The steady state radial heat loss of the furnace was typically no more than 70 watts per in. at 700°C. The shuttle payload bay cooling loop can cool at a maximum rate of 6400 watts (Ref 5). For this 48 in. furnace, the total heat rejection would be 3300 watts and therefore, the shuttle's cargo bay cooling loop appears adequate for the furnace conditions tested.

Standard electrical service for one quarter section of the shuttle cargo bay is 1750 watts continuous, and 3000 watts for 15 min out of each 3 hr period (Ref 5). Only two quarter sections are powered. If the two active quarters are both used, a total of 3500 watts continuous is possible. The two quarters must be kept electrically isolated. This amount of power is, at best, very marginal for the operation of the EDG furnace in the form tested, since radial heat loss alone is already 3300 watts at 700°C.

As the high energy consumption is a result of the cooling needed to generate a temperature gradient, the only method to use the EDG in space will be to either reduce the (already limited) temperature gradient, furnace length, furnace temperature, or to provide more power to the Space Shuttle.

8.2 LAUNCH SURVIVAL

Beside issues of cooling and power, in order to achieve flight readiness, the construction of the furnace must be able to survive the launch and space environments. Factors such as vibration survival and electronic packaging for space must be considered. The strength of the furnace as typified by the friable insulation material utilized in the furnace construction is questionable. It is clear that to adapt the EDG furnace system for space flight will require extensive modification of the furnace design to harden the furnace and electronics hardware.

9 - SUMMARY

The major considerations behind the multizone design and, specifically, the EDG furnace are summarized below. Advantages and disadvantages exist. These arise from the controller and the physical construction of the furnace. Numbers when presented are for the EDG system and conditions studied. With other multizone system designs, these values will change. The considerations are:

- o Temperature gradient limits - the thermal averaging needed to smooth the effect of discrete heating zones means that cooling cannot be localized. The result is a furnace limited to moderate or low temperature gradients. In the test furnace, for the sample size tested (0.5 in. diameter), temperature gradients up to approximately 75°C/in. are possible in stainless steel (16w/mC) and 30°C/in. in copper (300w/mC). The magnitude of a gradient is limited by the amount of axially transported heat that can be radially lost. Minimum gradients are limited by the accuracy of the control system, as the gradient produced is no better than the temperature sensors used to create it. Due to thermocouple errors, the lower limit is approximately 6°C/in. at 750°C.
- o Temperature gradient velocity limits - the upper limit of the gradient velocity is set by the cooling rate of the furnace zones involved. In the EDG, as the maximum cooling rate is axial heat flux dependent, the maximum gradient velocity will depend on operating temperature, gradient magnitude, and sample conductivity. Thermal gradient velocities up to 10 in./hr are possible for low conductivity materials (<16W/mC). The lower gradient velocity limit is set by the time-temperature stability and accuracy of the system. Sensitivity to temperature measurement error (due to electronic stability) as a results of room/electronics temperature variations sets a lower limit estimated at approximately 0.075 in./hr under conditions for a room temperature change of 5°C in 5 hr with a gradient of 20°C/in. and a 10% precision in gradient velocity. Under conditions where furnace temperature oscillation occurs (mostly at low temperatures) due to poor tuning and/or inadequate control resolution, the lower limit can be unacceptably high.

- o Experimental flexibility - parameters relating to temperatures and gradients (i.e., magnitude and length) are controlled by computer software. Many different thermal profiles can be programmed. (Without mechanical drivers, the furnace is more compact in size with little vibration.) A high degree of operator skill is needed to take advantage of this desirable features
- o Energy consumption - in the EDG furnace, power efficiency is sacrificed for temperature gradient magnitude. The overall power level is too high for Space Shuttle considerations (in the form tested). If lower temperature gradients or smaller sample lengths are acceptable, then the overall power requirements can reduced.

10 - CONCLUSIONS

The EDG furnace tested is a versatile moderate to low velocity, low gradient, directional solidification furnace. In its range of operation, its flexibility makes it a good tool for materials research. Its major handicaps are its high power consumption and the high dependence of the gradient and its motion on the control system. The EDG furnace tested was an early developmental prototype of the multizone design; future versions will no doubt have improved designs. In the complex area of crystal growth, more research into the multizone furnace design should be done to take full advantage of its capabilities.

11 - REFERENCES

1. United States Patent # 4423516, Dec 27, 1983.
2. Gordon, L. M., "Process Automation," Chem Eng, May, Aug, Sept, Nov, 1983.
3. Omega Engineering Handbook, 1985.
4. Pirich, R. G., Larson, D. J., and Busch, G., AIAA J, Vol 19, p589, 1981.
5. Communication between G. Knowles (Grumman) and M. Hendrix (NASA-JSC).

PRECEDING PAGE BLANK NOT FILMED